Dynamics of Structures

Arnaud Deraemaeker

Contents

1 Introduction

Vibration refers to mechanical oscillations about an equilibrium point. The oscillations may be periodic such as the motion of a pendulum or random such as the movement of a tire on a gravel road. In practice, every object is subject to a certain level of vibration, which can often not be seen with the naked eye. This does not mean that this phenomenon is not important, and it deserves, in many cases, to be studied. Examples of objects creating vibration in everyday life are a shaver, a vibrator in a cell phone, a loudspeaker, tools, rotating machines and vehicles in motion such as trains or trams.

1.1 Mechanism of Vibrations

The underlying mechanism of vibrations consists in the transfer of the potential energy into kinetic energy, and vice versa. Examples of the mass-spring system and the pendulum are illustrated in Figures 1 and 2.

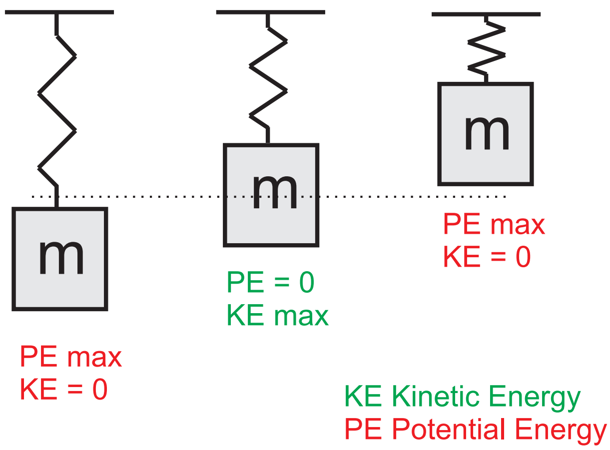

Figure 1: Transfer of the potential energy to kinetic energy and vice versa in the mass-spring system

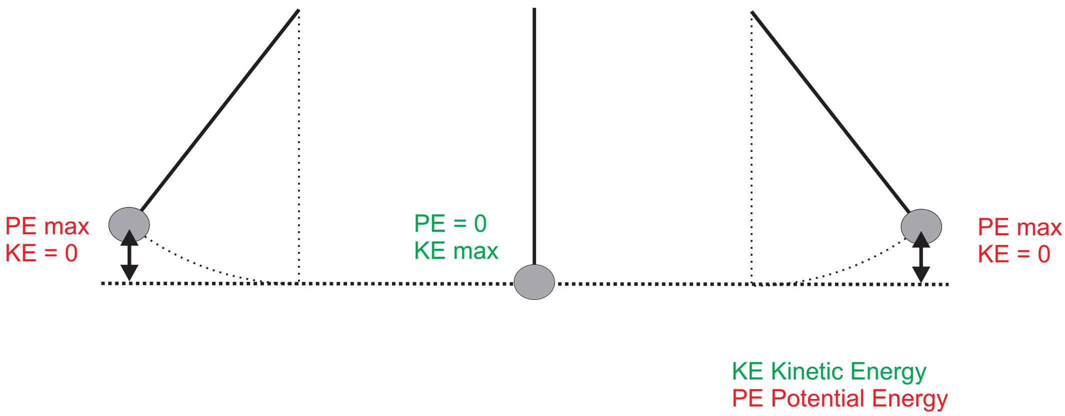

Figure 2: Transfer of the potential energy to kinetic energy and vice versa in the pendulum

1.2 Sources of excitations

In order for a body to vibrate, it has to be excited by a source. The sources of excitation can be divided in two main categories : free vibrations and forced vibrations. Free vibrations correspond to the case where the vibration is caused by an initial source which is then removed so that the structure vibrates without any force acting on it. Forced vibrations correspond to the case where an excitation is permanently applied to the structure.

1.2.1 Free vibration

A free vibration is generally induced by either an external force with a very short duration (shock), or by an initial displacement or velocity imposed to the structure. The simplest example is the mass-spring system: when the mass is pulled downwards, an initial displacement is imposed (Figure 3a). Once the mass is released, it starts vibrating freely. In a similar way, hitting a bell for a very short time makes it vibrate freely. The mechanical vibration is transmitted to the air and a sound is emitted. (Figure 3b)

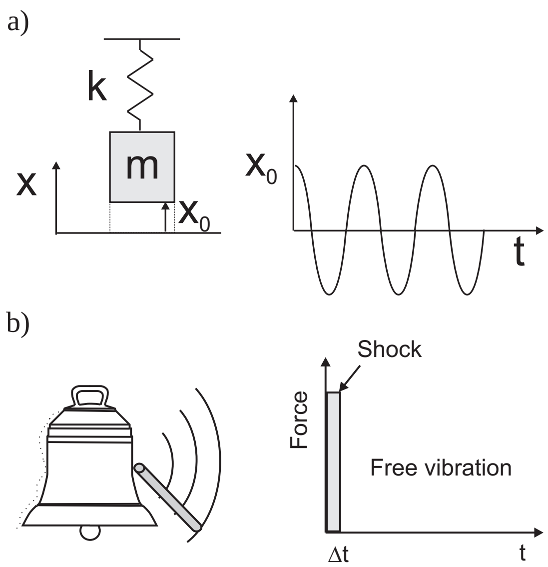

Figure 3: Examples of free vibrations: a) Free response of a mass-spring system due to an initial displacement b) Free response of a bell due to an initial shock

1.2.2 Forced vibrations

In forced vibrations, we can distinguish between three different types of excitation signals: harmonic, periodic, and random signals (Figure 4).

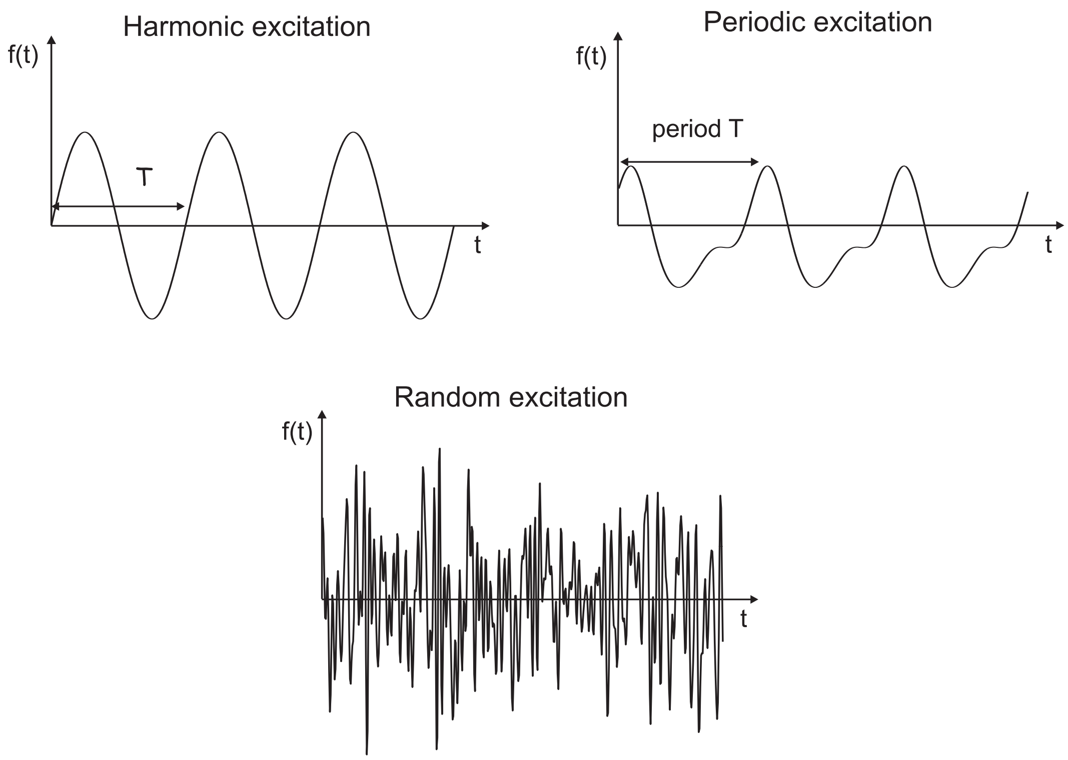

Figure 4: Three different types of forced excitation signals

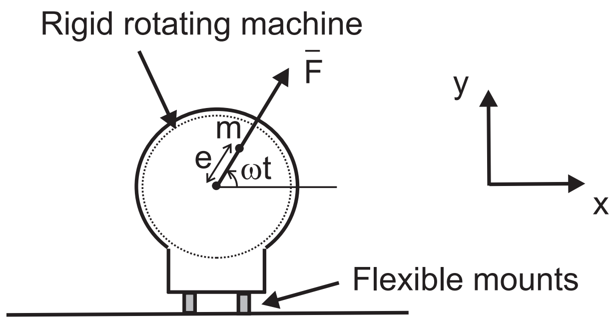

$$F_x = me\,\omega^2\cos(\omega t)$$
$$F_y = me\,\omega^2\sin(\omega t)$$

Figure 5: Forces generated by the unbalance of a rotating machine

- Harmonic excitation : the force applied to the body is a sine or a cosine function with a given period T. Rigid rotating machines are an example of source of harmonic excitation signal: as the rotor is never perfectly balanced (its center of gravity does not correspond to its geometric center), there exists an inertial force due to the unbalance. This force has a radial direction and an amplitude $me\omega^2$ (m= mass of the spring, e= distance between the center of gravity and the rotation center, ω = rotational speed, Figure 5) and can be decomposed into a vertical and an horizontal force varying with the rotation angle. Each of these components is a sine or cosine function and is transmitted to the environment through the fixations of the rotating machine. This excitation is therefore periodic and harmonic.

- Periodic excitation: this corresponds to excitation signals which repeat themselves over time with a certain period T. As an example, piston engines generate periodic excitation (the period corresponding to one full rotation of the crankshaft) which is not made of a single sine or cosine component (existence of harmonics of the fundamental frequency).

- Random excitation: a random excitation signal has no fundamental frequency and one cannot distinguish a pattern which repeats itself over time. Examples are the forces generated by wind, earthquakes (Figure 6), traffic, waves etc.

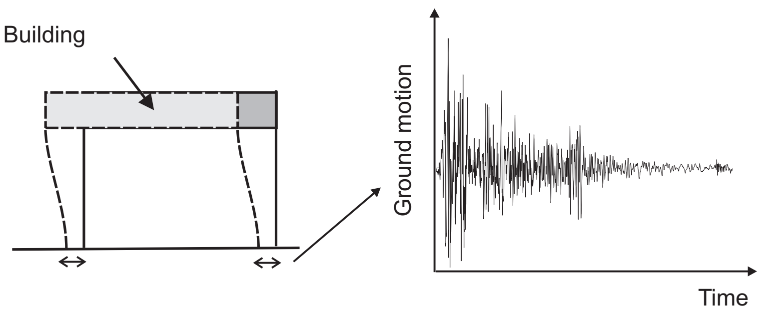

Figure 6: Example of excitation signal induced by an earthquake on a building

1.3 Vibration sources in civil engineering

In civil engineering, one can distinguish between internal and external sources of vibrations:

- Internal sources:
  - Ventilation systems
  - Elevator and conveyance systems
  - Fluid pumping equipment
  - Machines and generators
  - Aerobics and exercise rooms, human activity
- External sources:
  - Seismic activity
  - Subway, road and rail systems, airplanes
  - Construction equipment
  - Wind, Waves

Traditionally, vibrations have not been a big concern in civil engineering, except for high levels of vibrations caused by earthquakes. In recent years however, the sources and levels of excitations have increased, while at the same time the comfort demands are increasing and health issues are appearing. In some cases, novel high precision technologies require very low levels of vibrations. Another important change is the fact that new designs of structures make them more susceptible to vibrations. For example, where in the past, bridges where massive structures, they tend to a more and more slender design aimed at optimising the use of materials (Figure 7). The drawback is that such a design makes them much more prone to vibrations. The use of novel materials such as composites is also responsible for a lower level of damping, hence more vibrations.

Figure 7: Evolution in the design of bridges: from massive $[http://www.bridge2faith.net]$ to slender structures $[https://fr.wikipedia.org/wiki/Viaduc\_de\_Millau]$

We detail here below a few examples of structures where vibrations are problematic:

- **The Millenium Bridge** (Figure 8) in London is a steel suspension bridge for pedestrians crossing the River Thames. During its opening in June 2000, it was subjected to very high levels of lateral vibrations due to pedestrians walking on the bridge. The bridge was closed until a solution to the problem could be implemented.
- In **cable-stayed bridges** (Figure 8), wind excitation can cause excessive levels of vibrations in the cables. Damping systems are often implemented in order to solve this problem.
- In **high-rise buildings**, wind excitation can cause an oscillatory motion which is detrimental for comfort of the inhabitants in the top levels. These structures are also more vulnerable to earthquake excitation. An example is the Taipei 101 (Figure 9) building (509 m) in which a massive device called ”pendulum tuned mass damper” has been implemented. The device is designed to damp the vibrations due to earthquakes which could impact the structural integrity of the building.
- The original **Tacoma Narrows bridge** opened on July 1, 1940 and collapsed into the Puget Sound in Pierce County, Washington on November 7 1940 (Figure 9). The collapse was due to high wind conditions which caused excessive vibrations leading to the collapse of the bridge.

Millenium Bridge (London)

Cable-stayed bridge

Figure 8: The Millenium bridge [https : //fr.wikipedia.org/wiki/Millennium_Bridge_(Londres)] and a cable-stayed bridge (Dongting, China) [http : //sitesavisiter.com/pont − du − lac − dongting]

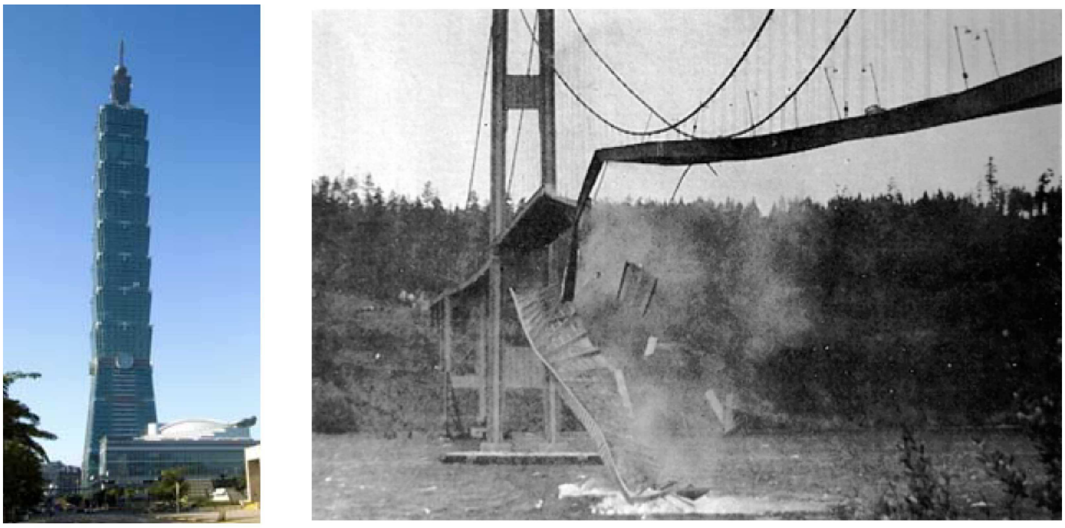

Taipei 101

Collapse of the Tacoma Narrows bridge

Figure 9: The Taipei building [http://blog.artnn.ru] and the original Tacoma Narrows bridge [http://www.maxisciences.com/construction/pont-de-tacoma-washington-1940_art3460.html]

1.4 Positive vs negative effects of vibrations

We have already listed negative aspects of vibrations: excessive levels of vibrations can cause fatigue, health and comfort issues, degrade the performance of systems and in the most catastrophic case can lead to collapse. There are however some cases in which vibrations are useful, examples are a loudspeaker (Figure 10) which requires vibrations to produce sound, an electric toothbrush, a sander, musical instruments, etc. Another example is the use of high-frequency vibrations in formula one engines to reduce the friction.

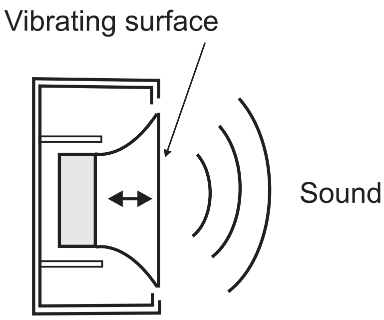

Figure 10: A loudspeaker uses vibrations of a moving membrane to produce sound

1.5 A first feeling about vibrations through movies and experiments

The reader is suggested to have a look at the following movies as an introduction to the concepts which will be developed in the coming chapters. The movies describe what is a simple harmonic motion, and introduce the concept of resonance.

```
Simple harmonic motion:
http://www.youtube.com/watch?v=SZ541Luq4nE

Mass spring system (finger excitation):
http://www.youtube.com/watch?v=_XTj_ePLvFI
```

2 Tools to describe an deal with dynamic signals

2.1 Harmonic signals

A periodic vibration of which the amplitude can be described by a sinusoidal function:

$$u(t) = A\cos(\omega t + \phi)$$
$$u(t) = A\sin(\omega t + \phi)$$

is called a *harmonic vibration* with:

- amplitude a
- angular frequency $\omega = 2\pi f$
- frequency f
- period $T = 1/f$ or $f = 1/T$
- phase angle ϕ at $t = 0$
- total phase angle $\omega t + \phi$

Harmonic signals are more conveniently represented in the complex plane. In order to do that, one writes:

$$u(t) = ae^{i(\omega t+\phi)} = a\cos(\omega t+\phi) + i\,a\sin(\omega t+\phi)$$

which can be written:

$$u(t) = ae^{i\phi}e^{i\omega t} = Ae^{i\omega t}$$

where

$$A = ae^{i\phi} = a\cos(\phi) + ia\sin(\phi)$$

which introduces the complex amplitude A which is independent of time (Figure 11). Note that introducing imaginary numbers is a kind of artefact: there exists no vibration which is imaginary, all vibration signals are real. The important point to remember is that the complex amplitude A carries the information of both the amplitude a and the phase angle ϕ and therefore contains all the information about the harmonic signal.

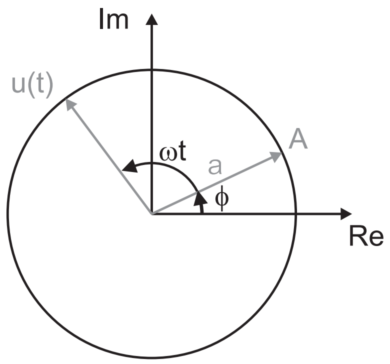

Figure 11: Representation of the harmonic signal as a complex number A with a phase and amplitude in the complex plane

The use of the complex notation is particularly useful when one wishes to calculate the first and second derivatives of a harmonic signal with respect to time:

$$\begin{aligned}
u(t) &= Ae^{i\omega t} \\
v(t) &= \frac{d\,u(t)}{dt} = i\omega Ae^{i\omega t} = i\omega u(t) \\
a(t) &= \frac{d\,v(t)}{dt} = -\omega^2 Ae^{i\omega t} = -\omega^2 u(t)
\end{aligned}$$

The displacement, velocity and accelerations are represented in the complex plane in Figure 12. One can see clearly that the derivation introduces a phase shift of 90° together with a multiplication of the amplitude by a factor ω. The signals are represented in the time domain for a phase angle of $\phi = 0$ in Figure 13.

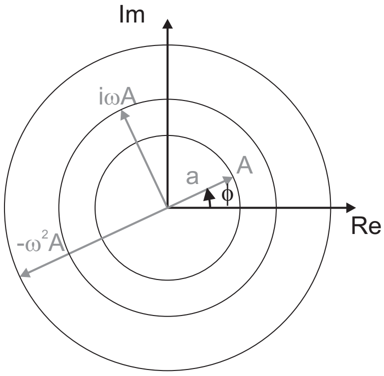

Figure 12: Displacement, velocity and acceleration represented in the complex plane

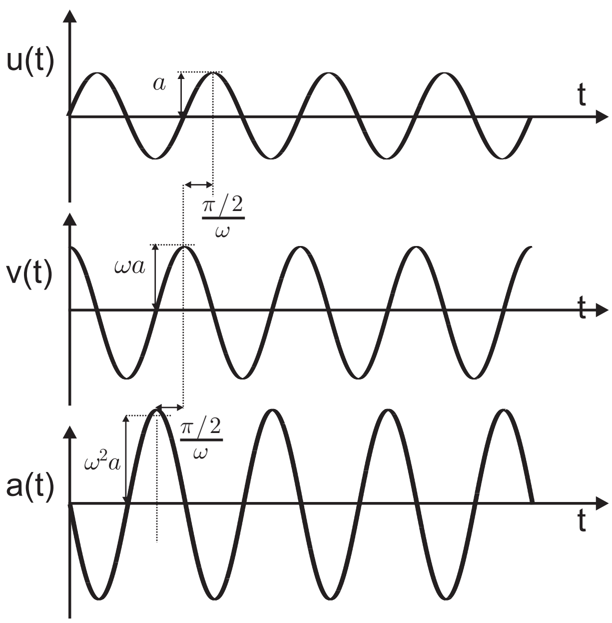

Figure 13: Displacement, velocity and acceleration represented in the time domain ($\phi = 0$)

2.2 Harmonic analysis: the discrete Fourier transform

Let $u(t)$ be a periodic function of period T. It can be decomposed into a discrete Fourier series of the form:

$$u(t) = a_0 + \sum_{n=1}^{\infty} [a_n \cos(n\omega_0 t) + b_n \sin(n\omega_0 t)] \tag{1}$$

with

$$\omega_0 = \frac{2\pi}{T}$$

is the fundamental frequency and

$$a_0 = \frac{1}{T}\int_0^T u(t)dt \tag{2}$$

$$a_n = \frac{2}{T}\int_0^T u(t)\cos(n\omega_0 t)dt \tag{3}$$

$$b_n = \frac{2}{T}\int_0^T u(t)\sin(n\omega_0 t)dt \tag{4}$$

In other words, a peridic function can be represented by an infinite sum of sine and cosine functions of discrete frequencies which are multiples of the fundamental frequency ω_0 (Figure 14).

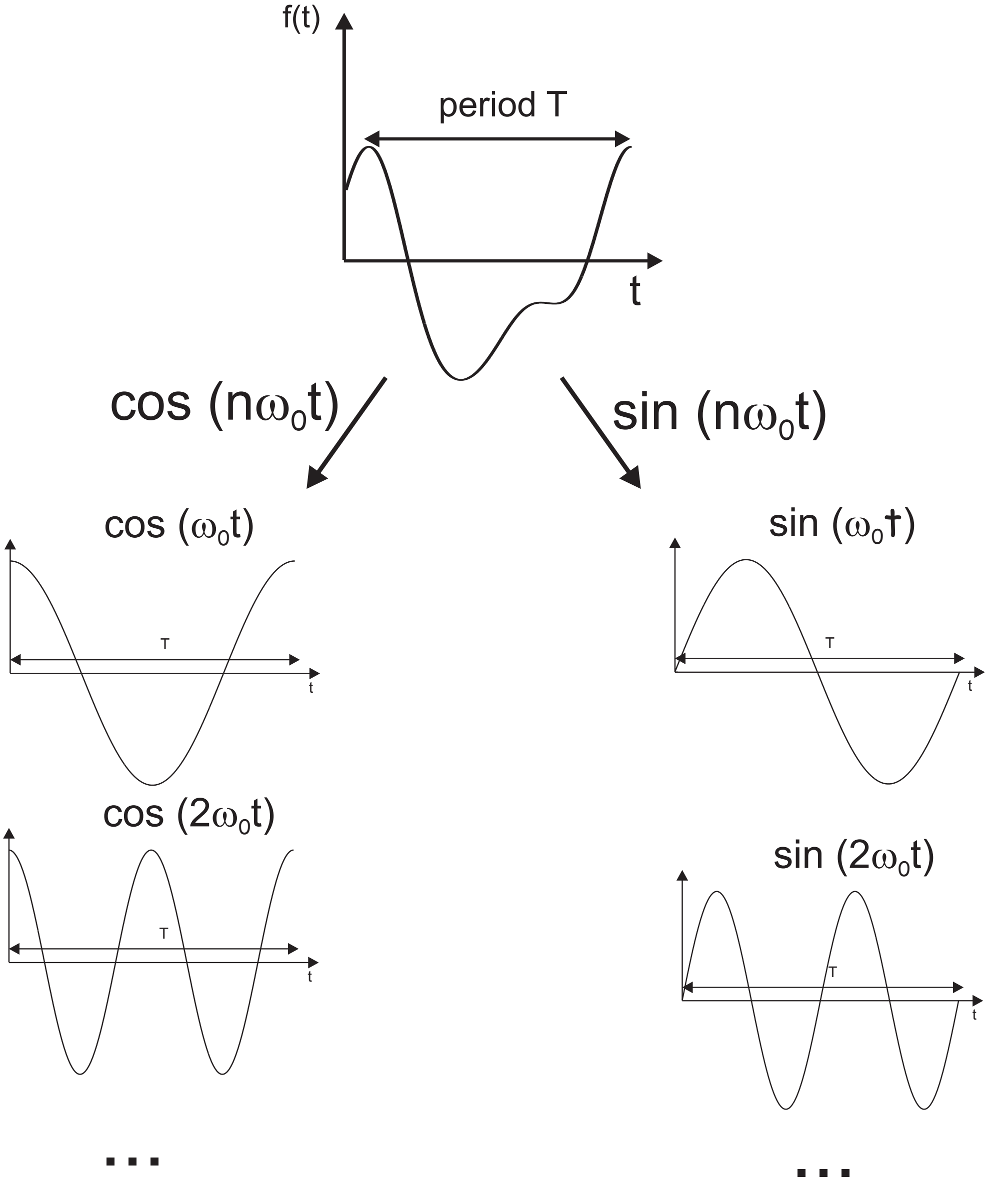

Figure 14: Fourier decomposition of a periodic signal

An alternative formulation is given by:

$$u(t) = \frac{a_0}{2} + \sum_{n=1}^{\infty} [a_n \cos(n\omega_0 t) + b_n \sin(n\omega_0 t)] \tag{5}$$

$$\begin{aligned}
a_0 &= \frac{2}{T}\int_0^T u(t)dt \\
a_n &= \frac{2}{T}\int_0^T u(t)\cos(n\omega_0 t)dt \\
b_n &= \frac{2}{T}\int_0^T u(t)\sin(n\omega_0 t)dt
\end{aligned}$$

2.2.1 Amplitude and phase formulation

Equation (5) can be written in the form of a single cosine function with amplitude an phase as follows:

$$u(t) = d_0 + \sum_{n=1}^{\infty} d_n \cos(n\omega_0 t - \phi_n) \tag{6}$$

where one can show (left as a demonstration) that:

$$\begin{aligned}
d_0 &= \frac{a_0}{2} \\
d_n &= \sqrt{a_n^2 + b_n^2} \\
\phi_n &= tg^{-1}\left(\frac{b_n}{a_n}\right)
\end{aligned}$$

2.2.2 Complex formulation

Equation (5) can also be written in a complex form. Using the following trigonometric equalities,

$$\cos(n\omega_0 t) = \frac{e^{in\omega_0 t} + e^{-in\omega_0 t}}{2}$$

$$\sin(n\omega_0 t) = \frac{e^{in\omega_0 t} - e^{-in\omega_0 t}}{2i}$$

one gets:

$$u(t) = \frac{a_0}{2} + \sum_{n=1}^{\infty}\left[a_n \frac{e^{in\omega_0 t} + e^{-in\omega_0 t}}{2} + b_n \frac{e^{in\omega_0 t} - e^{-in\omega_0 t}}{2i}\right]$$

$$u(t) = \frac{a_0}{2} + \sum_{n=1}^{\infty}\left[\frac{a_n - ib_n}{2} e^{in\omega_0 t} + \frac{a_n + ib_n}{2} e^{-in\omega_0 t}\right]$$

which can also be written

$$u(t) = \sum_{n=-\infty}^{n=\infty} c_n e^{in\omega_0 t}$$

with

$$
\begin{aligned}
c_0 &= \frac{a_0}{2} \\
c_n &= \frac{a_n - ib_n}{2} \\
c_{-n} &= \frac{a_n + ib_n}{2}
\end{aligned}
$$

Subsituting a_0, a_n and b_n using (2-4), we get:

$$
c_0 = \frac{a_0}{2} = \frac{1}{T}\int_0^T u(t)dt
$$

$$
c_n = \frac{a_n - ib_n}{2} = \frac{1}{T}\int_0^T u(t)\left(\cos(n\omega_0 t) - i\sin(n\omega_0 t)\right)dt = \frac{1}{T}\int_0^T u(t)e^{-in\omega_0 t}dt
$$

$$
c_{-n} = \frac{a_n + ib_n}{2} = \frac{1}{T}\int_0^T u(t)\left(\cos(n\omega_0 t) + i\sin(n\omega_0 t)\right)dt = \frac{1}{T}\int_0^T u(t)e^{in\omega_0 t}dt
$$

so that we can finally write:

$$
u(t) = \sum_{n=-\infty}^{n=\infty} c_n e^{in\omega_0 t} \tag{7}
$$

with

$$
c_0 = \frac{1}{T}\int_0^T u(t)dt
$$

$$
c_n = \frac{1}{T}\int_0^T u(t)e^{-in\omega_0 t}dt
$$

Note that c_n is complex and carries the phase and amplitude information of the n^{th} component of the Fourier transform. This can easily be shown knowing that:

$$
\begin{aligned}
c_n &= \frac{a_n - ib_n}{2} \\
d_n &= \sqrt{a_n^2 + b_n^2} \\
\phi_n &= tg^{-1}\left(\frac{b_n}{a_n}\right)
\end{aligned}
$$

where d_n and ϕ_n are the phase and amplitudes of the n^{th} component of the Fourier transform. Note also that c_n and c_{-n} are complex conjugate so that $u(t)$ is always real. The complex formulation can also be written in the following form where the integrals are taken from $-T/2$ to $T/2$ instead of from 0 to T:

$$
\begin{aligned}
u(t) &= \sum_{n=-\infty}^{n=\infty} c_n e^{in\omega_0 t} \\
c_0 &= \frac{1}{T}\int_{-\frac{T}{2}}^{\frac{T}{2}} u(t)dt \\
c_n &= \frac{1}{T}\int_{-\frac{T}{2}}^{\frac{T}{2}} u(t)e^{-in\omega_0 t}dt
\end{aligned}
$$

2.2.3 Examples of Fourier transforms of periodic signals

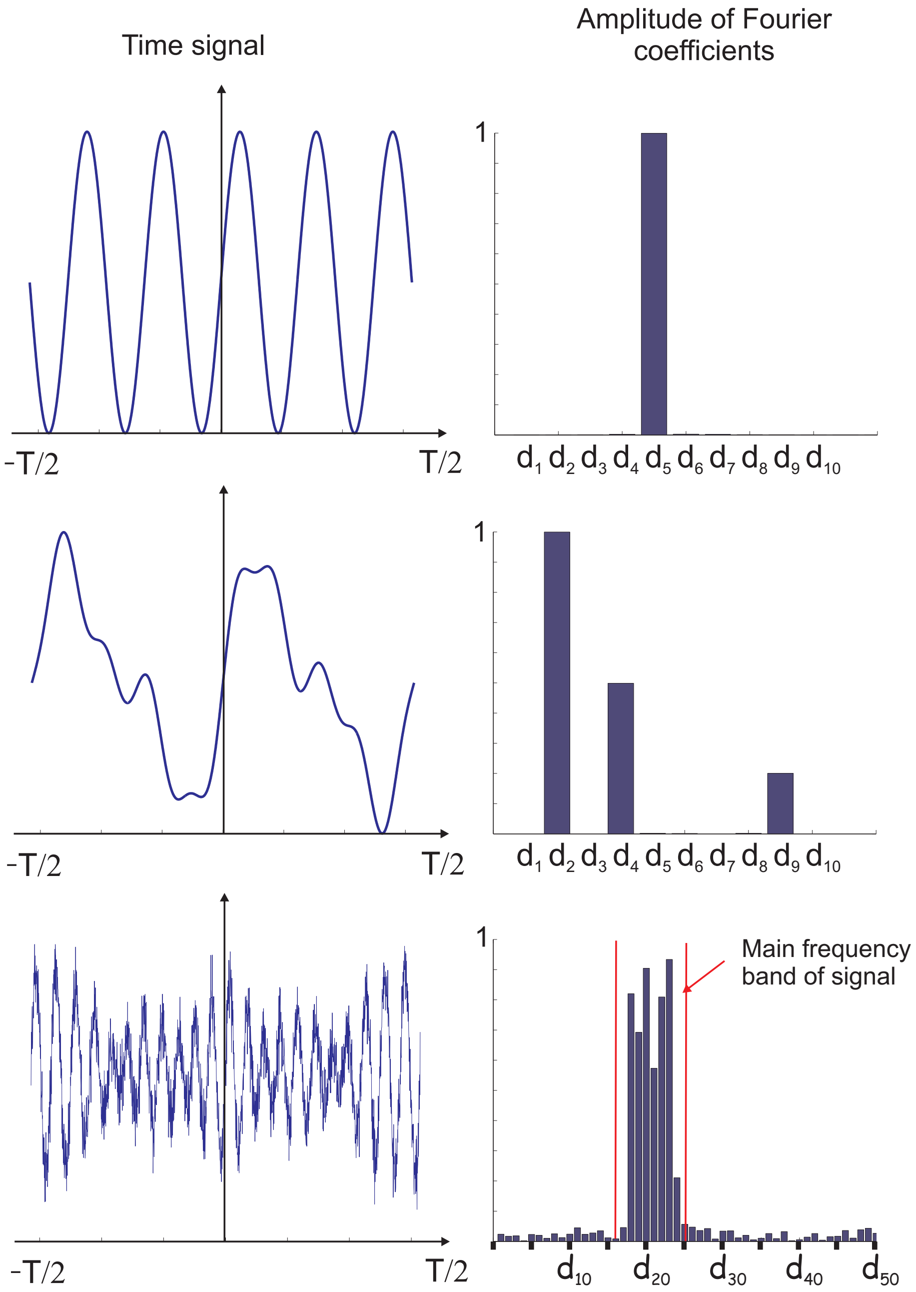

Figure 15: Examples of Fourier transforms of periodic signals: amplitudes of the Fourier components

Figure 15 shows three examples of periodic signals together with their respective discrete Fourier transforms. Only the amplitudes d_n of the Fourier components are represented. In the first two examples, the function has only one and three Fourier components. The third example is more complex. All the values of d_n are non-zero, but there is a specific frequency band in which they are very large. Outside of this frequency band, the Fourier components can be considered as negligible. This example shows the interest of the transformation in the frequency domain using the discrete Fourier transform:

if one wishes to compute the response of a structure to an excitation signal of that type, it should be performed only in the main frequency band where the excitation signal has large Fourier components.

2.3 The continuous Fourier transform

When the function u(t) is not periodic, the discrete Fourier transform cannot be applied. Instead, the continuous Fourier transform should be used. It can be obtained from the discrete transform considering that the period T of the signal tends to infinity. In this case, the discrete frequencies $n\omega_0$ used in the discrete transform tend to a continuous variable ω. The frequency spacing $\Delta\omega = \omega_0$ tends to $d\omega$ (Figure 16):

$$
\begin{aligned}
lim_{T\rightarrow\infty}\,\omega_0 &= lim_{T\rightarrow\infty}\,\Delta\omega = d\omega \\
lim_{T\rightarrow\infty}\,n\omega_0 &= \omega
\end{aligned}
$$

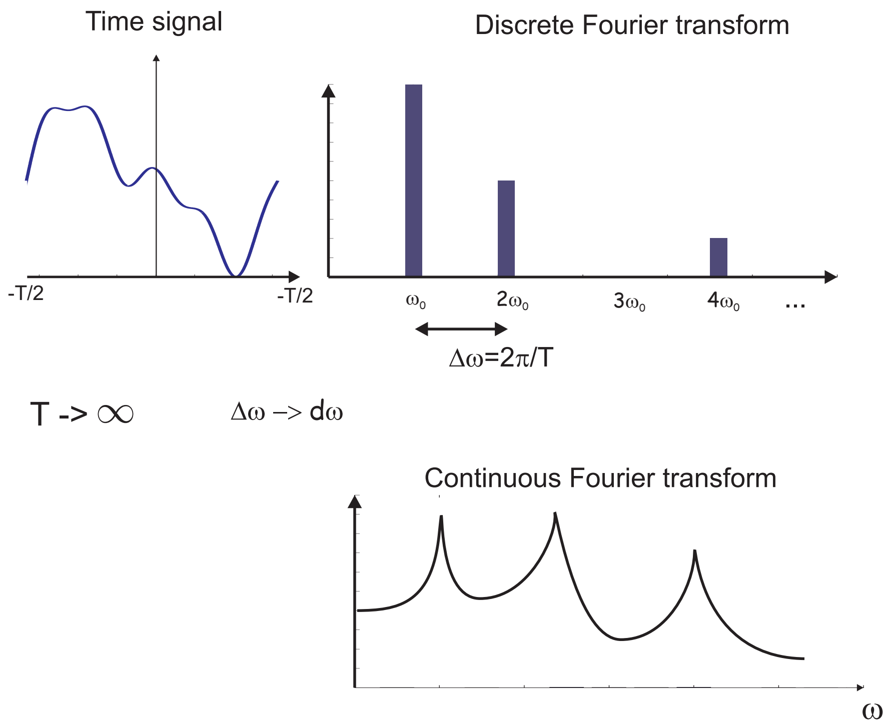

Figure 16: From the discrete Fourier transform to the continuous Fourier transform

Recalling the definition of c_n (8), we compute:

$$
lim_{T\rightarrow\infty}\,Tc_n = lim_{T\rightarrow\infty}\int_{-\frac{T}{2}}^{\frac{T}{2}} u(t)e^{-in\omega_0 t}dt = \int_{-\infty}^{\infty} u(t)e^{-i\omega t}dt = U(\omega)
$$

$U(\omega)$ is a continuous fonction of the variable ω and is the continuous Fourier transform of $u(t)$. We can now rewrite $u(t)$:

$$\begin{aligned} u(t) &= lim_{T\to\infty} \sum_{n=-\infty}^{n=\infty} c_n e^{in\omega_0 t} = lim_{T\to\infty} \sum_{n=-\infty}^{n=\infty} c_n \frac{T}{T} e^{in\omega_0 t} \\ &= lim_{T\to\infty} \sum_{n=-\infty}^{n=\infty} (c_n T) \frac{\omega_0}{2\pi} e^{in\omega_0 t} = \frac{1}{2\pi} \int_{-\infty}^{\infty} U(\omega) e^{i\omega t} d\omega \end{aligned}$$

which is the inverse continuous Fourier transform. Note that an alternative formulation consists in writing the Fourier transform as a function of f instead of ω. In this case, we have:

$$\omega = 2\pi f \Rightarrow d\omega = 2\pi df$$
$$U(f) = \int_{-\infty}^{\infty} u(t) e^{-i2\pi f t} dt$$
$$u(t) = \int_{-\infty}^{\infty} U(f) e^{i2\pi f t} df$$

where one sees that the factor $1/2\pi$ is not present anymore.

2.3.1 Examples of continuous Fourier transforms and properties

Table 1 and Figure 17 give a few examples of continuous Fourier transforms, while Table 2 gives some properties of the continuous Fourier transforms. These properties will be used in the demonstration of Parseval's theorem in section 2.4.

$u(t)$	$U(f)$
1	$\delta(f)$
$\delta(t)$	1
$\cos(2\pi f_0 t)$	$\frac{\delta(f-f_0)+\delta(f+f_0)}{2}$
$\sin(2\pi f_0 t)$	$\frac{\delta(f-f_0)+\delta(f+f_0)}{2i}$
$\sum_{n=-\infty}^{n=\infty} \delta(t-nT)$	$\frac{1}{T}\sum_{n=-\infty}^{n=\infty} \delta(f-\frac{n}{T})$

Table 1: Examples of continuous Fourier transforms

Time domain function	Frequency domain function	Property
$a\,f(t) + b\,g(t)$	$a\,F(f) + b\,G(f)$	Linearity
$f(kt)$	$\frac{1}{\lvert k\rvert} F\left(\frac{f}{k}\right)$	Time Scaling
$\frac{1}{k} f\left(\frac{t}{k}\right)$	$F(kf)$	Frequency scaling
$f(t - t_0)$	$e^{-i2\pi f t_0} F(f)$	Time shifting
$f(t)\, e^{i2\pi f_0 t}$	$F(f - f_0)$	Frequency shifting
$f(t)$ real even function	$F(f)$ real even function	
$f(t)$ real odd function	$F(f)$ imag odd function	
$f(t)$ real	$F(-f) = F(f)^*$	

Table 2: Properties of the continuous Fourier transform

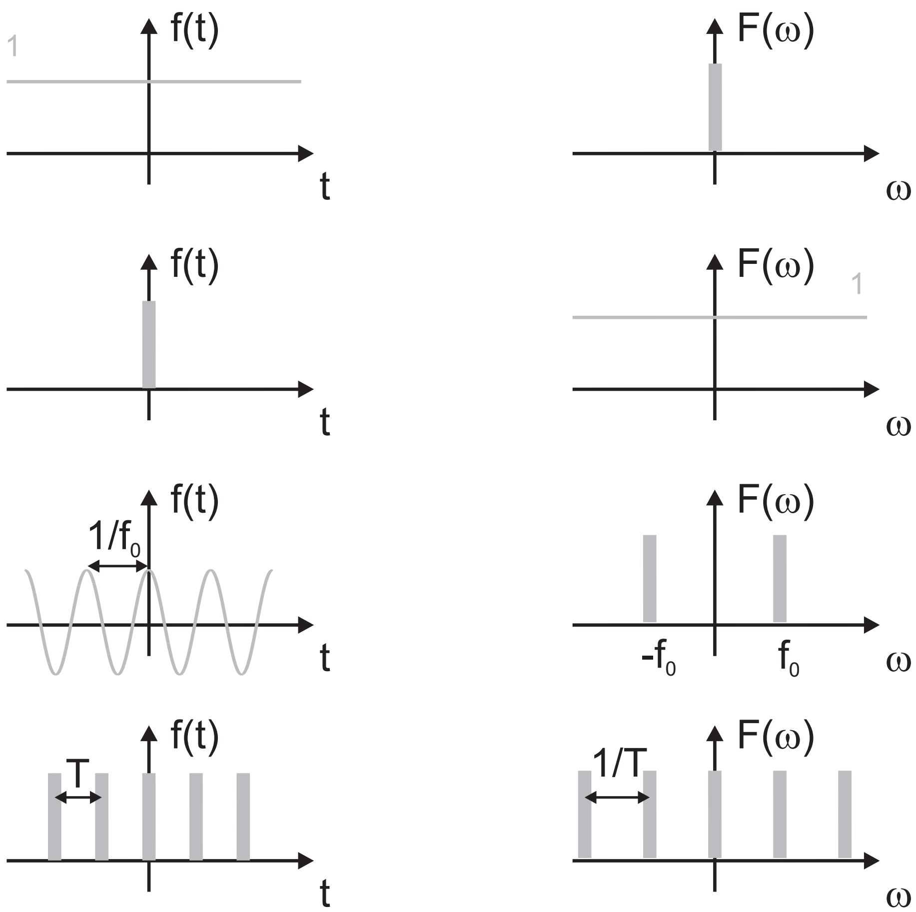

Figure 17: Examples of continuous Fourier transforms

In the following, we calculate the continuous Fourier transform of a cosine function, of a 'box' function and a triangular function. Consider the function $u(t) = \cos(2\pi f_0 t)$. Its Fourier transform is given by:

$$\begin{aligned} U(f) &= \int_{-\infty}^{\infty} \cos(2\pi f_0 t) e^{-i2\pi f t}\, dt \\ &= \int_{-\infty}^{\infty} \frac{1}{2}\left(e^{i2\pi f_0 t} + e^{-i2\pi f_0 t}\right) e^{-i2\pi f t}\, dt \\ &= \frac{1}{2}\int_{-\infty}^{\infty} e^{-i2\pi(f-f_0)t}\, dt + \frac{1}{2}\int_{-\infty}^{\infty} e^{-i2\pi(f+f_0)t}\, dt \\ &= \frac{1}{2}\delta(f-f_0) + \frac{1}{2}\delta(f+f_0) \end{aligned}$$

where we have used the definition of the $\delta(x)$ function :

$$\delta(x) = \int_{-\infty}^{\infty} e^{-2i\pi k x}\, dk$$

Consider now the box function represented in Figure 18 which is defined using the Heaviside step function $H(x)$:

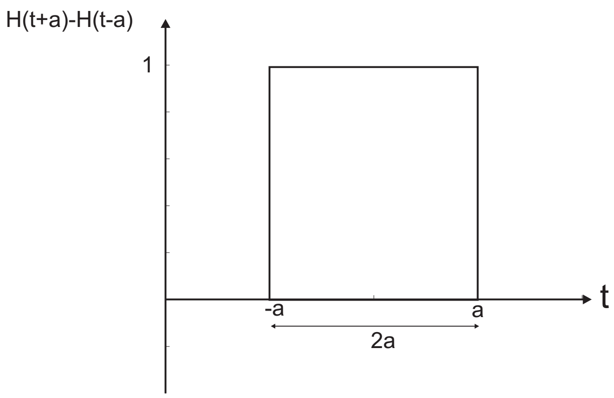

Figure 18: Box function of width $2a$

$$u(t) = H(t+a) - H(t-a) = \begin{cases} 1 & -a < t < 0 \\ 0 & |t| > a \end{cases}$$

The continuous Fourier transform is:

$$\begin{aligned} U(f) &= \int_{-\infty}^{\infty} u(t) e^{-i2\pi f t}\, dt = \int_{-a}^{a} e^{-i2\pi f t}\, dt = \frac{-1}{i2\pi f}\left[e^{-i2\pi f t}\right]_{-a}^{a} \\ &= \frac{(e^{i2\pi f a} - e^{-i2\pi f a})}{2i\pi f} = \frac{2\sin(2\pi f a)}{2\pi f} \end{aligned}$$

Using the definition of the $sinc$ function:

$$sinc(x) = \frac{\sin(\pi x)}{\pi x}$$

we get

$$U(f) = 2asinc(2fa)$$

The $sinc$ function is represented on Figure 19.

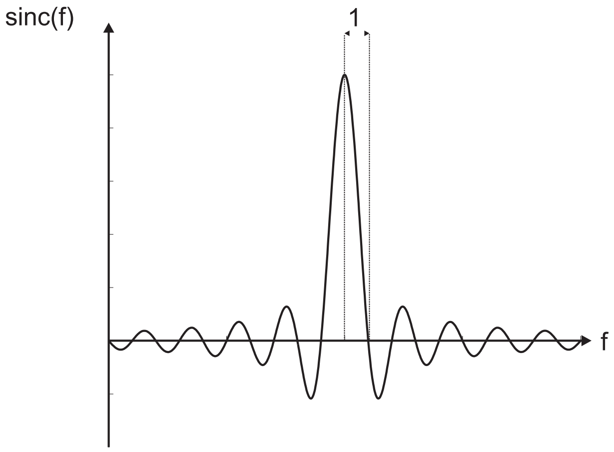

Figure 19: The $sinc$ function

The effect of the width a of the box is illustrated on Figure 20: as the width is divided by a factor of 5, the value of $U(0)$ is divided by 5 ($U(0)$ corresponds to the integral of $u(t)$, here the area of the box), and the first lobe of the $sinc$ function goes to zero for a value of 5 instead of 1. In order to see the effect of the width of the box for functions having the same "energy", we consider now three box functions of different widths, where the surface of the box is equal in Figure 21. The term "energy" is used here to refer to the case where $u(t)$ is an impulse input force of duration Δt and amplitude F, of which the energy is $F\Delta t$. For the same energy, we see that as the width of the box is smaller and smaller (i.e. the impact of the force is of shorter duration), the first lobe of the $sinc$ function is wider and wider so that the continuous Fourier transform tends to a constant in the frequency band considered in the graph. This illustrates the fact that in order to excite a wide band of frequencies with high amplitudes, the duration of the impact force must be as short as possible.

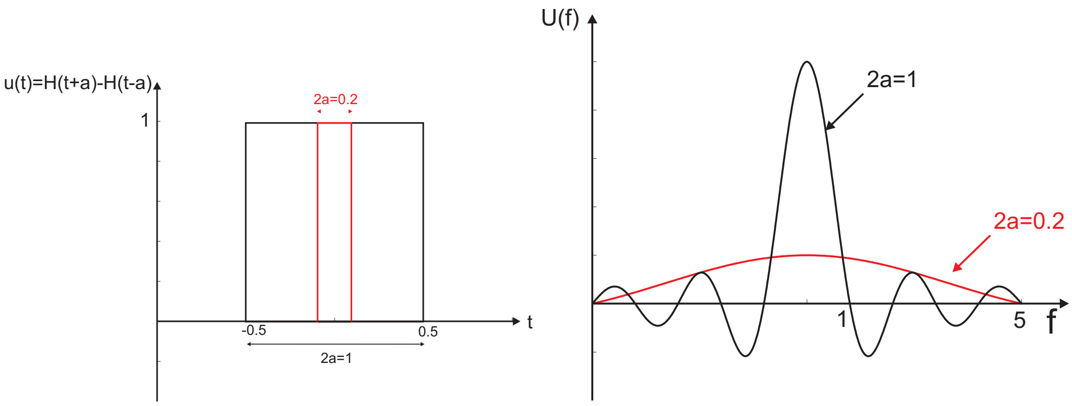

Figure 20: Effect of the width a of the box on the continuous Fourier transform

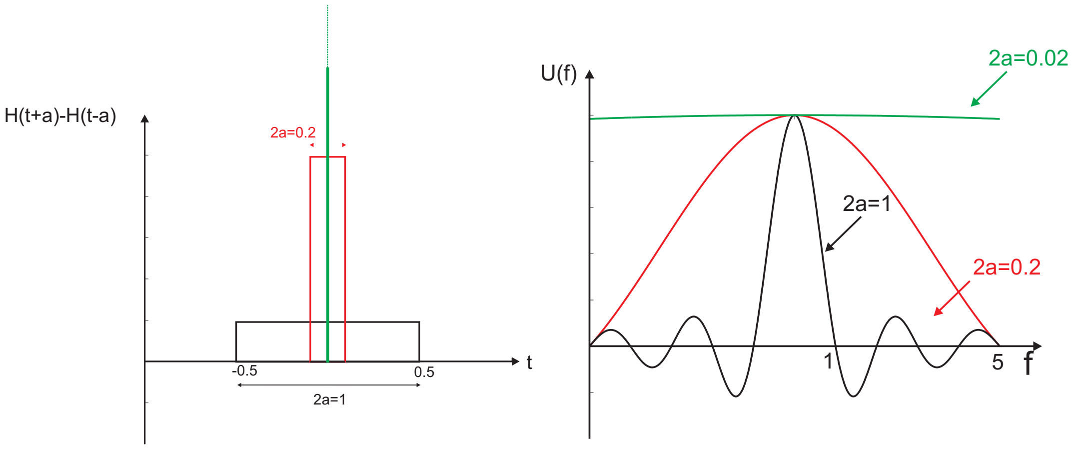

Figure 21: Effect of the width a of the box on the continuous Fourier transform for impulse functions having the same ”energy”

We now consider a triangle function $u(t)$ as represented in Figure 22:

$$u(t) = \begin{cases} a - |t| & -a < t < a \\ 0 & |t| > a \end{cases}$$

and compute its continuous Fourier transform

$$\begin{aligned} U(f) &= \int_{-\infty}^{\infty} u(t) e^{-i2\pi f t}\, dt \\ &= \int_{-a}^{0} (a+t) e^{-i2\pi f t}\, dt + \int_{0}^{a} (a-t) e^{-i2\pi f t}\, dt \end{aligned}$$

The first term of the sum is:

$$\begin{aligned} \int_{-a}^{0} (a+t) e^{-i2\pi f t}\, dt &= \left[\frac{(a+t) e^{-2\pi i f t}}{-2\pi i f} \right]_{-a}^{0} - \int_{-a}^{0} \frac{e^{-2\pi i f t}}{-2 i \pi f}\, dt \\ &= \left[\frac{(a+t) e^{-2\pi i f t}}{-2\pi i f} \right]_{-a}^{0} - \left[\frac{e^{-2 i \pi f t}}{4 i^2 \pi^2 f^2} \right]_{-a}^{0} \end{aligned}$$

and the second term gives

$$\int_{0}^{a} (a-t) e^{-i2\pi f t}\, dt = \left[\frac{(a-t) e^{-2\pi i f t}}{-2\pi i f} \right]_{0}^{a} + \left[\frac{e^{-2 i \pi f t}}{4 i^2 \pi^2 f^2} \right]_{0}^{a}$$

and finally the Fourier transform of the triangle function is:

$$\begin{aligned} U(f) &= \frac{2}{4\pi^2 f^2} - \frac{e^{2i\pi f a}}{4\pi^2 f^2} - \frac{e^{-2i\pi f a}}{4\pi^2 f^2} = \frac{-e^{-2i\pi f a}}{4\pi^2 f^2} \left(1 - 2e^{2i\pi f a} + e^{4 i \pi f a} \right) \\ &= \frac{-e^{-2i\pi f a}}{4\pi^2 f^2} \left(e^{2i\pi f a} - 1 \right)^2 = \frac{-e^{-2i\pi f a}}{4\pi^2 f^2} e^{2i\pi f a} \left(e^{i\pi f a} - e^{-i\pi f a} \right)^2 \\ &= \frac{-1}{4\pi^2 f^2} (2i)^2 \left(\sin^2(\pi f a) \right) = \frac{\sin^2(\pi f a)}{\pi^2 f^2} = a^2 sinc^2(f a) \end{aligned}$$

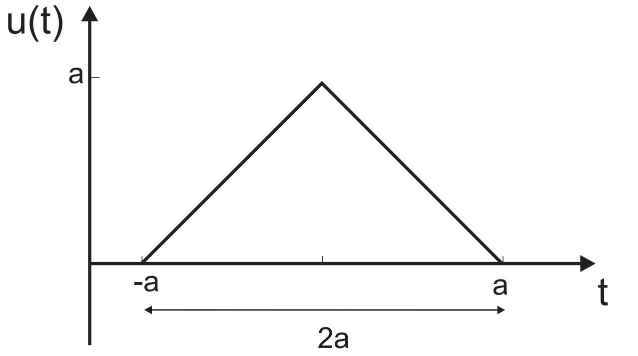

Figure 22: Triangle function of width $2a$

The continuous Fourier transform of a triangle function is compared to the Fourier transform of a box function in Figure 23 for a width of $a = 0.5$. The value of $U(0)$ for the triangle is 1/2 the value for the box function (the area of the triangle is 1/2 the area of the box), and the first lobe goes to zero for a value of 2 for the triangle and 1 for the box function. For the same duration of impact, one can expect therefore that the triangle function excites a wider frequency band than the box function.

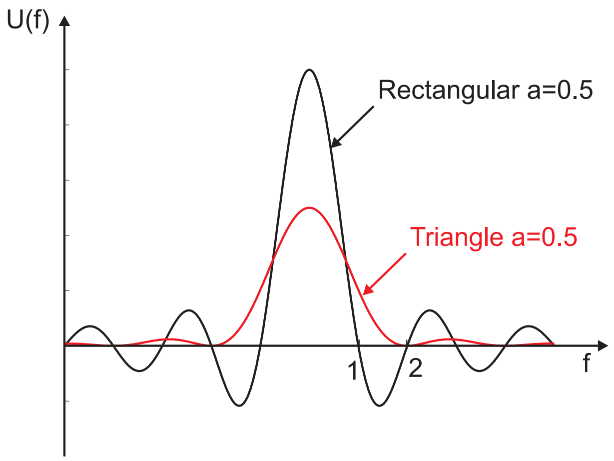

Figure 23: Comparison of $U(f)$ for the triangle and the box function ($a = 0.5$)

2.4 The convolution integral and the theorem of Parseval

2.4.1 The convolution integral

The convolution integral of two time functions $x(t)$ and $h(t)$ yields a new time function $y(t)$ defined as:

$$\begin{aligned} y(t) &= \int_{-\infty}^{\infty} x(\tau)h(t-\tau)d\tau \\ y(t) &= x(t) * h(t) \end{aligned}$$

The following steps help understand how the convolution of two functions yields a new function:

- Take the two functions $x(t)$ and $h(t)$ and replace t by the dummy variable τ
- Mirror the function $h(\tau)$ against the ordinate, this yields $h(-\tau)$
- Shift the function $h(-\tau)$ with a quantity t
- Determine for each value of t the product of $x(\tau)$ with $h(t-\tau)$
- Compute the integral of the product $y(t)$
- Let t vary from $-\infty$ (or a value small enough to make the product zero) to $+\infty$ (or a value of t that is big enough)

Let us illustrate these different steps with an example. We consider the box function $x(t)$ which has a unit value from $t = 0$ to $t = 1$, and the box function $h(t)$ which has a value of 1/2 from $t = 0$ to $t = 1$ (Figure 24).

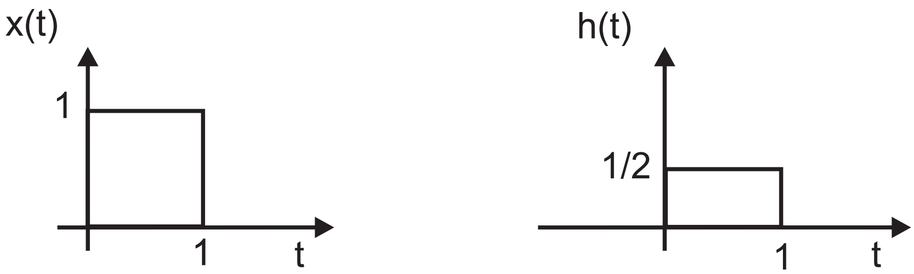

Figure 24: Box functions $x(t)$ and $h(t)$

We replace variable t by τ and mirror the $h(\tau)$ function (Figure 25).

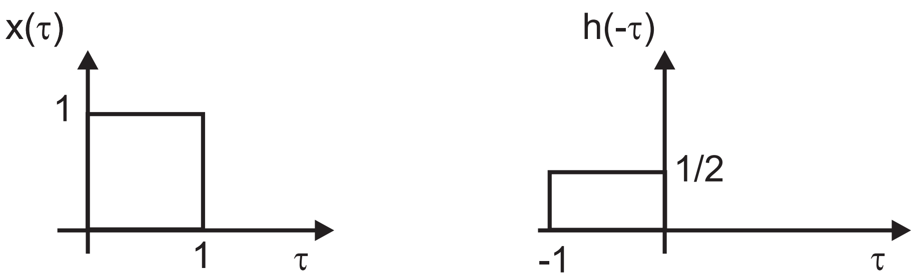

Figure 25: $x(\tau)$ and $h(-\tau)$

We then shift the function $h(-\tau)$ with a quantity t (Figure 26).

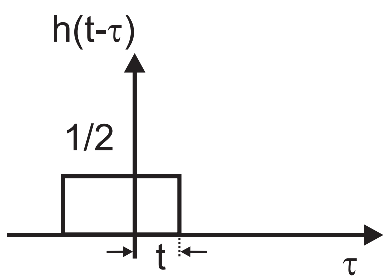

Figure 26: $h(t-\tau)$

For each value of t, we compute the product of $x(\tau)$ with $h(t-\tau)$ and compute the integral. The resulting function is a triangle function as shown in Figure 27.

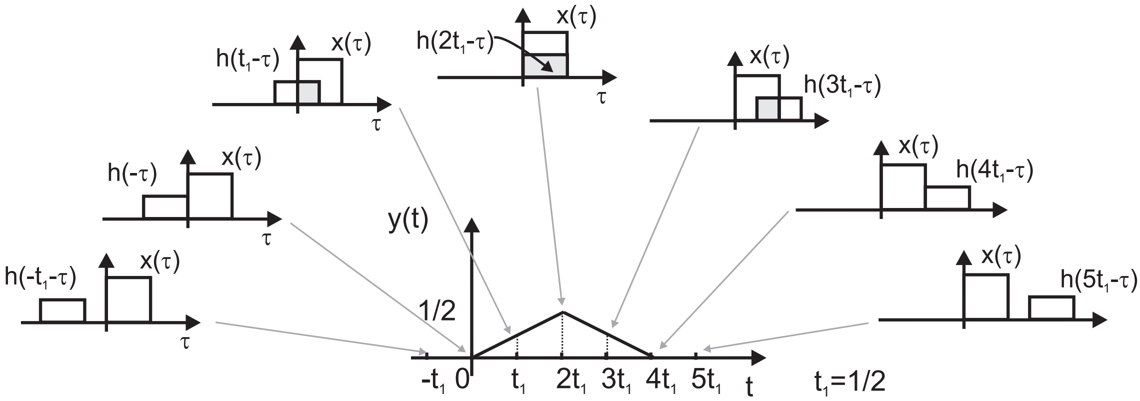

Figure 27: $h(t-\tau)$

Due to the definition of the convolution integral, one can easily show the following property:

$$y(t) = \int_{-\infty}^{\infty} x(\tau)h(t-\tau)d\tau = \int_{-\infty}^{\infty} x(t-\tau)h(\tau)d\tau$$

Another interesting property is given by the convolution theorem which states that :

Convolution in the time domain corresponds with a multiplication in the frequency domain:

$$y(t) = x(t) * h(t)$$
$$Y(f) = X(f).H(f)$$

Proof:

$$\begin{aligned} Y(f) &= \int_{-\infty}^{\infty} y(t)e^{-i2\pi ft}dt = \int_{-\infty}^{\infty} \left[\int_{-\infty}^{\infty} x(t-\tau)h(\tau)d\tau\right] e^{-i2\pi ft}dt \\ &= \int_{-\infty}^{\infty} h(\tau)\left[\int_{-\infty}^{\infty} x(t-\tau)e^{-i2\pi ft}dt\right] d\tau \end{aligned}$$

Make the change of variables : $u = t - \tau \Rightarrow du = dt$

$$\begin{aligned} Y(f) &= \int_{-\infty}^{\infty} h(\tau)\left[\int_{-\infty}^{\infty} x(u)e^{-i2\pi f(u+\tau)}du\right] d\tau \\ &= \int_{-\infty}^{\infty} h(\tau)e^{-i2\pi f\tau}d\tau \left[\int_{-\infty}^{\infty} x(u)e^{-i2\pi fu}du\right] \\ &= H(f).X(f) \end{aligned}$$

In the same way, one can prove that a convolution in the frequency domain corresponds to a multiplication in the time domain:

$$\begin{aligned} Y(f) &= X(f) * H(f) \\ y(t) &= x(t).h(t) \end{aligned}$$

2.4.2 The theorem of Parseval

The energy of a signal computed in the time domain is equal to the energy computed in the frequency domain :

$$\int_{-\infty}^{\infty} h^2(t)dt = \int_{-\infty}^{\infty} |H(f)|^2 df$$

Proof:

$$\begin{aligned}
\int_{-\infty}^{\infty} h^2(t)dt &= \int_{-\infty}^{\infty} \left[\int_{-\infty}^{\infty} H(f)e^{i2\pi ft}df\right] \left[\int_{-\infty}^{\infty} H(f')e^{i2\pi f't}df'\right] dt \\
&= \int_{-\infty}^{\infty} \int_{-\infty}^{\infty} H(f).H(f') \int_{-\infty}^{\infty} e^{i2\pi(f+f')t}dtdf'df \\
&= \int_{-\infty}^{\infty} \int_{-\infty}^{\infty} H(f).H(f') \int_{-\infty}^{\infty} 1\, e^{i2\pi(f+2f')t}e^{-i2\pi(f')t}dtdf'df
\end{aligned}$$

The term

$$\int_{-\infty}^{\infty} 1\, e^{i2\pi(f+2f')t}e^{-i2\pi(f')t}dt$$

is the Fourier transform of

$$1\, e^{i2\pi(f+2f')t} = f(t)\, e^{i2\pi(f+2f')t}$$

if we take $f(t)$=1. Knowing that the Fourier transform of $f(t)e^{2i\pi f_0 t}$ is equal to $F(f - f0)$ (see Table 2), and that the Fourier transform of 1 is $\delta(f)$ (Table 1), we have

$$\int_{-\infty}^{\infty} 1\, e^{i2\pi(f+2f')t}e^{-i2\pi(f')t}dt = \delta(f' - (f + 2f')) = \delta(-f - f')$$

and

$$\int_{-\infty}^{\infty} h^2(t)dt = \int_{-\infty}^{\infty}\int_{-\infty}^{\infty} H(f).H(f')\delta(-f - f')df'df = \int_{-\infty}^{\infty} H(f).H(-f)df$$

In addition, we know that h(t) is real so that we have (Table 2)

$$H(-f) = H^*(f)$$

and finally

$$= \int_{-\infty}^{\infty} H(f).H^*(f)df = \int_{-\infty}^{\infty} |H(f)|^2 df$$

The theorem of Parseval can also be written using the variable $\omega = 2\pi f$:

$$\int_{-\infty}^{\infty} h^2(t)dt = \int_{-\infty}^{\infty} |H(f)|^2 df = \frac{1}{2\pi}\int_{-\infty}^{\infty} |H(\omega)|^2 d\omega$$

3 Single degree of freedom system

The study of the single degree of freedom (dof) system is the foundation of structural dynamics. Such a system is represented by a mass attached to the ground with a spring. One may argue that such a system is not of practical importance, as buildings are not a large mass attached to the ground by a spring. While this is true, we will see in the next chapters that the theory of the single degree of freedom system can be used to study the dynamic behavior of all structures, once the concept of mode shapes is understood (Section 5.1). There are also cases for which the structure can be simplified to the extent that it corresponds to a single dof system. This is the subject of the next section.

3.1 One degree of freedom systems in real life

The simplification of the model of a real structure to a one dof system requires to assume the existence of a rigid body, whose motion due to an excitation source is in a single direction. This body needs to be attached to a motionless reference through a flexible element whose dynamical behavior can be neglected and acts like a spring. In practice, all the bodies, when subjected to a force, tend to deform, but one can consider that when this deformation is small, the body can be considered as rigid. On the contrary, if the body is deformed by the application of a force, it is considered as flexible (Figure 28). Note that the flexibility of the body will generally depend on the direction of the applied force.

Figure 28: Rigid body / flexible body

This classification is however not as clear as it may appear. When the force applied to the body is dynamic, the deformation of the body depends also on the frequency at which it is excited. In order to illustrate this, let us consider the example of a one story building. In the first case, the building is excited by a ground motion due to an earthquake. The excitation frequency of the earthquake is rather low (typically below 20 Hz), and the floor is quite rigid when excited laterally. On the other hand, the columns, when excited at their tip, are very flexible. In this case, the floor can be regarded as a rigid body, and the columns act as a spring element attaching the large mass of the floor to a fixed reference (the ground, Figure 29)

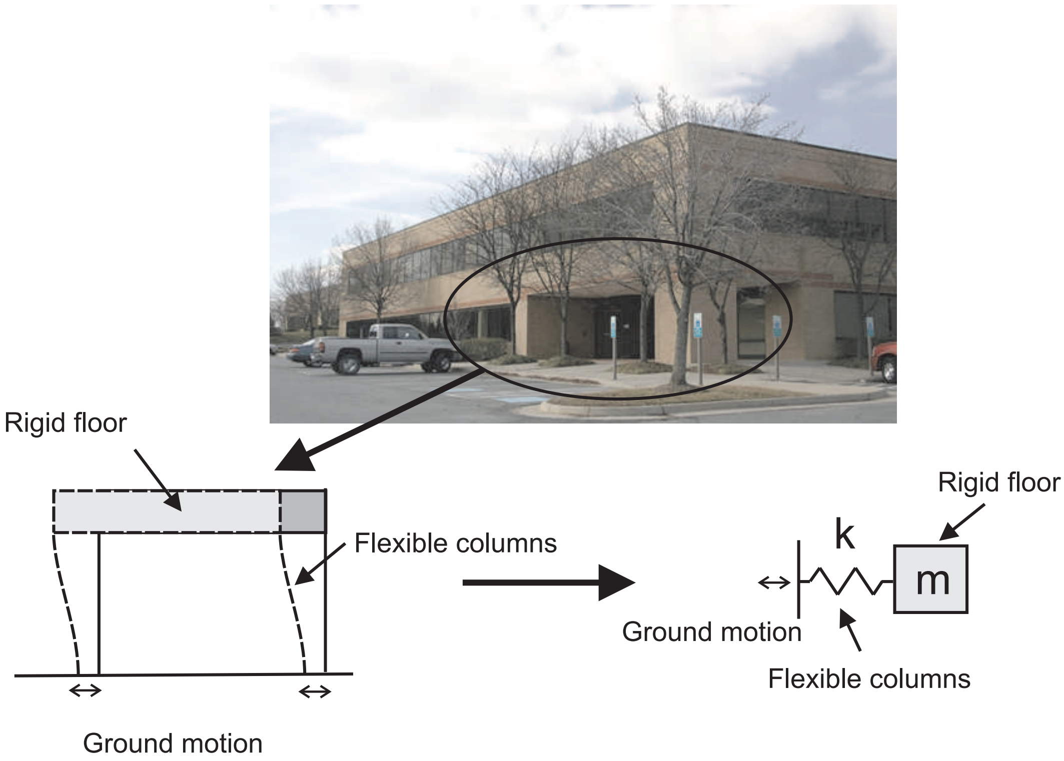

Figure 29: One story Building excited by an earthquake

In the second case, if the building is excited by a rotating machine (such as a power generator) which is in the middle of the floor (Figure 30) , the frequency of excitation is much higher and can reach several hundreds of Hertz. The excitation of the rotating machine acts both in the vertical and in the horizontal direction. The horizontal direction corresponds to the case previously studied. For the vertical direction however, the columns have a much higher stiffness in that direction, and can be considered as rigid supports of the floor which is now excited in bending, a direction in which it is much more flexible. The system can therefore be modeled by a beam on its supports which is excited in the middle by a vertical force. In such a case, it is not straightforward to simplify the system to a one dof system (we will see however in section 6 how this can be done).

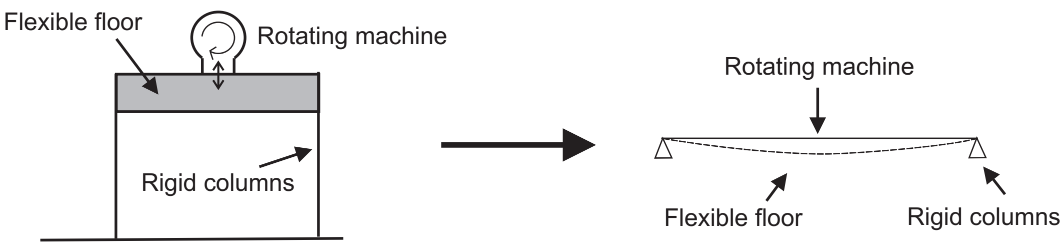

Figure 30: One story building excited by a rotating machine

The first example shows how a real-life system can, in some cases, be simplified to a one dof system. In the second example, such a simplification is not as straightforward. Note also that elements which are considered flexible in the first case, are considered rigid in the second case, and vice versa, the only difference being the direction of the excitation.

Figure 31 represents a series of systems which can be modeled with an equivalent one dof system.

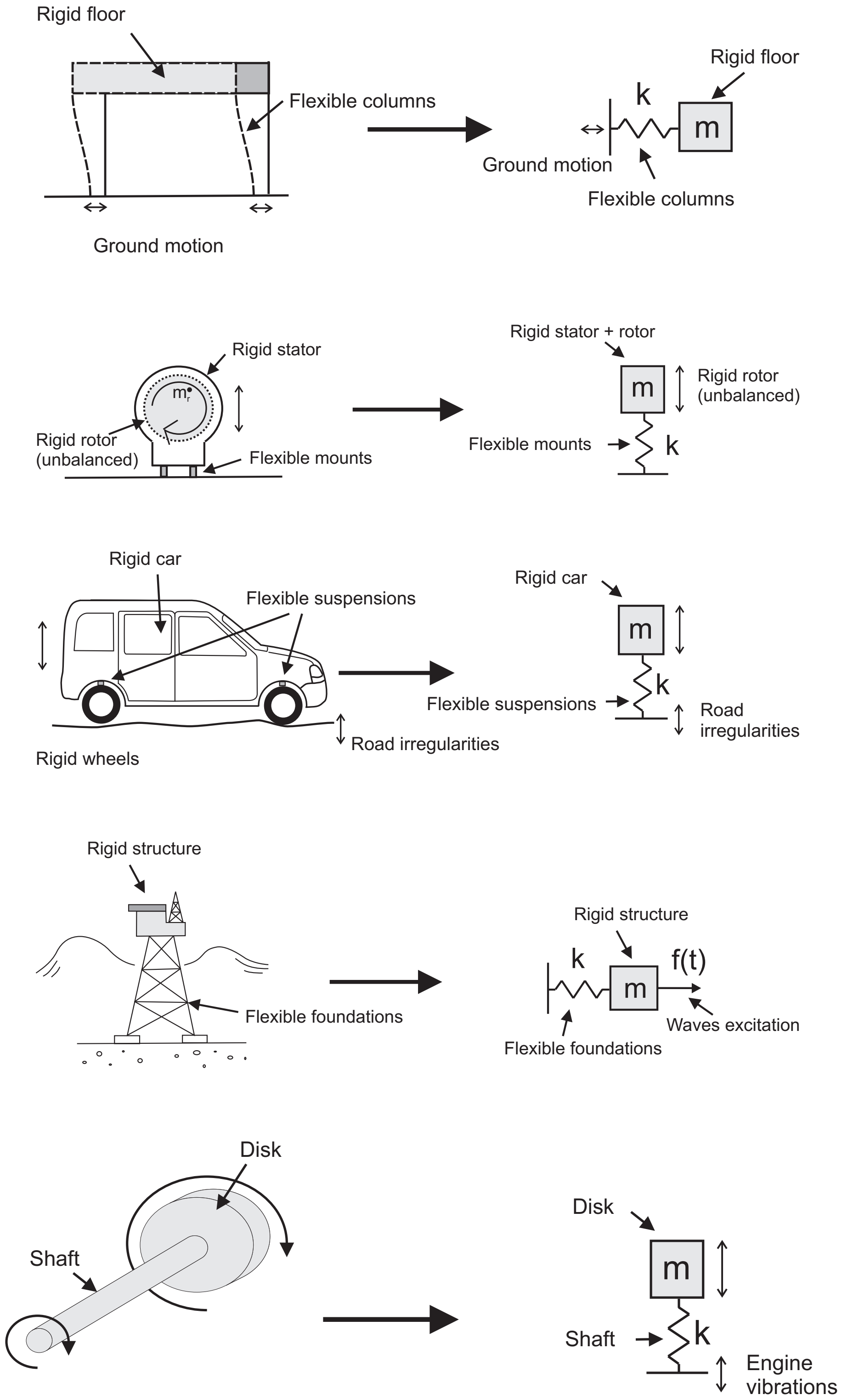

Figure 31: Examples of equivalent one dof systems

3.2 Response of a single degree of freedom system without damping

Let us consider a mass-spring system without damping, represented in Figure 32. The first law of Newton applied to this system gives:

$$m\ddot{x} = \sum F_x \tag{8}$$

where $\sum F_x$ is the sum of forces action on mass m in direction x:

- Spring force: $-kx$, where k is the stiffness of the spring. Note that the position $x = 0$ corresponds to the static equilibrium of the hanging mass attached to the spring. As the equation of motion is written with respect to this reference position, the force of gravity must not be considered in the equilibrium of forces: it is in equilibrium with the spring force $k\Delta l$ in the static equilibrium position (Fiugre 33)
- External force f acting on the mass. It is the force which causes the mass to move, it is called the ”excitation force”.

Putting all the terms dependent on x on the left hand side, we get the equation of motion of the 1 dof system:

$$m\ddot{x} + kx = f \tag{9}$$

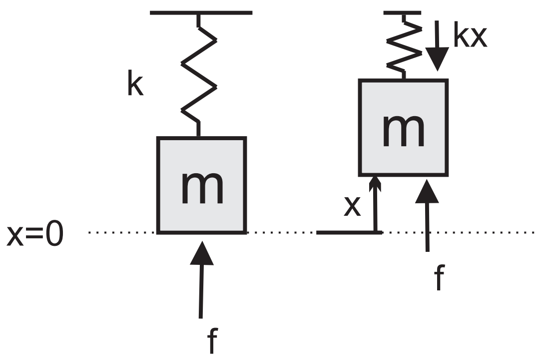

Figure 32: Forces acting on a one dof mass-spring system

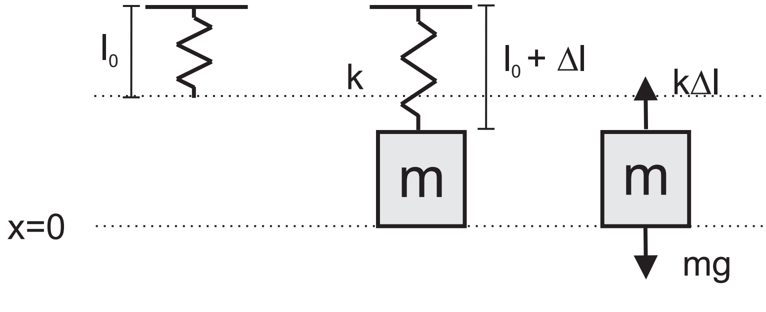

Figure 33: Definition of the reference position $x = 0$ of the mass for the mass-spring system

3.2.1 General solution of the equation of motion

The characteristics equation of (9) is obtained assuming $x = A\,e^{rt}$ which leads to:

$$mr^2 + k = 0 \tag{10}$$

The roots of this equation are purely imaginary:

$$r = \pm i\sqrt{k/m}$$

The general solution can therefore be written in the form of :

$$x = A\cos\omega_n t + B\sin\omega_n t$$

where

$$\omega_n = \sqrt{k/m}$$

is the natural angular frequency. In the absence of external excitation force, the motion is oscillatory with a frequency $f = \frac{1}{2\pi}\sqrt{k/m}$ which is defined by the values of k and m.The motion is initialized by imposing initial conditions on the displacement x_0 and on the velocity $\dot{x}_0$. In this case, the motion is given by:

$$x(t) = x_0\cos\omega_n t + \frac{\dot{x_0}}{\omega_n}\sin\omega_n t$$

Figure 34 illustrates the vibration of a one dof system to which an initial displacement x_0 with a zero initial velocity $\dot{x_0}$ are imposed.

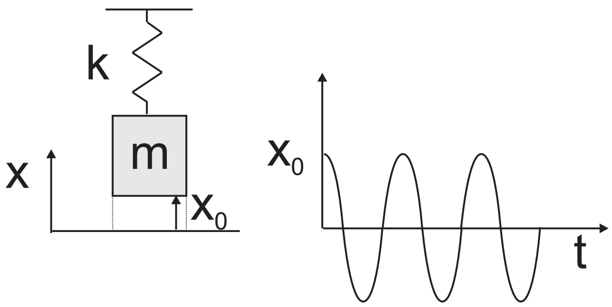

Figure 34: Free vibration of a 1 dof system to which an initial displacement x_0 is imposed

The solution can also be written in the general form of a cosine with amplitude a and a phase ϕ:

$$x(t) = a\cos(\omega_n t + \phi)$$

where we have:

$$x_0 = a\cos\phi$$
$$\dot{x_0}/\omega_n = a\sin\phi$$

which leads to:

$$\tan\phi = \frac{\dot{x_0}}{\omega_n x_0}$$

The phase ϕ is a function of both x_0 and $\dot{x_0}$. It is equal to zero when $\dot{x_0} = 0$ and equal to $90°$ when $x_0 = 0$.

3.2.2 Particular solution

Consider the continuous inverse Fourier transform of the excitation force $f(t)$:

$$f(t) = \frac{1}{2\pi}\int_{-\infty}^{\infty} F(\omega)e^{-i\omega t}d\omega$$

and isolate a single component at frequency ω:

$$F(\omega)e^{-i\omega t} = F(\omega)\cos(\omega t) + iF(\omega)\sin(\omega t)$$

Let us first consider an excitation of the form $F(\omega)\cos(\omega t)$. The equilibrium equation is written:

$$m\ddot{x} + kx = F\cos\omega t \tag{11}$$

and the particular solution can be written in the general form

$$x(t) = A\cos\omega t + B\sin\omega t = a\cos(\omega t + \phi)$$

If we now consider an excitation of the form $F(\omega)\sin(\omega t)$, the form of the general solution is

$$x(t) = a\sin(\omega t + \phi)$$

Therefore the general solution to an excitation $F(\omega)e^{i\omega t}$ is

$$x(t) = a\cos(\omega t + \phi) + i\ \sin(\omega t + \phi) = ae^{i(\omega t+\phi)} = Xe^{i\omega t}$$

where $X = ae^{i\phi}$ is a complex number carrying the information of both the phase and the amplitude of the response at frequency ω (Figure 35)

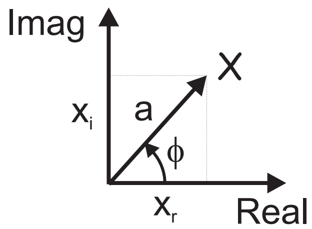

Figure 35: Representation of the complex amplitude X in the complex plane

Replacing $x(t) = X\,e^{i\omega t}$ and $f(t) = F\,e^{i\omega t}$ in (9), we get

$$\left(k - \omega^2 m\right)Xe^{i\omega t} = Fe^{i\omega t}$$

which can be solved for X:

$$X = \frac{F}{k - \omega^2 m}$$

Let us define X_0, the amplitude of the static displacement of the mass ($\omega = 0$) :

$$X_0 = F/k$$

The solution can then be expressed as:

$$\frac{X}{X_0} = \frac{1}{1 - \omega^2/\omega_n^2} \tag{12}$$

where we have used the fact that $\omega_n = \sqrt{k/m}$ is the natural angular frequency of the system. For an undamped system, the value of X/X_0 is always real. It is positive when $\omega < \omega_n$. This means that when the excitation frequency is lower than the natural angular frequency of the system, the displacement X is in phase with the excitation force ($\phi = 0°$). When the excitation frequency is equal to the natural angular frequency of the system, the amplitude tends to infinity. In practice, the displacement can never reach infinity as there is always a small amount of dissipation which is not considered here. When the excitation frequency is higher than the natural angular frequency of the system, the displacement is in opposition of phase with respect to the excitation ($\phi = 180°$): the mass will have an upward motion when the force applied is downwards. The value of X/X_0 as a function of the excitation frequency is plotted in Figure 36. Such a plot is called a Bode diagram.

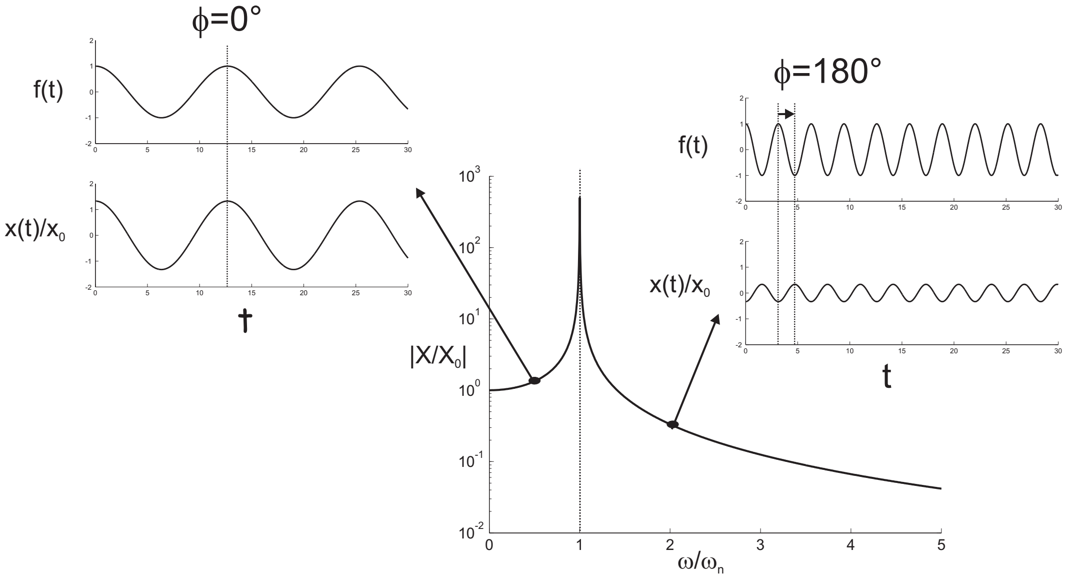

Figure 36: Amplitude of X/X_0 as a function of the excitation frequency (Bode diagram)

Note that in structural dynamics, it is usual to represent the Bode diagram containing both the amplitude and the phase with a linear frequency axis and a logarithmic scale for the amplitudes, while in the domain of control and automatics, a logarithmic scale is often used for the frequencies, and a scale in decibels (dB) (also logarithmic) is used for the amplitudes. When using a log-log scale, the Bode diagram of a second order system such as a mass-spring system has a slope of -40 dB/decade after resonance (Figure 37)

If one wishes to compute the response $x(t)$ in the time domain, it can be done using the inverse continuous Fourier transform given by:

$$x(t) = \frac{1}{2\pi} \int_{-\infty}^{\infty} X(\omega) e^{-i\omega t} d\omega$$

where

$$X(\omega) = \frac{F(\omega)}{k - \omega^2 m}$$

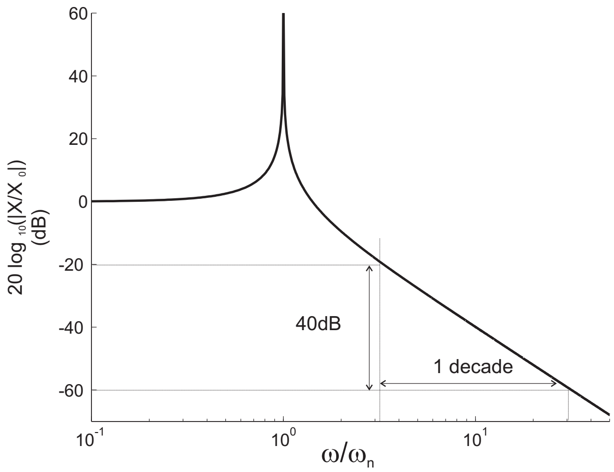

Figure 37: Bode diagram of a mass-spring system using a logarithmic scale for both the frequencies and the amplitudes

The Bode diagram is a very useful tool. It allows to clearly point out the resonance of dynamic systems. In the case of a 1 dof system, one sees clearly that the frequencies close to the resonant frequency are strongly amplified while the frequencies away from the resonant frequency are diminished. The 1 dof system can therefore be seen as a mechanical filter.

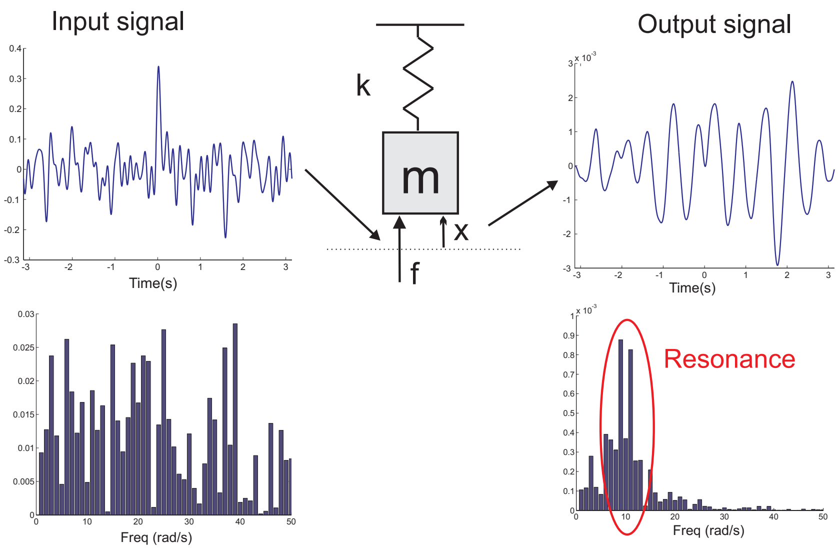

Figure 38: Illustration of the resonance : the one dof system acts as a mechanical filter which enhances the frequency components close to the natural frequency of the system

This is illustrated in Figure 38 where we consider a periodic excitation force $f(t)$ whose discrete Fourier transform is computed, showing the relative amplitudes of the different components. The discrete Fourier transform is then applied to the output $x(t)$ of the system. One sees clearly that the relative amplitudes of the different components have changed: the amplitudes close to resonance are much higher than the other components. Resonance can be used to induce very large displacements in a system. The entertaining exercise of breaking a wine glass with the voice is one example: if one emits a sounds whose frequency is close to one of the natural frequencies of the glass, the effect can be strong enough to break it. The reader can see a demonstration in the following videos:

http://www.youtube.com/watch?v=10lWpHyN0Ok
http://www.youtube.com/watch?v=JiM6AtNLXX4

3.3 Response of a single degree of freedom system with damping

Equation (9) represents a conservative system in which there is an exchange between the kinetic and potential energy without dissipation of energy. In reality, there is always a certain amount of energy dissipated somewhere in the system, which is responsible for a certain amount of damping. For mass-spring systems, the most common form of damping adopted is the viscous damping, represented by a dashpot element. In the equation of motion, an additional force due to the dashpot is added in the following form:

$$F_b = -b\dot{x}$$

The equation of motion is given by (Figure 39) :

$$m\ddot{x} + b\dot{x} + kx = f \tag{13}$$

In order to simplify the notations, equation (13) can be rewritten by dividing it by m and introducing the damping coefficient $\xi = b/(2\sqrt{km})$:

$$\ddot{x} + 2\xi\omega_n\dot{x} + \omega_n^2 x = f/m \tag{14}$$

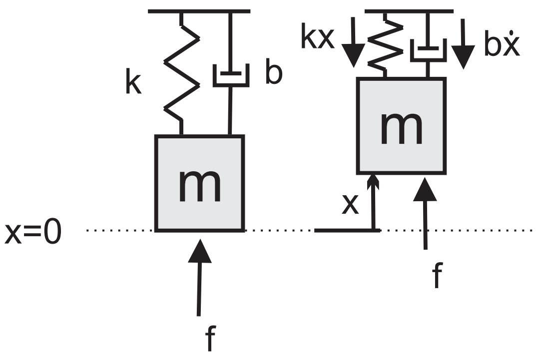

Figure 39: Forces acting on a one dof mass-spring-dashpot system

3.3.1 General solution of the equation of motion

The characteristics equation is given by:

$$r^2 + 2\xi\omega_n r + \omega_n^2 = 0$$

In most structures, the damping coefficient ξ is smaller than one. In this case, the roots of the characteristics equations are given by:

$$r = -\xi\omega_n \pm i\omega_n\sqrt{1-\xi^2}$$

or

$$r = -\xi\omega_n \pm i\omega_d$$

with

$$w_d = \omega_n \sqrt{1 - \xi^2}$$

The general solution can be written in the form of:

$$x(t) = e^{-\xi \omega_n t} \left(A \cos \omega_d t + B \sin \omega_d t \right)$$

In the absence of external forces, the system will vibrate due to initial conditions on the displacement x_0 and the velocity $\dot{x_0}$. The free vibration is given by:

$$x(t) = e^{-\xi \omega_n t} \left(x_0 \cos \omega_d t + \frac{\dot{x_0} + \omega_n \xi x_0}{\omega_d} \sin \omega_d t \right) \tag{15}$$

The system will oscillate at a frequency ω_d which is different from the natural frequency ω_n, and the motion will decrease with time due to the exponential term $e^{-\xi \omega_n t}$ which is a function of the damping coefficient ξ and the natural frequency of the system ω_n. The free response is represented for different values of ξ in Figure 40.

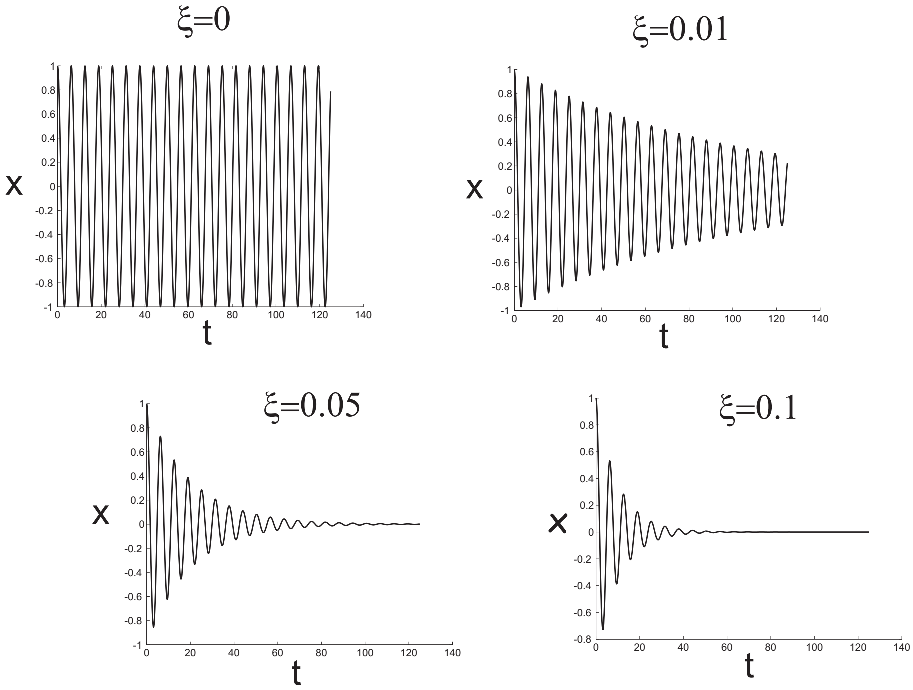

Figure 40: Free vibration of a one dof mass-spring-dashpot system due to an initial unit displacement $x_0 = 1$ as a function of the damping coefficient ξ

When $\xi = 0$, the mass oscillates with a constant amplitude. As the damping increases, the amplitude decreases faster with time. For a value of $\xi = 0.01$, the amplitude is divided by 2 after about 10 oscillations. On Figure 41, we represent the number n of oscillations needed to decrease the amplitude by one half as a function of ξ, in a log-log scale. The figure shows clearly that as the damping coefficient is divided by 10, 10 times more oscillations are needed to reduce the amplitude by one half. The time needed for the motion of the mass to be reduced by one half is a function of ξ and the natural frequency ω_n: the higher ω_n, the shorter this time will be. For a system with a low natural frequency and a low level of damping, a very long time will be needed to attenuate the vibration.

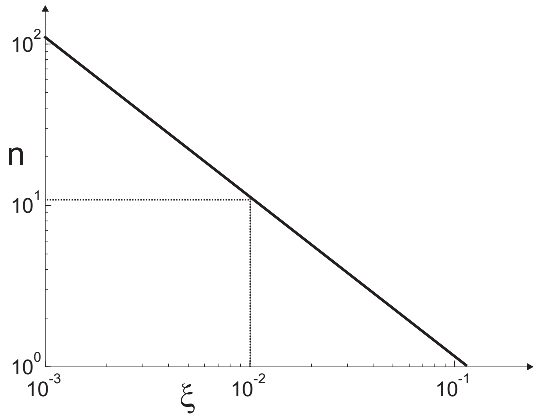

Figure 41: Number n of oscillations needed to reduce the vibration amplitude by one half as a function of the damping coefficient ξ

When the damping coefficient is very high ($\xi > 1$), the solution of the equation of motion is:

$$x(t) = e^{-\xi\omega_n t}\left(x_0 \cosh \mu t + \frac{\dot{x_0} + \omega_n \xi x_0}{\mu} \sinh \mu t\right)$$

with

$$\mu = \omega_n \sqrt{\xi^2 - 1}$$

This solution is not oscillatory. The higher the damping, the slower the response decreases because of the $\cosh$ and $\sinh$ terms which grow with time. For a limit value of $\xi = \infty$, the mass is blocked by the damper in the initial position ($x(t) = x_0$, Figure 42). The value $\xi = 1$ represents the limit between the oscillatory motion and the non-oscillatory motion. This value is called the critical damping. The roots of the characteristics equation are double and given by:

$$r = -\omega_n$$

The solution is given by:

$$x(t) = e^{-\omega_n t}\left(\left(\dot{x_0} + \omega_n x_0\right) t + x_0\right)$$

It is represented on Figure 42. Note that the critical damping corresponds to the value of damping for which the motion of the mass is the fastest to reach a zero value.

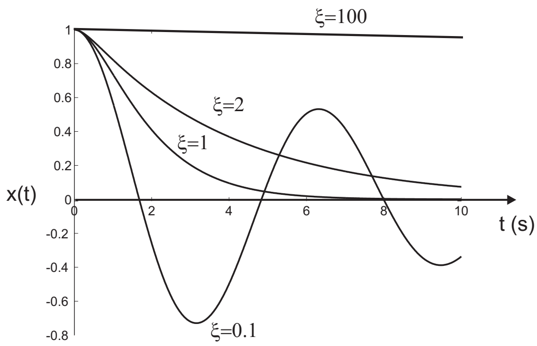

Figure 42: Response of a one dof mass-spring-dashpot system to an initial unit displacement ($x_0 = 1$) for high values of damping coefficients ξ

3.3.2 The impulse response

An impulse excitation is defined as a force of amplitude F applied during a short time Δt. The energy of the impulse is given by $F\Delta t$ (Figure 43). Let us consider the equation of motion (13) with initial conditions $x_0 = 0$ and $\dot{x_0} = 0$ and integrate it from $t = 0$ to $t = \Delta t$:

$$m\dot{x_0}|_{\Delta t} = F\Delta t - \int_0^{\Delta t} kxdt - \int_0^{\Delta t} b\dot{x}dt$$

As the initial conditions are $x_0 = 0$ and $\dot{x_0} = 0$ and the time interval Δt is very short, the last two terms tend to zero, we get:

$$\dot{x_0}|_{\Delta t} = \frac{F\Delta t}{m}$$

which shows that in order to compute the response of a system to an impulse $F\Delta t$, one has to compute the response to an imposed velocity $F\Delta t/m$ at time $t = \Delta t$. The impulse response of the system is defined as the response to a unit value of $F\Delta t$. Using (15), the impulse response is given by:

$$x(t) = \frac{e^{-\xi\omega_n t}}{m\omega_d}\sin(\omega_d t) \tag{16}$$

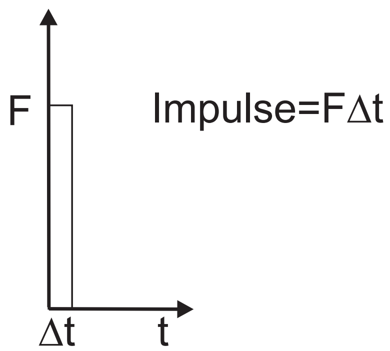

Figure 43: Definition of an impulse excitation

3.3.3 Particular solution of the equation of motion

In a similar way to what was done for the undamped system, we assume $f(t) = Fe^{i\omega t}$ and $x(t) = Xe^{i\omega t}$ and replace in (14) to get:

$$(\omega_n^2 + 2i\xi\omega\omega_n - \omega^2)X = F/m$$

The complex amplitude X is given by:

$$X = \frac{F}{m}\left(\frac{1}{\omega_n^2 + 2i\xi\omega\omega_n - \omega^2}\right) = \frac{F}{k}\left(\frac{1}{1 - \frac{\omega^2}{\omega_n^2} + 2i\xi\frac{\omega}{\omega_n}}\right) = X_0\left(\frac{1}{1 - \frac{\omega^2}{\omega_n^2} + 2i\xi\frac{\omega}{\omega_n}}\right)$$

The real and imaginary parts of X are given by:

$$X_r = X_0 \frac{1 - \frac{\omega^2}{\omega_n^2}}{\left(1 - \frac{\omega^2}{\omega_n^2}\right)^2 + \left(2\xi \frac{\omega}{\omega_n}\right)^2}$$

$$X_i = X_0 \frac{-2\xi \frac{\omega}{\omega_n}}{\left(1 - \frac{\omega^2}{\omega_n^2}\right)^2 + \left(2\xi \frac{\omega}{\omega_n}\right)^2}$$

and the amplitude and phase of X/X_0 are given by:

$$|X/X_0| = \sqrt{\frac{1}{\left(1 - \frac{\omega^2}{\omega_n^2}\right)^2 + \left(2\xi \frac{\omega}{\omega_n}\right)^2}}$$

$$\tan\phi = \frac{-2\xi \frac{\omega}{\omega_n}}{1 - \frac{\omega^2}{\omega_n^2}}$$

The Bode diagram (amplitude and phase) of X/X_0 is represented in Figure 44 for different values of ξ.

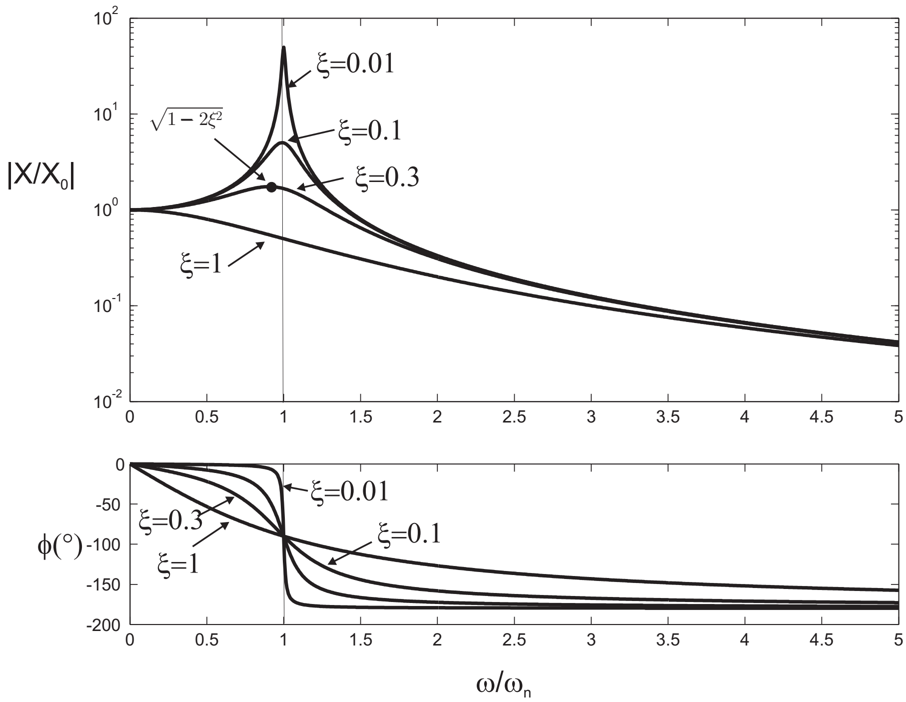

Figure 44: Bode diagram for the one dof mass-spring-dashpot system. Influence of the damping coefficient ξ

The influence of ξ is as follows: as ξ is increased, the amplitude of the peak is reduced and the phase transition from $0°$ to $180°$ around the resonance is smoother. At the resonant frequency, the phase is always equal to $90°$. The frequency at which the amplitude is maximum is slightly different from ω_n and ω_d:

$$\omega/\omega_n = \sqrt{1 - 2\xi^2}$$

The maximum amplitude is given by

$$|X/X_0| = \frac{1}{2\xi\sqrt{1-\xi^2}}$$

For small values of ξ, we have however:

$$\omega/\omega_n = 1$$
$$|X/X_0| = \frac{1}{2\xi}$$

Up to now we have represented the displacement $x(t) = Xe^{i\omega t}$ in the Bode diagram. The velocity $v(t) = \frac{d(x(t))}{dt} = i\omega X$, and the acceleration $a(t) = \frac{d^2(x(t))}{dt} = -\omega^2 X$ are represented and compared to the displacement in Figure 45. Note the change of slope before and after the resonance frequency due to the multiplication by a factor $i\omega$ and $-\omega^2$ respectively.

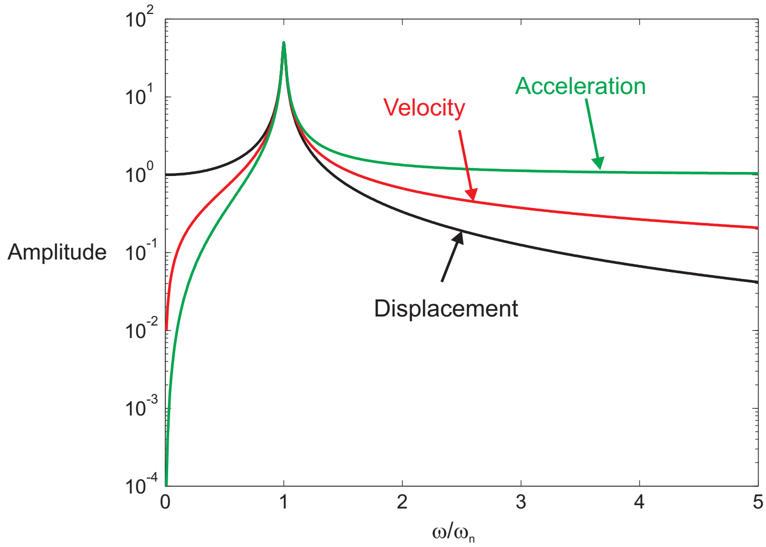

Figure 45: Bode diagram for the one dof mass-spring-dashpot system: displacement X, velocity $j\omega X$ and acceleration $-\omega^2 X$

An alternative way to represent the response X/X_0 as a function of the frequency is the Nyquist diagram in which the real and imaginary parts are plotted in the complex plane (Figure 46). For a 1 dof system, the Nyquist plot is close to a circle with a diameter = $1/2\xi$. The Nyquist plot makes a zoom around the natural frequency of the system: frequencies close to the natural frequency spread along the circle in the Nyquist plot.

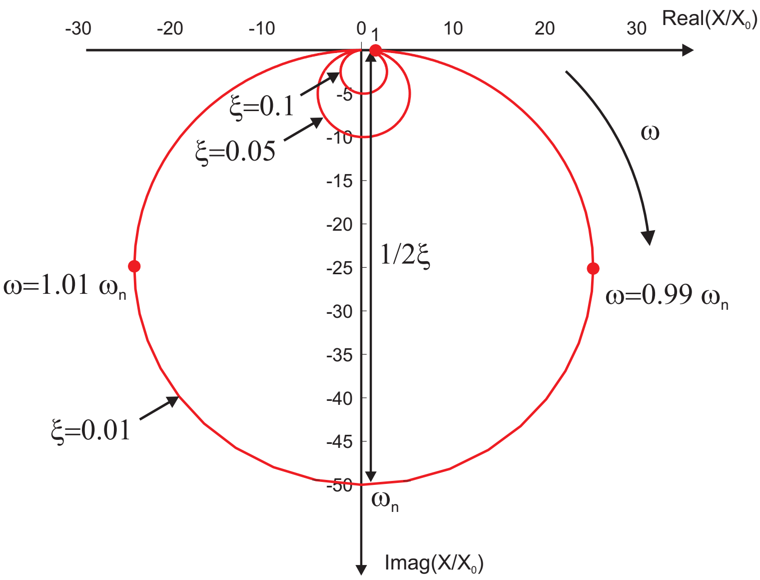

Figure 46: Nyquist plot for the one dof mass-spring-dashpot system for different values of damping ξ

3.3.4 Duhamel's integral

Consider a 1 dof system excited by an arbitrary force $f(t)$ (Figure 47). $f(t)$ is decomposed into a series of short impulses at time τ. The contribution of one impulse $f(\tau)d\tau$ to the response of the system is given by :

$$f(\tau)d\tau h(t-\tau)$$

where $h(t)$ is the impulse response. The total contribution is therefore:

$$x(t) = \int_0^t f(\tau)h(t-\tau)d\tau$$

knowing that $f(t) = 0$ and $h(t) = 0$ for $t > 0$ we have:

$$x(t) = \int_{-\infty}^{\infty} f(\tau)h(t-\tau)d\tau = f(t) * h(t)$$

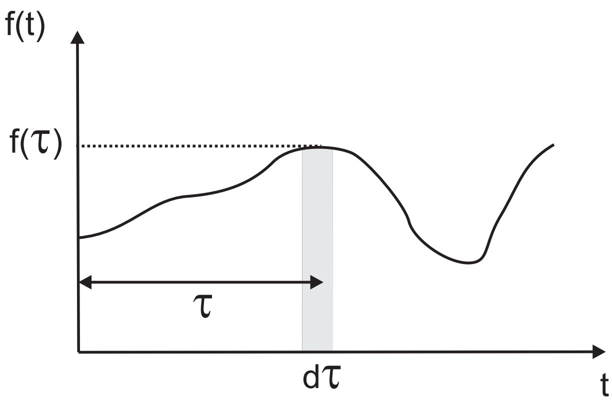

Figure 47: Decomposition of $f(t)$ in a series of short pulses at times τ

In the particular case where $f(t) = Fe^{i\omega t}$, we have:

$$\begin{aligned} x(t) = Xe^{i\omega t} &= \int_{-\infty}^{\infty} Fe^{i\omega t} h(t-\tau) d\tau = \int_{-\infty}^{\infty} Fe^{i\omega(t-\tau)} h(\tau) d\tau \\ &= Fe^{i\omega t} \int_{-\infty}^{\infty} h(\tau) e^{-i\omega\tau} d\tau = Fe^{i\omega t} H(\omega) \end{aligned}$$

which can be rewritten:

$$H(\omega) = \frac{X}{F}$$

showing that the continuous Fourier transform of the impulse response $h(t)$ is the ratio X/F which is the transfer function of the one dof system.

3.3.5 Base excitation

In some cases, the excitation is not in the form of an applied force $f(t)$. An example is the excitation of an earthquake which imposes a displacement of the base of the buildings. Let us consider the mass-spring-dashpot system to which a base displacement $x_0(t)$ is imposed (Figure 48).

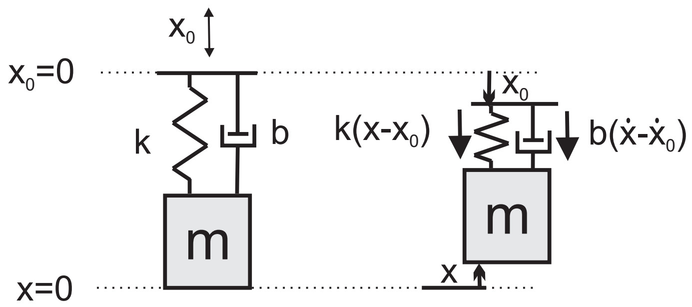

Figure 48: Forces acting on a 1 dof system excited by the base

The equilibrium of forces is written

$$m\ddot{x} = -k(x - x_0) + b(\dot{x} - \dot{x_0})$$

the equation can be rewritten as a function of the relative displacement of mass m with respect to the base $x_r = x - x_0$:

$$m\ddot{x_r} + b\dot{x_r} + kx_r = -m\ddot{x}_0 \tag{17}$$

This equation corresponds to the equation of motion of a one dof mass-spring-system where the displacement is the relative displacement x_r and the excitation $f(t) = -m\ddot{x}_0$ is a function of the imposed acceleration at the base and the mass m. The response can therefore be computed using the tools described in the previous sections.

3.4 Reduction to a one dof system

With some assumptions, the systems represented in Figure 31 can be reduced to a single dof mass-spring system. If one wishes to take into account the dissipation, a dashpot must be added. There are thus three parameters which need to be known when representing a real structure with an equivalent single dof mass-spring-dashpot system:

- The equivalent stiffness k
- The equivalent mass m
- The equivalent viscous damping coefficient b

One should always keep in mind that the equivalent single dof system is a simplification of the reality, and that it is valid only in a certain frequency range. This will be discussed in more details in section 3.4.4. With the help of simple examples, we illustrate the methodology to compute the equivalent stiffness, mass and damping parameters of a system.

3.4.1 Equivalent stiffness

The most general method to compute the equivalent stiffness of the flexible element of the system consists in applying a force of amplitude F in the direction of motion, and computing the resulting displacement x in the same direction. The equivalent stiffness is given by $k = F/x$ (Figure 49).

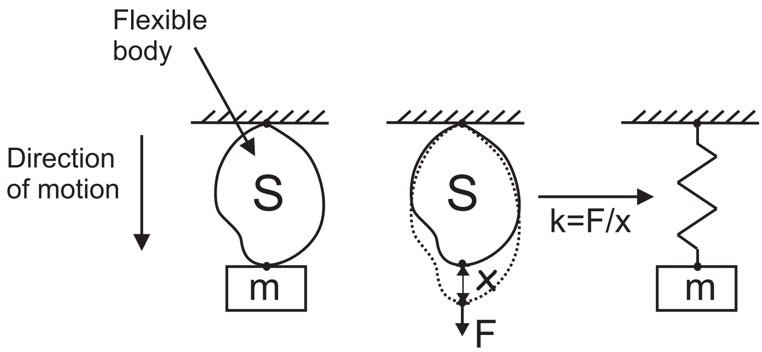

Figure 49: Principle to compute the equivalent stiffness k of a flexible body S

In the following, this methodology is applied to simple flexible bodies, for which analytical solutions can be computed.

Bar in traction
For a bar in traction (Figure 50), the constitutive equation is given by:

$$N = EA\frac{du}{dx}$$

where E is the Young's modulus, A the area of the section and $u(x)$ the axial displacement (in direction x). For a bar in pure traction, the normal force N is constant and equal to F so that the general form of $u(x)$ is

$$u(x) = \frac{F}{EA}x + Cst$$

The bar is fixed (u(x)=0) at $x = 0$, so that we have :

$$u(x) = \frac{F}{EA}x$$

The displacement at the free tip of the bar is equal to

$$d = \frac{F}{EA}L$$

and the equivalent stiffness is given by:

$$k = \frac{EA}{L}$$

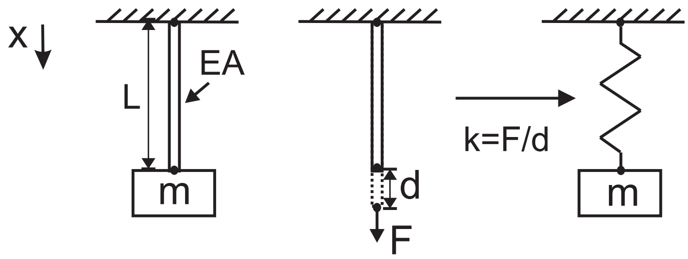

Figure 50: Reduction of a bar in traction of length L, Young's modulus E and section area A to an equivalent spring k

Bar in torsion

For a bar in torsion, the direction of motion is a rotation, so that the force to be applied needs to be a moment C. The equivalent stiffness is computed through the calculation of the rotation angle at the position where the moment is applied (Figure 51). The constitutive equation is given by:

$$M_x = GJ\frac{d\theta}{dx}$$

where $G = \frac{E}{2(1+\nu)}$ is the shear modulus and J is the polar inertia ($J = \pi R^4/2$ for a circular section of radius R). For a bar in pure torsion, the torsional moment M_x is constant and equal to the applied moment C, so that the general form of $\theta(x)$ is:

$$\theta(x) = \frac{C}{GJ}x + Cst$$

The bar is fixed at $x = 0$ so that $Cst = 0$ and we finally have:

$$\theta(x) = \frac{C}{GJ}x$$

The rotation at the tip of the bar is

$$\theta(L) = \frac{CL}{GJ}$$

so that the equivalent stiffness is equal to

$$K = \frac{GJ}{L}$$

Note that while the motion is a rotation and the force is a moment, it is usual to represent it with an equivalent system in translation, as this is much easier from a visual point of view.

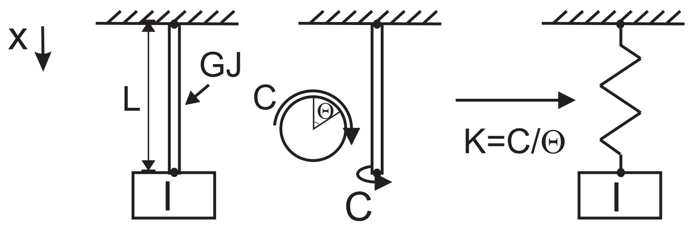

Figure 51: Reduction of a bar in torsion of length L and torsional stiffness GJ to an equivalent spring K

Beam in bending

For beams in bending, we can follow the same approach as the one detailed for the bar in traction and in torsion. In most cases however, it is more convenient to use solutions directly available in tables. As an example, we consider a cantilever beam in bending (Figure 52). From the tables, we can directly get the displacement $y(x)$ as a function of x:

$$y(x) = \frac{Fx^2}{6EI}(3L - x)$$

and deduce the tip displacement

$$y(L) = d = \frac{FL^3}{3EI}$$

The equivalent stifness is therfore

$$k = \frac{3EI}{L^3}$$

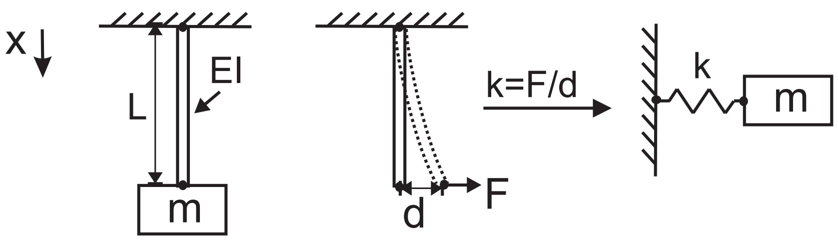

Figure 52: Reduction of a beam in bending of length L and bending stiffness EI to an equivalent spring k

Let us take a second example of a portal frame represented in Figure 53. The direction of motion is supposed to be horizontal. Due to the symmetry of the structure, the problem can be studied by considering only one half of the structure. The force applied in the direction of motion is thus $F/2$. Note that the boundary conditions of the beam in bending are different from the previous example, because the rotation at the tip is zero due to fixation to the rigid floor. For these boundary conditions, the displacement is given by:

$$y(x) = \frac{F}{24EI}x^2(3L - 2x)$$

The tip displacement is

$$d = y(L) = \frac{FL^3}{24EI}$$

which gives us the value of the equivalent stiffness

$$k = \frac{24EI}{L^3}$$

If we neglect the weight of the columns, the natural frequency of the equivalent one dof system is

$$f = \frac{1}{2\pi}\sqrt{\frac{24EI}{L^3 M_{floor}}}(Hz)$$

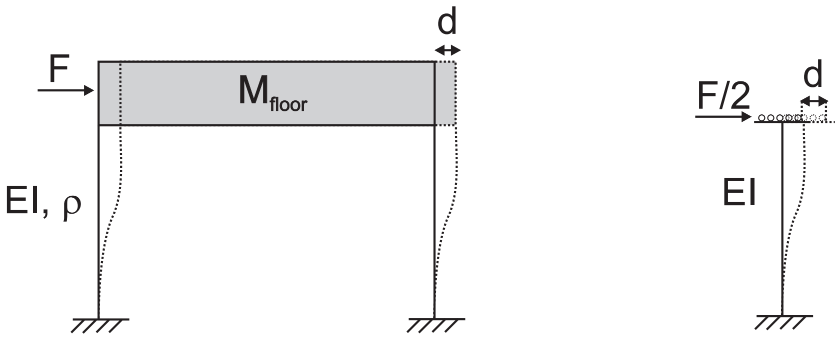

Figure 53: Reduction of a portal frame to an equivalent mass-spring system

An alternative method can be used to compute the equivalent stiffness. It is based on the equality of the strain energy of the real structure and the one dof mass-spring system which is given by

$$E_s = \frac{kx^2}{2} = \frac{F^2}{2k} \tag{18}$$

The principle consists in computing the strain energy of the real system and then identifying the equivalent stiffness by expressing the equality with (18). Let us consider the first three examples:

- For a bar in traction, the strain energy is

$$E_s = \frac{1}{2}\int_0^L \frac{N^2}{EA}dx$$

  and the normal force N is constant and equal to F leading to

$$E_s = \frac{1}{2}\frac{F^2 L}{EA} = \frac{F^2}{2k} \Rightarrow k = \frac{EA}{L}$$

- For a bar in torsion, the strain energy is

$$E_s = \frac{1}{2}\int_0^L \frac{M_x^2}{GJ}dx$$

  and the torsional moment M_x is constant and equal to C leading to

$$E_s = \frac{1}{2}\frac{C^2 L}{GJ} = \frac{C^2}{2K} \Rightarrow K = \frac{GJ}{L}$$

- For a beam in bending the strain energy is

$$E_s = \frac{1}{2}\int_0^L \frac{M^2}{EI}dx$$

and for the cantilever beam we have $M(x) = -Fx$ so that

$$E_s = \frac{1}{2}\frac{F^2}{EI}\frac{L^3}{3} \Rightarrow k = \frac{3EI}{L^3}$$

This method is fairly simple to apply and gives the same results as the general methodology presented above. Note that when the flexible body cannot be represented by a simple bar in traction or torsion, or a beam, the general methodology can still be applied. In order to compute the displacement d due to a force F applied in the direction of motion, an effective approach is to discretize the flexible body using the finite element method. The value of d computed allows to compute the equivalent stiffness $k = F/d$.

3.4.2 Equivalent mass

The computation of the equivalent mass allows to replace the flexible body by a massless spring. This approach is valid when the mass of the flexible body is small compared to the moving mass m. When such is not the case, it is possible to take into account the mass of the flexible body using an energy approach, in a manner analogous to what was done for the equivalent stiffness using the strain energy. The idea is to express the equality of the kinetic energy of an additional mass attached to the spring with the kinetic energy of the flexible body. This is illustrated with the following examples.

Equivalent mass of a spring

Consider a mass-spring system represented in Figure 55. If the mass of the spring is not small with respect to m, it can be modeled by an additional mass m_s. In order to do that, we express the kinetic energy of this additional mass:

$$E_k = \frac{1}{2}m_a\dot{x}^2 \tag{19}$$

We now compute the kinetic energy of the spring. We assume that when the spring is deformed, the displacement along the spring is linear:

$$u(x) = u(L)\frac{x}{L}$$

so that the velocity at each point x is given by

$$v(x) = \dot{u}(L)\frac{x}{L}$$

where $\dot{u}(L)$ is the velocity at the tip of the spring and is equal to $\dot{x}$ in equation (19). The total kinetic energy of the spring is

$$\begin{aligned} E_{ks} &= \frac{1}{2}\int_0^L \rho v(x)^2\, dx = \frac{1}{2}\int_0^L \rho\frac{x^2}{L^2}\dot{u}^2(L) = \frac{1}{2}\rho\frac{L}{3}\dot{u}^2(L) \\ &= \frac{1}{2}\frac{m_s}{3}\dot{u}^2(L) = \frac{1}{2}\frac{m_s}{3}\dot{x}^2 = \frac{1}{2}m_a\dot{x}^2 \end{aligned}$$

where m_s is the mass of the spring ($m_s = \rho L$). The additional mass due to the spring is $m_a = m_s/3$.

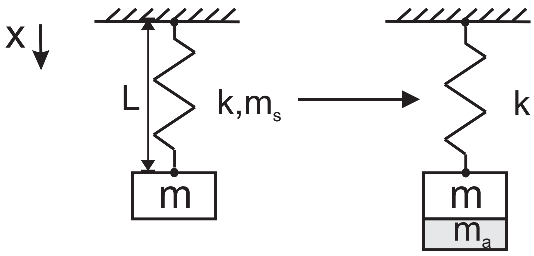

Figure 54: Equivalent 1D model of a mass-spring system taking into account the additional mass due to the spring

Bar in traction

The second example is a mass hanging from a bar. We have already calculated the equivalent stiffness of the bar in traction $k = EA/L$. When the mass of the bar is not small compared to the mass m, its equivalent additional mass m_a needs to be computed. Again, we assume that the displacement is in the form

$$u(x) = u(L)\frac{x}{L}$$

the velocity is

$$v(x) = \dot{u}(L)\frac{x}{L}$$

where $\dot{u}(L)$ is the velocity at the tip of the bar and is equal to $\dot{x}$ in equation (19). Following the same calculations as for the spring, the additional mass m_a is equal to $m_b/3$ where m_b is the mass of the bar.

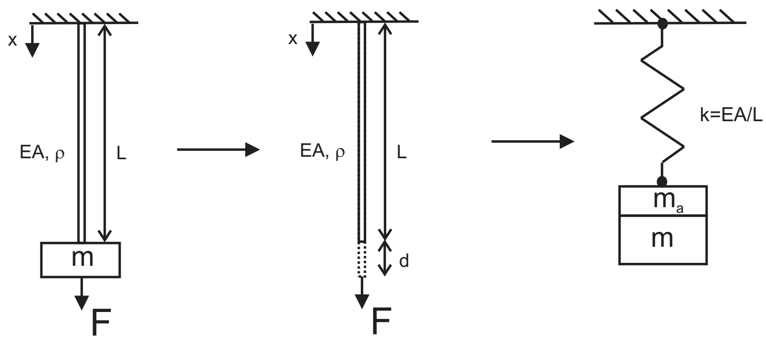

Figure 55: Equivalent mass-spring model of a mass hanging from a bar taking into account the additional mass due to the bar

3.4.3 Equivalent damping

In real structures, damping is a complex phenomenon which comes mainly from two types of sources: external and internal (Figure 56).

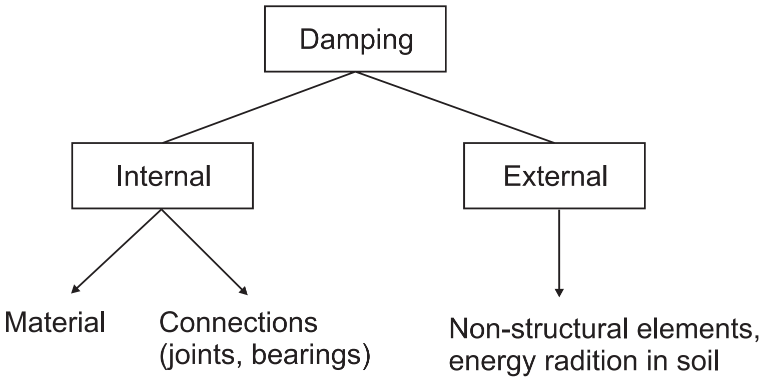

Figure 56: Sources of damping in real structures

When dissipation is present, the stress is not in phase with the strain, which results in a hysteresis loop if one plots the stress as a function of the strain (Figure 57).

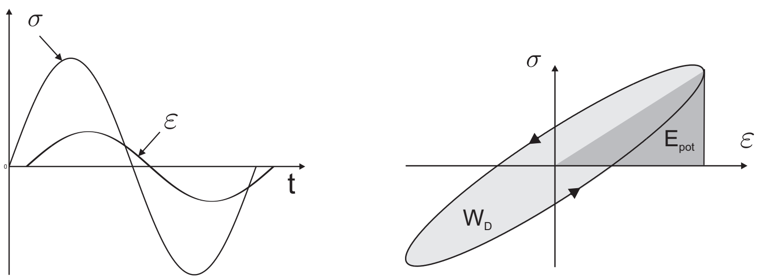

Figure 57: When the stress is not in phase with the strain (left), this results in a hysteresis loop in the stress-strain plane (right)

The mechanical energy dissipated in one cycle per unit volume W_D is given by the area inside the loop :

$$W_D = \int_0^T \sigma \dot{\varepsilon}\, dt = \int \sigma d\varepsilon$$

where T is the period of one cycle. The damping factor ψ of a material is proportional to the ratio of energy dissipated in one cycle to the maximum strain potential energy:

$$\psi = \frac{1}{2\pi} \frac{W_D}{E_{pot}}$$

where E_{pot} is the maximum strain energy. The damping factor of a structure is given by

$$\psi_S = \int_V \psi\, dV = \frac{1}{2\pi} \frac{W_{DS}}{E_{potS}}$$

It is equal to the damping factor of the material if the structure is homogeneous. The methodology to compute an equivalent viscous damping coefficient consists in expressing the equality of ψ_S for the structure studied, with the value of ψ_S for a one dof mass-spring-dashpot system.

Computation of ψ_S for a single dof mass-spring dashpot system

Let us consider the mass-spring-dashpot system represented in Figure 58 and compute the dissipated energy in one cycle:

$$W_{DS} = \int_0^T b\dot{x}\,\dot{x}dt$$

with $x(t) = |X|cos(\omega t)$ we have

$$\begin{aligned} W_{DS} &= \int_0^T \omega^2 b|X|^2 sin^2(\omega t)dt = \int_0^T \omega^2 b|X|^2 \frac{1-cos(2\omega t)}{2}dt \\ &= \omega^2 b|X|^2 \frac{T}{2} = \pi b\omega|X|^2 \end{aligned}$$

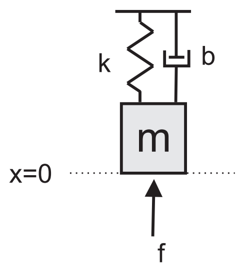

Figure 58: One dof mass-spring-dasphot system

The maximum potential energy is given by

$$E_{potS} = \frac{1}{2}kx_{max}^2 = \frac{1}{2}k|X|^2$$

and the damping factor of the mass-spring-dashpot system is given by:

$$\begin{aligned} \Psi_S &= \frac{1}{2\pi}\frac{W_D S}{E_{potS}} = \frac{2\pi}{2\pi}\frac{b\omega|X|^2}{k|X|^2} \\ &= \frac{\omega b}{k} \end{aligned}$$

Note that the damping factor the mass-spring-dashpot system computed at the natural frequency $\omega = \sqrt{k/m}$ is:

$$\psi_S(\omega_n) = \sqrt{\frac{k}{m}}\frac{b}{k} = \frac{b}{\sqrt{km}} = 2\xi$$

showing the link with the damping coefficient ξ defined earlier.

Examples of computation of an equivalent damping

Let us consider a few examples of computation of an equivalent damping b.

- In the general case where ψ_S is a known function of ω, we have:

$$b(\omega) = \frac{k\psi_S(\omega)}{\omega}$$

Note that this model introduces a dependency of b with respect to the frequency ω. The major drawback is that it cannot be used for time domain computations (such as when using the Duhamel's integral). A good approximation can be obtained by using a viscous damping where b is a constant by equating ψ_S at the natural frequency of the system (Figure 59).

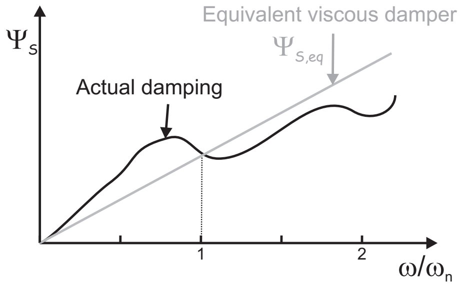

Figure 59: Determination of the value of an equivalent viscous damper

$$\frac{b}{\sqrt{km}} = \psi_S(\omega_n) \Rightarrow b = \psi_S(\omega_n)\sqrt{km}$$

For moderate values of damping, this will lead to a good representation of the damping because the frequency response of a one dof system is affected by the damping only in a narrow frequency band around the resonance (Figure 44). Therefore, it is necessary to have an accurate model of damping only in the frequencies close to the resonant frequency.

- For some structures, the **hysteretic damping model is often adopted**, which consists in assuming ψ_S as constant. In this case, we have (Figure 60):

$$\psi_S = \frac{\omega b}{k} \Rightarrow b(\omega) = \frac{k\psi_S}{\omega}$$

Note again that this model introduces a dependency of b with respect to the frequency ω.

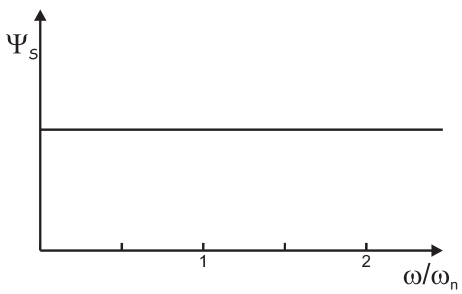

Figure 60: value of ψ_S for the hysteretic damping model

- In Coulomb friction damping, the damping force is proportional to the weight of the mass and its sign is opposite to the sign of the velocity. The equation of motion for a single dof system with Coulomb friction is:

$$m\ddot{x} + F_c sgn(\dot{x}) + kx = f$$

where $sgn(x) = 1$ for $x > 0$ and $sgn(x) = -1$ or $x < 0$

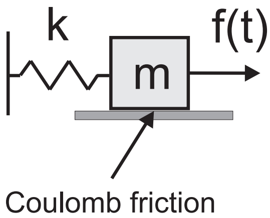

Figure 61: One dof system with Coulomb friction

Figure 62 (left) shows an example of $x(t)$, $\dot{x}(t)$ and $F_c sgn(\dot{x})$. The energy dissipated in one cycle is given by:

$$W_D = \int_0^T F_c sgn(\dot{x})\, \dot{x} dt = \int F_c sgn(\dot{x})\, dx$$

which can be computed easily by plotting the coulomb friction force as a function of the displacement of the mass (Figure 62, right).

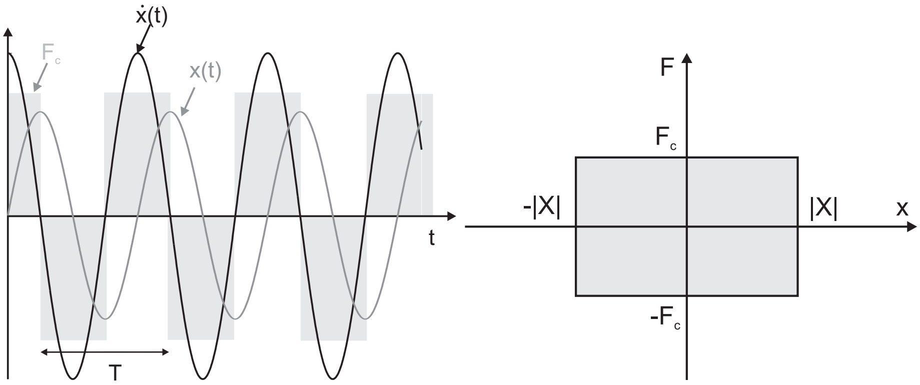

Figure 62: Example of displacement, velocity and friction force for a one dof system with Coulomb friction

$$W_{DS} = 4 \int_0^{T/4} F_c\, \dot{x} dt = \int_0^{|X|} 4 F_c dx$$

The damping factor of the system is thus

$$\Psi_S = \frac{1}{2\pi} \frac{4F_c|X|}{\frac{1}{2}k|X|^2} = 4\frac{F_c}{\pi k|X|}$$

and the value of the equivalent damping

$$b(\omega, |X|) = 4\frac{F_c}{\pi\omega|X|}$$

The equivalent damping is a function of both the frequency and the amplitude of the displacement of the mass.

Measurement of damping in one dof systems

Typical values of damping for materials used in civil engineering structures are given in Table 3. Because the damping in structures comes from the materials but also from the connections, it is very difficult to predict the damping coefficient of a structure. Because of that, it is often necessary to measure the damping coefficient after the structure has been built in order to make sure that the structure is safe. There are two fast and simple techniques to measure this damping coefficient.

Material	ξ
Reinforced concrete	0.004-0.012
Composite	0.002-0.003
Steel	0.001-0.002

Table 3: Typical values of damping in civil engineering structures

The first technique is called the **logarithmic decrement method**. It is based on the measurement of the impulse response of the structure. When a structure is excited by an impulse force, the response contains mainly its first mode. This is because the form of the impulse response is a sine function with an exponentially decaying enveloppe where the coefficient of the exponential is $-\xi\omega_n t$. The higher modes decrease therefore faster and their contribution to the response is negligible after a few oscillations. A typical impulse response containing only the first mode of vibration (single dof) is represented in Figure 63.

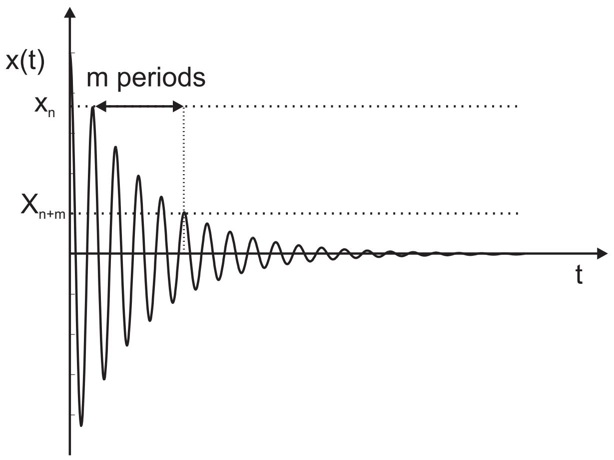

Figure 63: Impulse response containing the first mode (single dof)

The general form of the response at time t is:

$$x(t) = e^{-\xi\omega_n t}\left(Acos(\omega_d t) + Bsin(\omega_d t)\right)$$

The response m periods after time t is:

$$\begin{aligned} x(t+mT) &= e^{-\xi\omega_n (t+mT)}\left(Acos(\omega_d (t+mT)) + Bsin(\omega_d (t+mT))\right) \\ x(t+mT) &= e^{-\xi\omega_n (t+mT)}\left(Acos(\omega_d t) + Bsin(\omega_d t)\right) \end{aligned}$$

and we have

$$\frac{x(t)}{x(t+mT)} = \frac{e^{-\xi\omega_n t}}{e^{-\xi\omega_n (t+mT)}} = e^{\xi\omega_n (mT)}$$

we define the logarithmic decrement

$$\Lambda = ln\left(\frac{x(t)}{x(t+mT)}\right) = \xi\omega_n(mT) = \xi m\frac{2\pi}{\omega_d}\omega_n = 2m\pi\xi\frac{1}{\sqrt{1-\xi^2}}$$

For small values of ξ we have $\xi^2 << 1$ which gives:

$$\Lambda \simeq 2m\pi\xi$$

The damping coefficient is given by:

$$\xi = \frac{1}{2\pi m}\Lambda$$

The second technique is called the half-power bandwidth. It is based on the frequency response of the system (Figure 64). It consists in identifying the maximum amplitude A at resonance, followed by the two points at the left and right of the resonance where the amplitude is $A/2$ (half power). The frequencies Ω_1 and Ω_2 correspond to these two points, and it can be shown that the damping coefficient can be approximated by:

$$\xi = \frac{\Omega_2 - \Omega_1}{\Omega_2 + \Omega_1}$$

The approximation is valid for values of $\xi < 0.1$.

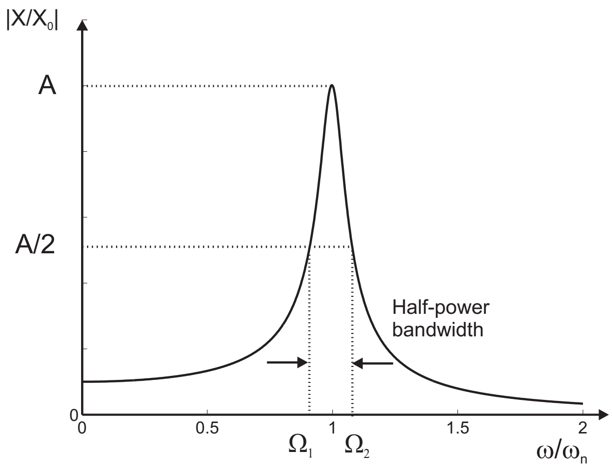

Figure 64: Frequency response of a structure focusing on one mode: the half-power bandwidth method

3.4.4 Reduction to a single dof system : limitations

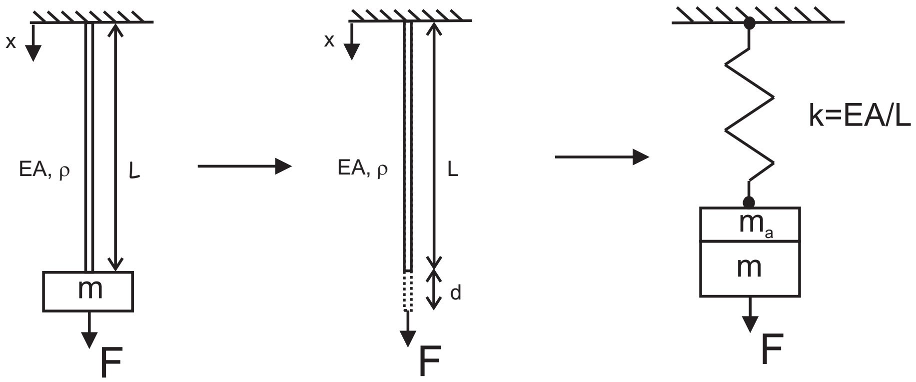

Figure 65: Mass hanging from a bar and equivalent representation with a single dof system with an equivalent stiffness and an additional mass

Let us consider the structure in Figure 65 which consists of a bar to which a mass is hanging. We have already discussed the reduction of such a system to a single dof system with an equivalent stiffness $k = EA/L$, and an additional mass m_a=$m_b/3$ where m_b is the mass of the bar. The mass is $100kg$ and the bar is made of steel ($E = 210GPa$, $\rho = 7800kg/m^3$) and has a length $L = 1m$ and a square section of $2cm$ x $2cm$.

The frequency response function $X(\omega)/F$ is plotted in Figure 66 where the exact solution (considering the bar as a continuous system, see section 6), and the equivalent single dof system (with and without the additional mass of the bar) are compared. Below 2500 Hz, all three models are in very good agreement. Around the natural frequency, there is a slight difference in the resonant frequency: the model taking into account the additional mass matches with the exact solution, while the model neglecting the additional mass has a resonant frequency slightly higher, but the difference is less than 1%. Above 2500 Hz, the exact solution contains an additional peak. This peak is due to the first resonant frequency of the bar which is coupled with the mass. This additional resonant frequency cannot be represented by a single dof system.

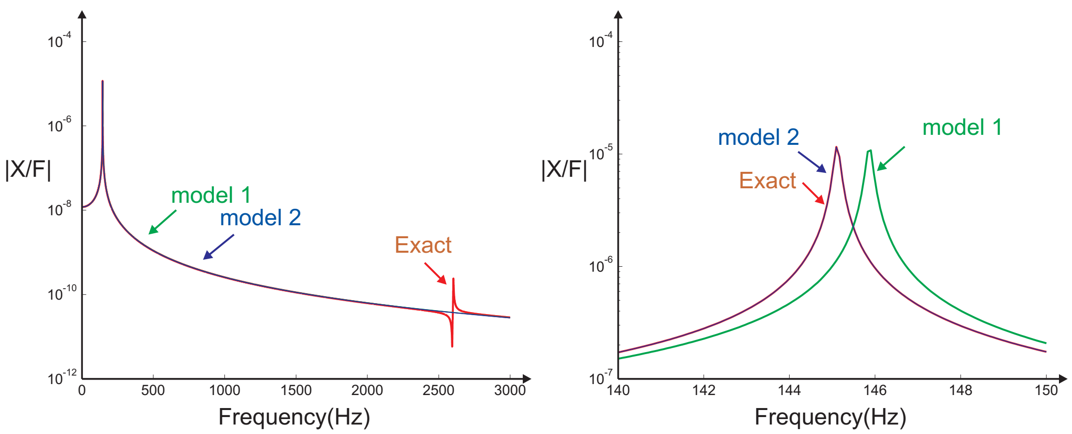

Figure 66: Frequency response function of the mass hanging from a bar excited by a vertical force. Exact response and approximation using a single dof system (with and without additional mass)

The next graphs in Figure 67 are plotted using a value of ρ 10 times higher (i.e. $\rho = 78000kg$) for the bar. While this value is not representative of a real material, the purpose is to illustrate the fact that in such a case, the mass of the bar cannot be neglected anymore. We see indeed that if the mass of the bar is neglected, a significant difference is found for the first natural frequency. Another difference is that the equivalent single dof model is only valid below 500 Hz due to the appearance of several peaks above this value. These peaks are due to several resonant frequencies of the continuous bar coupled to the mass. Such additional peaks can again not be represented by a single dof system.

In summary, the examples shown above illustrate the fact that the single dof equivalent system is only valid in a certain frequency band which depends on dynamic properties of the bodies which are replaced by an equivalent mass and spring.

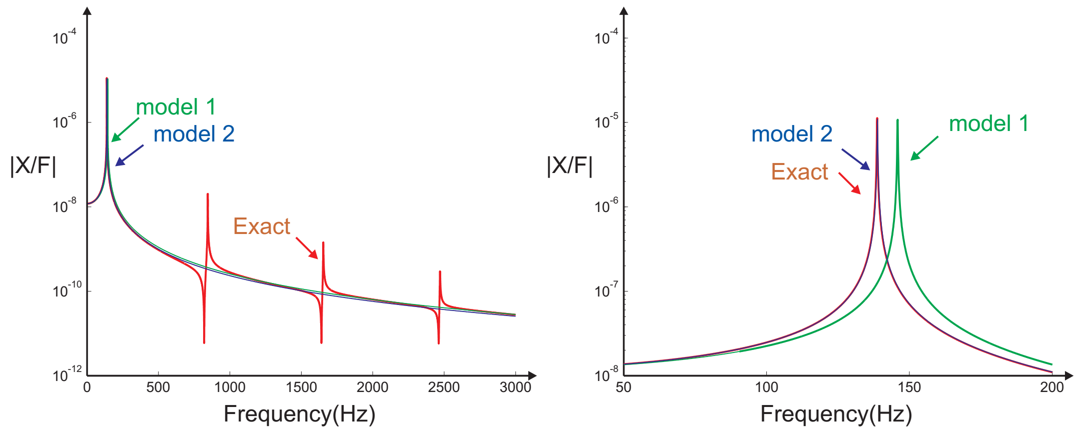

Figure 67: Frequency response function of the mass hanging from a heavy bar excited by a vertical force. Exact response and approximation using a single dof system (with and without additional mass)

3.5 One DOF application: the accelerometer

By far the most common sensor for measuring vibrations is the accelerometer. The basic working principle of such a device is presented in Figure 68(a). It consists of a moving mass on a spring and dashpot, attached to a moving solid. The acceleration of the moving solid results in a differential displacement x between the mass M and the solid. The governing equation is given by,

$$M\ddot{x} + c\dot{x} + kx = -M\ddot{x}_0 \tag{20}$$

In the frequency domain $x/\ddot{x}_0$ is given by,

$$\frac{x}{\ddot{x}_0} = \frac{-1}{-\omega^2 + \omega_n^2 + 2i\xi\omega\omega_n} \tag{21}$$

with $\omega_n = \sqrt{\frac{k}{m}}$ and $\xi = b/2\sqrt{km}$ and for frequencies $\omega << \omega_n$, one has,

$$\frac{x}{\ddot{x}_0} \simeq \frac{-1}{\omega_n^2} \tag{22}$$

showing that at low frequencies compared to the natural frequency of the mass-spring system, x is proportional to the acceleration $\ddot{x}_0$. Note that since the proportionality factor is $\frac{-1}{\omega_n^2}$, the sensitivity of the sensor is increased as ω_n^2 is decreased. At the same time, the frequency band in which the accelerometer response is proportional to $\ddot{x}_0$ is reduced.

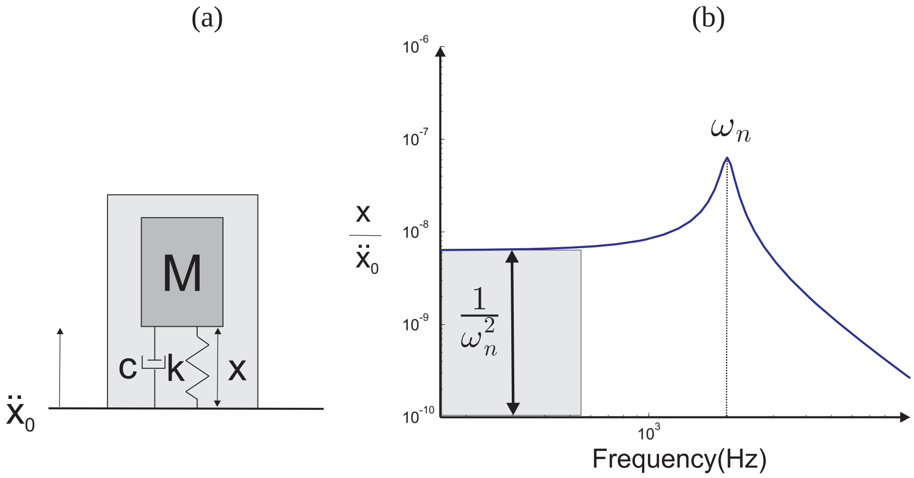

Figure 68: Working principle of an accelerometer

The relative displacement x can be measured in different ways among which the use of piezoelectric material, either in longitudinal or shear mode (Figure 69). In such configurations, the strain applied to the piezoelectric material is proportional to the relative displacement between the mass and the base. If no amplifier is used, the voltage generated between the electrodes of the piezoelectric material is directly proportional to the strain, and therefore to the relative displacement. For frequencies well below the natural frequency of the accelerometer, the voltage produced is therefore proportional to the absolute acceleration of the base.

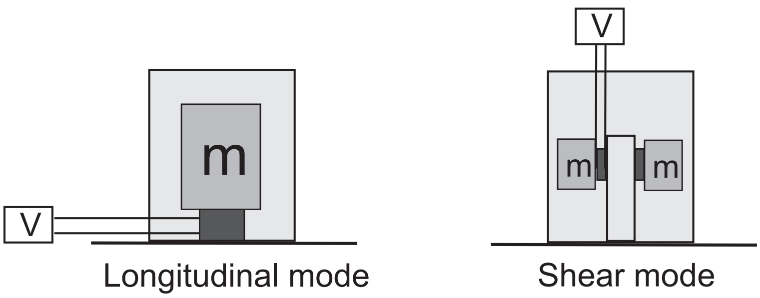

Figure 69: Different sensing principles for standard piezoelectric accelerometers

4 Vibration isolation

4.1 Direct vibration isolation

The problem of direct vibration isolation consists in preventing the vibrations coming from a given source to propagate in the building, or in the surroundings. A typical example is the washing mashine which, when vibrating, transmits the vibration to the floor. Depending on the design of the building, such vibrations can propagate through several floors. Another example is a power station located near other buildings such as a school or a hotel. The vibrations generated by the power station can propagate into the neighboring buildings and cause noise and discomfort. Schematically, the source of vibrations is represented by a force f acting on a rigid body of mass m. This rigid body is fixed to the ground through some elements which are represented by a spring and a damper in parallel (Figure 70).

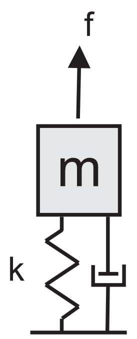

Figure 70: Direct vibration isolation

The equation of motion is:

$$m\ddot{x} + b\dot{x} + kx = f$$

The force transmitted to the ground (surroundings) is :

$$f_T = b\dot{x} + kx$$

In the frequency domain, we have

$$F = \left(k - \omega^2 m + i\omega b\right) X \Rightarrow |F| = \sqrt{(k-\omega^2 m)^2 + \omega^2 b^2}|X|$$

and

$$F_T = (k + i\omega b)\, X \Rightarrow |F_T| = \sqrt{k^2 + \omega^2 b^2}|X|$$

The isolation factor is given by:

$$\frac{|F_T|}{|F|} = \frac{\sqrt{k^2 + \omega^2 b^2}}{\sqrt{(k-\omega^2 m)^2 + \omega^2 b^2}}$$

and using the definitions of $\xi = b/(2\sqrt{km})$ and $\omega_n = \sqrt{k/m}$ we get :

$$\frac{|F_T|}{|F|} = \frac{\sqrt{1 + (2\xi\frac{\omega}{\omega_n})^2}}{\sqrt{(1-(\frac{\omega}{\omega_n})^2)^2 + (2\xi\frac{\omega}{\omega_n})^2}} \tag{23}$$

The isolation factor is a function of the frequency ω and is plotted in Figure 71.

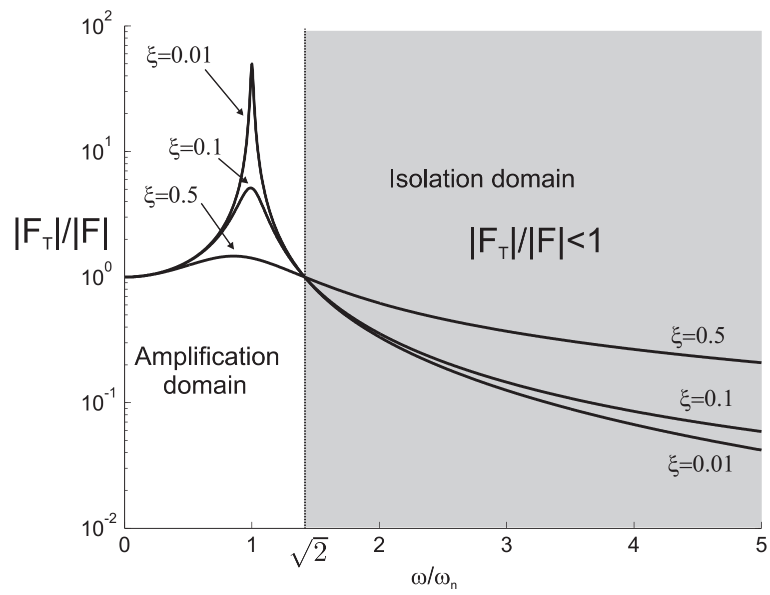

Figure 71: Isolation factor for the direct vibration isolation problem

One can distinguish two different domains:

- for frequencies $\omega < \sqrt{2}\omega_n$, $|F_T|/|F| > 1$, this is the amplification domain where no isolation is achieved, the amplitude of the force transmitted to the ground is greater than the force applied to the body. In this domain, adding damping improves the situation: the amplification at resonance decreases.

- for frequencies $\omega > \sqrt{2}\omega_n$ we are in the isolation domain: the force transmitted to the ground is smaller than the force f. In this domain, adding damping has a negative impact on the isolation which decreases.

For the damping, an ideal situation would be to have a damper which has a high damping at low frequencies and a low damping at high frequencies. Materials such as rubber and elastomers exhibit that type of damping properties. The problem of direct vibration isolation consists in designing the one dof system such that for the excitation frequencies considered, we are in the isolation domain. If these excitation frequencies are low, it requires to have a very low resonant frequency of the single dof system. There are two ways to achieve this: the first one is to have a very soft spring. Note that the spring must be strong enough to sustain the static load of the mass which in general does not allow to use very flexible springs. The second way is to increase the mass of the system. This can be done for example by adding a rigid and heavy foundation to the rigid body of mass m.

4.2 Inverse vibration isolation

The problem of inverse vibration isolation consists in designing an isolator on which sensitive equipment is attached in order to prevent the vibrations from the environment to reach the sensitive equipment. Examples are precision devices such as microscopes or lithography machines which need to be isolated from ground motion, or buildings which need to be isolated from the ground motion due to earthquakes. Schematically, the vibrations from the environment are represented by a ground motion x, and the sensitive equipment is the rigid body m attached to the ground through a spring and a damper (Figure 72).

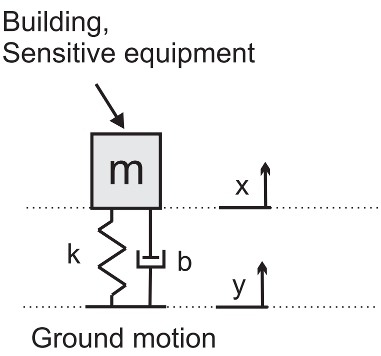

Figure 72: Inverse vibration isolation

The equation of motion is:

$$m\ddot{x} + k(x - y) + b(\dot{x} - \dot{y}) = 0$$

which can be rewritten

$$m\ddot{x} + kx + b\dot{x} = ky + b\dot{y}$$

In the frequency domain we have:

$$\left(k - \omega^2 m + i\omega b\right) X = (k + i\omega b)\, Y$$

The transmissibility of the one dof system is defined as:

$$\frac{|Y|}{|X|} = \frac{\sqrt{k^2 + \omega^2 b^2}}{\sqrt{(k - \omega^2 m)^2 + \omega^2 b^2}}$$

One can note that while the physical problem is different, the transmissibility has the same expression as the isolation factor in (23). The transmissibility is a function of the frequency and represented in Figure 73. The same remarks as for the isolation factor concerning the damping and the design of the isolation device hold.

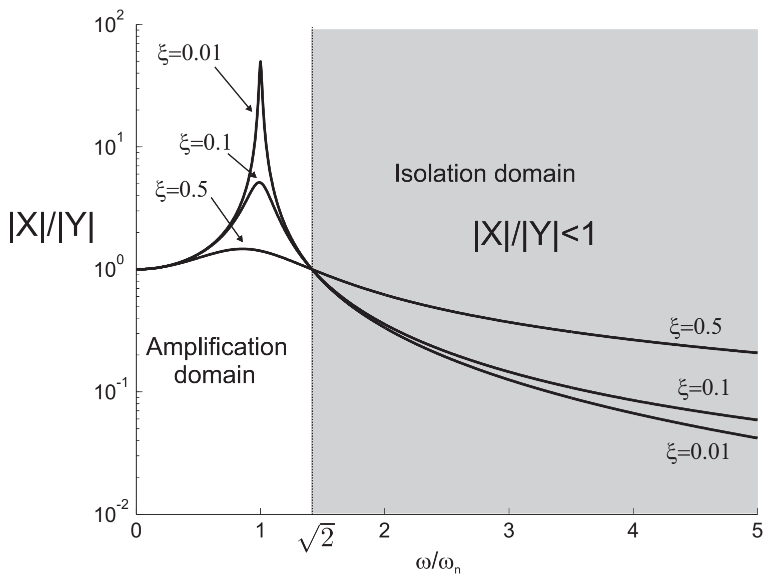

Figure 73: Transmissibility for the inverse isolation problem

The following movies illustrate the effect of an isolator for different problems such as building isolation for earthquakes:

```
Vibration isolation demonstrations :
    http://www.youtube.com/watch?v=ntV6LQF1GxA
    http://www.youtube.com/watch?v=reYtUNLXvt8
    http://www.youtube.com/watch?v=YPAOZXc33gE
    http://www.youtube.com/watch?v=MboMuAzRUF0
    http://www.youtube.com/watch?v=ChaqMDc4ces
    http://www.youtube.com/watch?v=ZqlXp3czrrM
    http://www.youtube.com/watch?v=Fw7aQwMmBNM

Application to buildings:
http://www.youtube.com/watch?v=phgdkqn9aTI
http://www.youtube.com/watch?v=Nc4JcWn6nYs
http://www.youtube.com/watch?v=Es0Bp7XYJbk
http://www.youtube.com/watch?v=5zVUDyBaN3E
```

5 Multiple degree of freedom systems

Figure 74 represents a series of systems which can be modeled as multiple degree of freedom systems. In the example of the automobile suspension, the motion has been extended to multiple degrees of freedom by considering both the vertical translation and the rotation of the car, as well as the flexibility of the tires (which adds two degrees of freedom).

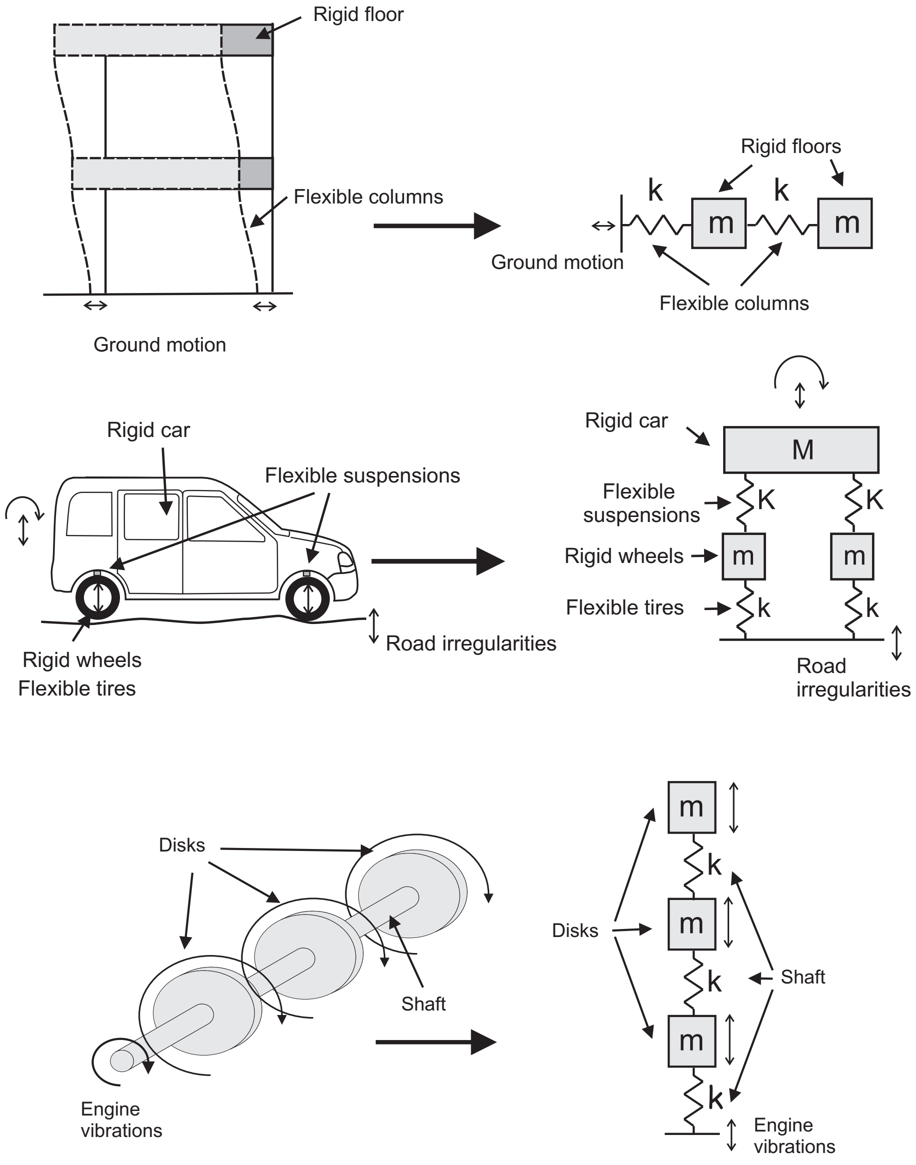

Figure 74: Examples of multiple dofs systems

5.1 Response of a multiple degrees of freedom system without damping

Let us consider the two dofs system represented in Figure 75. A force f is applied to the second mass. The first law of Newton is applied to each mass:

$$m\ddot{x}_1 = -kx_1 - k\left(x_1 - x_2\right) \tag{24}$$
$$m\ddot{x}_2 = k\left(x_1 - x_2\right) - kx_2 + f \tag{25}$$

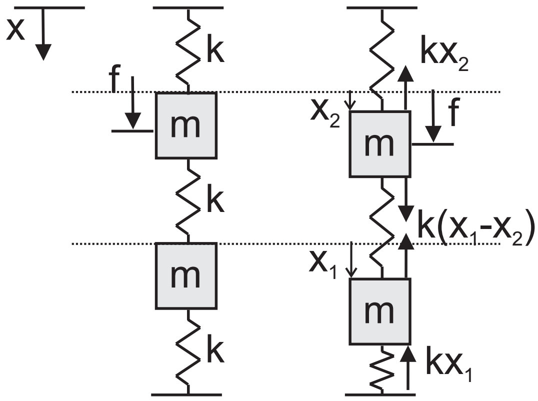

Figure 75: Forces acting on a two dofs system with two masses and three springs

This set of equations can be written in a matrix form:

$$\begin{bmatrix} m & 0 \\ 0 & m \end{bmatrix} \begin{Bmatrix} \ddot{x}_1 \\ \ddot{x}_2 \end{Bmatrix} + \begin{bmatrix} 2k & -k \\ -k & 2k \end{bmatrix} \begin{Bmatrix} x_1 \\ x_2 \end{Bmatrix} = \begin{Bmatrix} 0 \\ f \end{Bmatrix} \tag{26}$$

or in a more compact form

$$M\ddot{x} + Kx = F \tag{27}$$

where M is the mass matrix, K is the stiffness matrix, F is the vector of forces, and x is the vector containing the dofs of the system (here x_1 and x_2). The form of equations in (27) can be generalized to write the equations of motion of a system with n dofs. In such a case, the size of the matrices is n x n and the size of the vectors is n.

5.1.1 General solution of the equations of motion

The general solution of (27) can be obtained assuming

$$\begin{Bmatrix} x_1(t) \\ x_2(t) \end{Bmatrix} = \begin{Bmatrix} A_1 \\ A_2 \end{Bmatrix} e^{rt} = \psi e^{rt}$$

Equation (27) becomes:

$$\left(K + r^2 M\right)\psi = 0$$

This set of equations admits a non-trivial solution if

$$det(K + r^2 M) = 0$$

The roots of the determinant are purely imaginary and appear as complex conjugate pairs (this is due to the nature of the matrices K and M which are positive definite). They can be written

$$r^2 = -\omega^2$$

so that equation (27) can be written:

$$\left(K - \omega^2 M\right)\psi = 0$$

This set of equations is an eigenvalue problem. Its solution will give a set of eigenvalues called the eigenfrequencies (ω_i, i=1..n, where n is the number of dofs) and the associated eigenvectors ψ_i called the mode shapes. The general solution of the equation of motion can be written as the sum of functions in the spatial domain (the mode shapes) and oscillatory functions in the time domain (oscillations at frequencies ω_i):

$$x(t) = \sum_{i=1}^{n} \left(Z_{i1}cos(\omega_i t) + Z_{i2}sin(\omega_i t)\right)\psi_i$$

The coefficients Z_{ij} are a function of the initial conditions (displacement and velocity).

Illustration: two degrees of freedom system
The eigenfrequencies and mode shapes of the system represented in Figure 75 satisfy the set of equations:

$$\left(K - \omega^2 M\right)\psi = 0 \tag{28}$$

A non-trivial solution exists if

$$det(K - \omega^2 M) = det\begin{pmatrix} 2k - \omega^2 m & -k \\ -k & 2k - \omega^2 m \end{pmatrix} = 0$$

which leads to

$$(2k - \omega^2 m)(2k - \omega^2 m) - k^2 = m^2\omega^4 - 4km\omega^2 + 3k^2 = 0$$

The solutions of this second order equation (ω^2 is the unknown) are:

$$\omega_1^2 = k/m$$
$$\omega_2^2 = 3k/m$$

The mode shapes associated to these two eigenfrequencies are obtained by replacing ω successively by ω_1 and ω_2 in the first (or the second) line of (28):

For $\omega_1^2 = k/m$

$$\left(2k - \frac{k}{m}m\right)A_1 - kA_2 = 0$$
$$kA_1 = kA_2 \Rightarrow A_1 = A_2$$

For $\omega_2^2 = 3k/m$

$$\left(2k - \frac{3k}{m}m\right)A_1 - kA_2 = 0$$
$$-kA_1 = kA_2 \Rightarrow A_1 = -A_2$$

The two mode shapes are then given by (note that a mode shape is always known up to a constant)

$$\psi_1 = \left\{ \begin{array}{c} 1 \\ 1 \end{array} \right\}$$
$$\psi_2 = \left\{ \begin{array}{c} 1 \\ -1 \end{array} \right\}$$

The first mode shape corresponds to a translation of the two masses in phase (there is no strain in the middle spring), while the second mode shape corresponds to a motion of the two masses in opposition of phase (Figure 76).

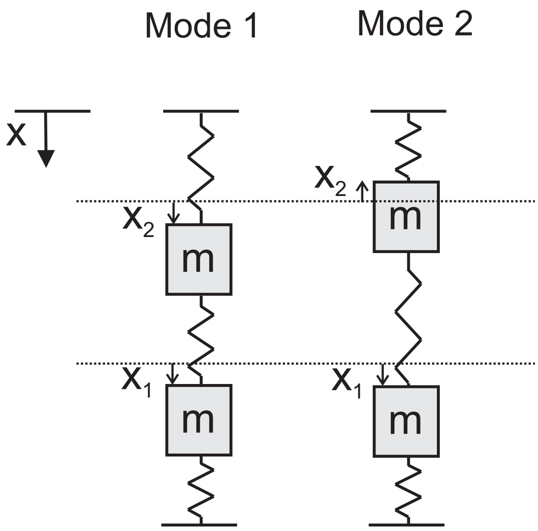

Figure 76: Mode shapes of the two dofs system represented in Figure 75

The general solution can be written in the form:

$$\left\{ \begin{array}{c} x_1(t) \\ x_2(t) \end{array} \right\} = (Z_{11}\cos\omega_1 t + Z_{12}\sin\omega_1 t) \left\{ \begin{array}{c} 1 \\ 1 \end{array} \right\} + (Z_{21}\cos\omega_2 t + Z_{22}\sin\omega_2 t) \left\{ \begin{array}{c} 1 \\ -1 \end{array} \right\}$$

Let us assume that a zero initial velocity is imposed to the two masse ($\dot{x_1}(0) = \dot{x_2}(0) = 0$) and that an initial displacement is imposed in the form of

$$\left\{ \begin{array}{c} x_1(0) \\ x_2(0) \end{array} \right\} = \left\{ \begin{array}{c} 0 \\ 1mm \end{array} \right\}$$

These four conditions allow to determine the four constants Z_{ij}. The solution is

$$\left\{ \begin{array}{c} x_1(t) \\ x_2(t) \end{array} \right\} = \left(\begin{array}{c} \frac{1}{2}\cos\omega_1 t - \frac{1}{2}\cos\omega_2 t \\ \frac{1}{2}cos\omega_1 t + \frac{1}{2}cos\omega_2 t \end{array} \right) (mm)$$

The free vibration of the two dofs system subject to these initial conditions is shown in Figure 77. The presence of two frequencies, due to the existence of two eigenfrequencies can be noticed. As the number of dofs increases in a system; the number of eigenfrequencies also inscreases and the free vibration contains more and more frequencies.

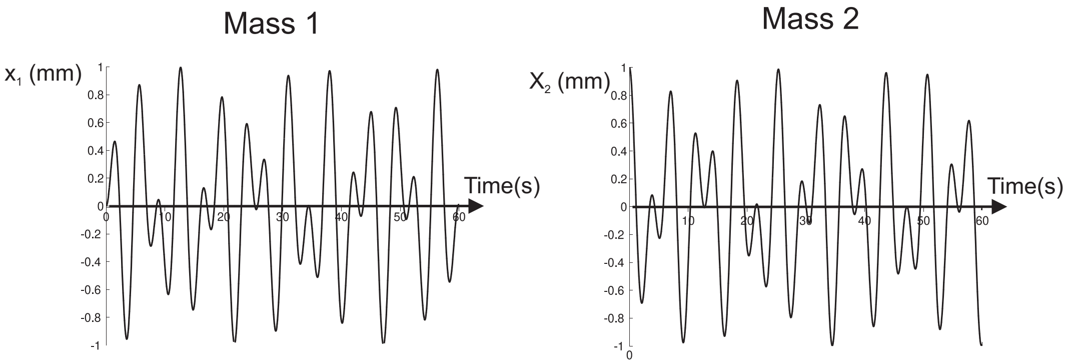

Figure 77: Free vibration of a two dofs system subject to an initial zero velocity and an imposed displacement $x_1 = 0$, $x_2 = 1(mm)$

5.1.2 Orthogonality of the mode shapes

In the following, we will demonstrate the property of orthogonality of the modeshapes:

$$\begin{aligned}\psi_i^T M \psi_j &= \delta_{ij}\mu_i \\ \psi_i^T K \psi_j &= \delta_{ij}\mu_i\omega_i^2\end{aligned}$$

Proof:
Let us take two eigenfrequencies ω_i and ω_j such that $\omega_i \neq \omega_j$. The associated mode shapes are ψ_i and ψ_j. We have:

$$\begin{gathered}\left(K - \omega_i^2 M\right)\psi_i = 0 \\ \left(K - \omega_j^2 M\right)\psi_j = 0\end{gathered}$$

Let us premultiply the first expression by ψ_j^T and the second by ψ_i^T and make a substraction:

$$\psi_j^T M \psi_i \left(\omega_i^2 - \omega_j^2\right) = 0$$

where we have used the fact that matrix K is symmetric so that $\psi_i^T K \psi_j = \psi_j^T K \psi_i$. As we have assumed $\omega_i \neq \omega_j$, we find:

$$\psi_j^T M \psi_i = 0 \qquad i \neq j$$

For $i = j$; we define

$$\psi_i^T M \psi_i = \mu_i$$

The second orthogonality relationship is easily deduced, as we have $K\psi_i = \omega_i^2 M \psi_i$ and therefore

$$\begin{aligned}\psi_j^T K \psi_i &= \omega_i^2 \psi_j^T M \psi_i = 0 \qquad i \neq j \\ \psi_i^t K \psi_i &= \omega_i^2 \psi_j^T M \psi_i = \omega_i^2 \mu_i\end{aligned}$$

The orthogonality conditions can also be written in a matrix form. Let us define the matrix of mode shapes whose columns are the mode shapes:

$$\Psi = \left[\begin{array}{cccc} \psi_1 & \psi_2 & ... & \psi_n \end{array}\right]$$

we have:

$$\Psi^T M \Psi = diag(\mu_i)$$
$$\Psi^T K \Psi = diag(\mu_i \omega_i^2)$$

where $diag(\mu_i)$ is a diagonal matrix with the values μ_i on the diagonal:

$$diag(\mu_i) = \begin{bmatrix} \mu_1 & 0 & ... & 0 \\ 0 & \mu_2 & ... & 0 \\ ... & ... & ... & ... \\ 0 & 0 & ... & \mu_n \end{bmatrix}$$

These relationships express the fact that the mode shapes are orthogonal with respect to the matrices M and K. They can therefore be used as a basis of orthogonal functions to represent the solution of the problem.

5.1.3 Particular solution of the equation of motion

Let us start from equation (27) and decompose the solution of the problem in the basis of the mode shapes:

$$x(t) = \sum_{i=1}^{n} z_i(t)\psi_i$$

which can be written in a matrix form :

$$x = \Psi z$$

where z is the vector of modal amplitudes. Let us replace x by Ψz in (27) and premultiply by Ψ^T, we have:

$$\Psi^T M \Psi \ddot{z} + \Psi^T K \Psi z = \Psi^T f$$

and using the orthogonality conditions, we find:

$$diag(\mu_i)\ddot{z} + diag(\mu_i \omega_i^2) z = \Psi^T f$$

which is a set of n uncoupled equations of the type

$$\mu_i \ddot{z}_i + \mu_i \omega_i^2 z_i = F_i \tag{29}$$

Equation (29) corresponds to the equation of motion of a single dof system with

- a mass μ_i, called the modal mass
- a stiffness $\mu_i \omega_i^2$
- a natural frequency $\omega_i = 2\pi f_i$
- a force $F_i = \psi_i^T f$ (modal excitation)

In summary, by writing the particular solution $x(t)$ as a function of the modal amplitudes $z_i(t)$ and the mode shapes ψ_i, it is possible to transform the initial set of n coupled equations into a set of n uncoupled equations. Each independent equation corresponds to the equation of motion of a single dof system. All the tools presented in Section 3 can therefore be used to find the solution of the equations of motions of a mdof system.

The particular solution can be calculated in the frequency domain following the same approach, assuming $x(t) = Xe^{i\omega t}$ and $f(t) = Fe^{i\omega t}$ where X and F are vectors of size n, we have:

$$\left(K - \omega^2 M\right) X = F \tag{30}$$

While this equation can be solved directly by inverting the matrix $\left(K - \omega^2 M\right)$ at each frequency, a simpler and more efficient method consists in assuming that the solution X can be written as a function of the mode shapes:

$$X(\omega) = \sum_{i=1}^{n} Z_i(\omega)\psi_i$$

which can be written in a matrix form:

$$X = \Psi Z$$

where Z is a vector of modal amplitudes. Let us replace in (30), and premultiply by Ψ^T, we have:

$$\left(\Psi^T K \Psi - \omega^2 \Psi^T M \Psi\right) Z = \Psi^T F$$

and using the orthogonality properties:

$$\left(\begin{bmatrix} \mu_1\omega_1^2 & 0 & ... & 0 \\ 0 & \mu_2\omega_2^2 & ... & 0 \\ ... & ... & ... & ... \\ 0 & 0 & ... & \mu_n\omega_n^2 \end{bmatrix} - \omega^2 \begin{bmatrix} \mu_1 & 0 & ... & 0 \\ 0 & \mu_2 & ... & 0 \\ ... & ... & ... & ... \\ 0 & 0 & ... & \mu_n \end{bmatrix} \right) \left\{ \begin{array}{c} Z_1 \\ Z_2 \\ ... \\ Z_n \end{array} \right\} = \left\{ \begin{array}{c} \psi_1^T F \\ \psi_2^T F \\ ... \\ \psi_n^T F \end{array} \right\}$$

We obtain a set of n decoupled equations. The unknowns Z_i can easily be solved for:

$$Z_j(\omega) = \psi_j^T F \frac{1}{\mu_j(\omega_j^2 - \omega^2)}$$

The Bode diagram of Z_i is identical to the Bode diagram of a single dof system and will present a resonant peak at the angular frequency ω_i. In the absence of damping, Z_i is always real (positive or negative). The displacement $X(\omega)$ can be retrieved by summing the contributions of the different mode shapes (Figure 78):

$$X(\omega) = \sum_{j=1}^{n} Z_j(\omega)\psi_j = \sum_{j=1}^{n} \frac{\psi_j^T F \psi_j}{\mu_j(\omega_j^2 - \omega^2)}$$

The Bode diagram of $X(\omega)$ will therefore present a maximum of n resonant peaks.

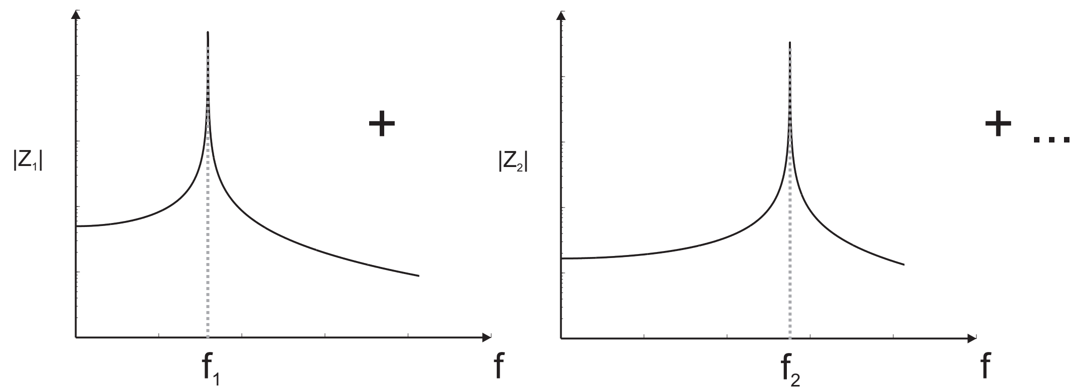

Figure 78: The response $X(\omega)$ is the sum of the response of single dof systems with amplitude Z_j, j=1...n

Illustration: two degrees of freedom system

We consider again the two dofs system represented in (Figure 75). The matrix of the mode shapes is written:

$$\Psi = \begin{bmatrix} 1 & 1 \\ 1 & -1 \end{bmatrix}$$

We compute the values of μ_i:

$$\Psi^T M \Psi = \begin{bmatrix} 1 & 1 \\ 1 & -1 \end{bmatrix} \begin{bmatrix} m & 0 \\ 0 & m \end{bmatrix} \begin{bmatrix} 1 & 1 \\ 1 & -1 \end{bmatrix} = \begin{bmatrix} 2m & 0 \\ 0 & 2m \end{bmatrix} \Rightarrow \mu_1 = \mu_2 = 2m$$

and the values of $F_i = \Psi^T F$:

$$\Psi^T F = \begin{bmatrix} 1 & 1 \\ 1 & -1 \end{bmatrix} \left\{ \begin{array}{c} 0 \\ F \end{array} \right\} = \left\{ \begin{array}{c} 1 \\ -1 \end{array} \right\}$$

The modal amplitudes Z_i are given by:

$$Z_1 = \frac{1}{2m(\frac{k}{m} - \omega^2)}$$
$$Z_2 = \frac{-1}{2m(\frac{3k}{m} - \omega^2)}$$

and the response of the system is:

$$X(\omega) = \left\{ \begin{array}{c} X_1(\omega) \\ X_2(\omega) \end{array} \right\} = \frac{1}{2m(\frac{k}{m} - \omega^2)} \left\{ \begin{array}{c} 1 \\ 1 \end{array} \right\} + \frac{-1}{2m(\frac{3k}{m} - \omega^2)} \left\{ \begin{array}{c} 1 \\ -1 \end{array} \right\}$$

The Bode diagrams of $X_1(\omega)$ and $X_2(\omega)$ are represented on Figure 79, where the modal amplitudes Z_1 and Z_2 are also represented. It is interesting to take a closer look at what happens between the eigenfrequencies f_1 and f_2. For mass 1, the contributions Z_1 and Z_2 are in phase, so that the amplitudes are added, resulting in a higher amplitude of X_1. For mass 2, the contributions Z_1 and Z_2 have an opposite phase. At the frequency at which their amplitude is equal, the sum of the contributions is therefore zero: at that frequency, mass 2 is not moving. **This frequency is called an**

anti-resonance. The resonant frequencies of a system are a global property (they are present on the Bode diagram for each dof of the system), while the anti-resonances are a local property of the system (they are present only at specific dofs of the system).

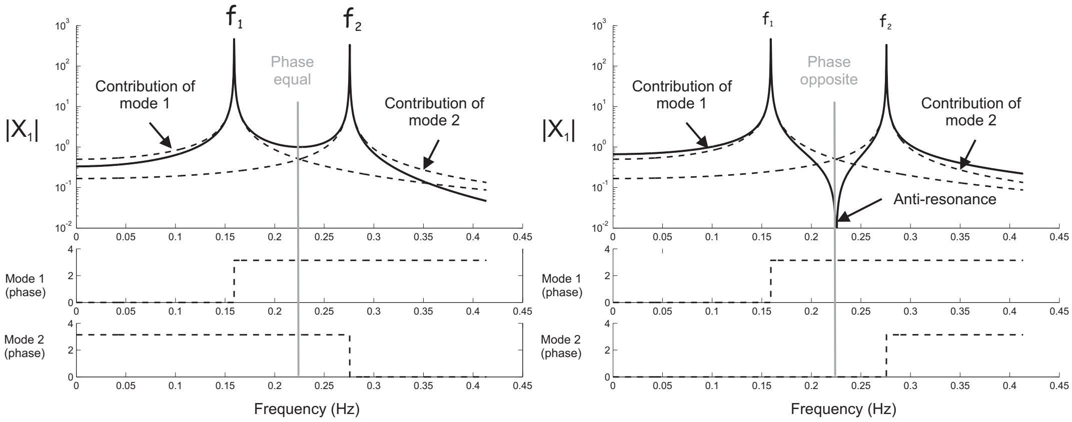

Figure 79: Bode diagram of the response of the two dofs systems (X_1 and X_2)

The following videos illustrate the resonance of single dofs and a three dofs systems:

```
3 SDOF systems : http://www.youtube.com/watch?v=iyw4AcZuj5k
3 DOFS system : http://www.youtube.com/watch?v=OaXSmPgl1os
```

5.2 Response of a multiple degrees of freedom system with damping

Let us consider the two dofs system represented in Figure 80. Damping has been introduced through three viscous dampers.

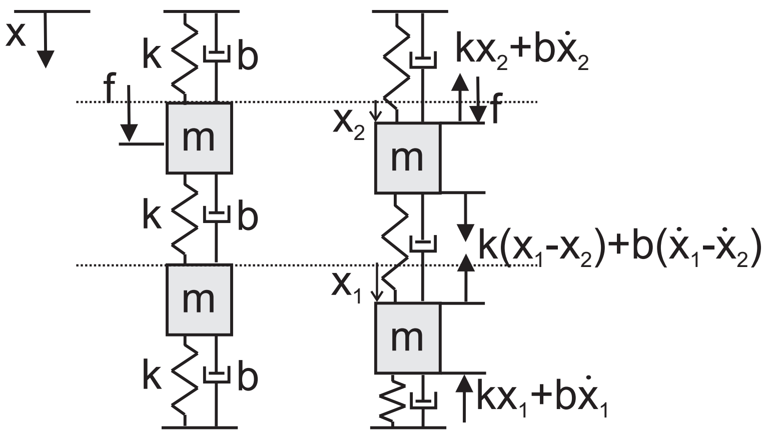

Figure 80: Two dofs system with damping

The equations of motion are obtained as in Section 5.1, taking into account the forces due to the dampers. In a matrix form, we have:

$$\begin{bmatrix} m & 0 \\ 0 & m \end{bmatrix} \begin{Bmatrix} \ddot{x_1} \\ \ddot{x_2} \end{Bmatrix} + \begin{bmatrix} 2b & -b \\ -b & 2b \end{bmatrix} \begin{Bmatrix} \dot{x_1} \\ \dot{x_2} \end{Bmatrix} + \begin{bmatrix} 2k & -k \\ -k & 2k \end{bmatrix} \begin{Bmatrix} x_1 \\ x_2 \end{Bmatrix} = \begin{Bmatrix} 0 \\ f \end{Bmatrix}$$

which can be written in a compact form

$$M\ddot{x} + C\dot{x} + Kx = f \tag{31}$$

where C is the damping matrix.

5.2.1 General solution of the equations of motion

The general solution of the equations of motion of a damped mdof system can be obtained by posing

$$\left\{ \begin{array}{c} x_1(t) \\ x_2(t) \end{array} \right\} = \left\{ \begin{array}{c} A_1 \\ A_2 \end{array} \right\} e^{rt} = \psi e^{rt}$$

Equation (31) becomes

$$\left(K + rC + r^2 M\right) \psi = 0$$

which admits non-trivial solutions for the roots of

$$det(K + rC + r^2 M) = 0$$

The roots of this determinant are complex, and the free response is characterised by oscillatory functions with an exponentially decaying envelope in the time domain. The associated eigenvectors are also complex, which means that their different components are not in phase. As it is not very common to use complex mode shapes in structural dynamics, we will not discuss them in further details.

5.2.2 Particular solution of the equations of motion

An alternative to the use of complex mode shapes is to calculate the response of the system using the real mode shapes associated to the K and M matrices. Let us start from equation (31) and decompose the solution of the problem in the basis of the mode shapes:

$$x(t) = \sum_{i=1}^{n} z_i(t) \psi_i$$

which can be written in a matrix form :

$$x = \Psi z$$

where z is the vector of modal amplitudes. Let us replace x by Ψz in (31) and premultiply by Ψ^T, we have:

$$\Psi^T M \Psi \ddot{z} + \Psi^T C \Psi \dot{z} + \Psi^T K \Psi z = \Psi^T f$$

In general, the term $\Psi^T C \Psi$ is not diagonal and the equations remain coupled. An approximation can be obtained however in the following cases:

- Rayleigh damping: this damping model assumes that the matric C can be written as:

  $$C = \alpha K + \beta M$$

  In such a case, the term $\Psi^T C \Psi$ reduces to:

  $$\Psi^T C \Psi = \Psi^T (\alpha K + \beta M) \Psi = diag(\alpha \mu_i \omega_i^2 + \beta \mu_i)$$

  This model is often used as an approximation in order to decouple the equations, but the model has no physical meaning.

- Modal damping: when the damping is small, the off-diagonal terms of $\Psi^T C \Psi$ can be neglected, and it reduces to:

$$\Psi^T C \Psi = \begin{bmatrix} 2\mu_1\xi_1\omega_1 & 0 & ... & 0 \\ 0 & 2\mu_2\xi_2\omega_2 & ... & 0 \\ ... & ... & ... & ... \\ 0 & 0 & ... & 2\mu_n\xi_n\omega_n \end{bmatrix}$$

  where we have introduced the modal damping ξ_i.

The modal damping is a more general and flexible model than Rayleigh damping. This can easily be shown by equating the result of the product $\Psi^T C \Psi$ in the two models:

$$diag(\alpha\mu_i\omega_i^2 + \beta\mu_i) = diag(2\xi_i\mu_i\omega_i)$$

which leads to :

$$\xi_i = \frac{1}{2}\left(\alpha\omega_i + \frac{\beta}{\omega_i}\right)$$

In the modal damping model, the damping coefficient of each mode can be set independently, while in the Rayleigh damping model, the modal damping coefficients have a specific evolution which is a function of only two coefficients α and β. An example of evolution of the coefficients ξ_i for a Rayleigh damping model is shown in Figure 81, where it can be seen that the model leads to very high values of damping at low frequencies and at high frequencies. Such values are in general not in accordance with the damping level at those frequencies, and the Rayleigh model can only fit to two values of ξ_i. In general, it is difficult to obtain an accurate model of matrix C and to determine the modal damping coefficients ξ_i. In the absence of experimental results which could be used to identify these values, a fixed value can be used. This fixed value depends on the type of structure considered. It is of common practice to use a fixed value of $\xi = 0.01$ in the absence of information about the damping.

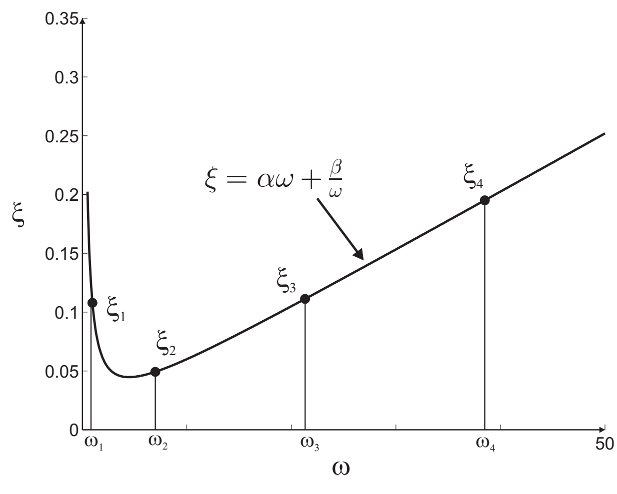

Figure 81: Evolution of the modal damping coefficients for the Rayleigh damping model

Using the more general form of the modal damping model, we find:

$$diag(\mu_i)\ddot{z} + diag(2\xi_i\mu_i\omega_i)\dot{z} + diag(\mu_i\omega_i^2)z = \Psi^T f$$

which is a set of n uncoupled equations of the type

$$\mu_i \ddot{z}_i + 2\xi_i \mu_i \omega_i z + \mu_i \omega_i^2 z_i = F_i \tag{32}$$

Equation (32) corresponds to the equation of motion of a damped single dof system with

- a mass μ_i, called the modal mass
- a stiffness $\mu_i \omega_i^2$
- a damping coefficient ξ_i
- a natural frequency $\omega_i = 2\pi f_i$
- a force $F_i = \psi_i^T f$ (modal excitation)

The particular solution can be calculated in the frequency domain following the same approach, assuming $x(t) = Xe^{i\omega t}$ and $f(t) = Fe^{i\omega t}$ where X and F are complex vectors of sine n, we have:

$$\left(K + i\omega C - \omega^2 M\right) X = F \tag{33}$$

the solution X is written as a function of the mode shapes:

$$X(\omega) = \sum_{j=1}^{n} Z_j(\omega)\psi_j$$

which can be written in a matrix form:

$$X = \Psi Z$$

where Z is a complex vector of modal amplitudes. Let us replace in (30), and premultiply by Ψ^T, we have:

$$\left(\Psi^T K \Psi + i\omega \Psi^T C \Psi - \omega^2 \Psi^T M \Psi\right) Z = \Psi^T F$$

and using the orthogonality properties and the modal damping model:

$$\mu_j(\omega_j^2 - \omega^2 + 2i\xi_j \omega \omega_j) Z_j = F_j$$

We obtain a set of n decoupled equations. The unknowns Z_j can easily be solved for:

$$Z_j(\omega) = \frac{\psi_j^T F}{\mu_j(\omega_j^2 - \omega^2 + 2i\xi_j \omega \omega_j)}$$

The Bode diagram of Z_i is identical to the Bode diagram of a damped single dof system and will present a damped resonant peak at the angular frequency ω_i. Due to the damping, Z_i is complex. The displacement $X(\omega)$ can be retrieved by summing the contributions of the different mode shapes:

$$X(\omega) = \sum_{j=1}^{n} Z_j(\omega)\psi_j = \sum_{j=1}^{n} \frac{\psi_j^T F \psi_j}{\mu_j(\omega_j^2 - \omega^2) + 2i\xi_j \omega \omega_j}$$

Illustration: two degrees of freedom system

Let us consider the system represented in Figure 80, and take the following values for the different coefficients: $k = 1N/m$, $m = 1kg$ and $b = 0.04Ns/m$. In the present case, matrix C is proportionnal to matrix K and the product $\Psi^T C \Psi$ is diagonal. We calculate the valus of ξ_j: $\xi_1 = 2\%$ and $\xi_2 = 3.5\%$. The forced response of mass 2 as a function of the frequency is represented on Figure 82. Note that the second peak is more damped than the first one due to the fact that $\xi_2 > \xi_1$.

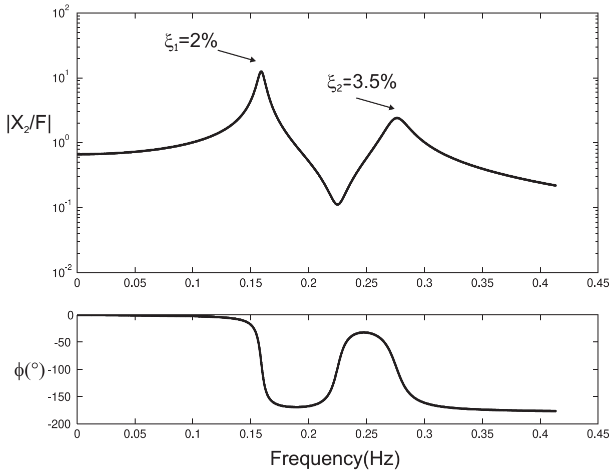

Figure 82: Bode diagram for mass 2 of the two dofs system with a damping matrix propotionnal to the stiffness matrix

Let us now remove the damper between mass 1 and the ground (Figure 83). Matrix C is not proportional to matrix K anymore so that the product $\Psi^T C \Psi$ is not diagonal. Let us neglect the off-diagonal terms and compute the modal damping coefficients. We get $\xi_1 = 1\%$ eand $\xi_2 = 2.9\%$. On Figure 84, the Bode diagram for mass 2 is plotted and the solution found neglecting the off-diagonal terms is compared to the solution obtained with the coupled equations (no terms neglected). The figure shows that the solutions are almost identical. It is therefore justified to neglect the off-diagonal terms because the damping is small.

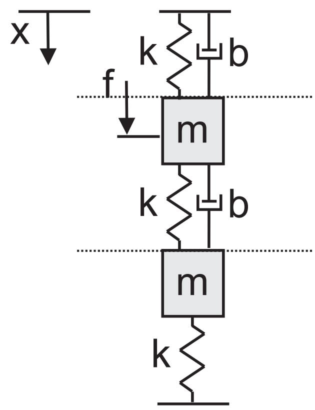

Figure 83: Two dofs system with damping - the viscous damper between the ground and mass 1 has been removed

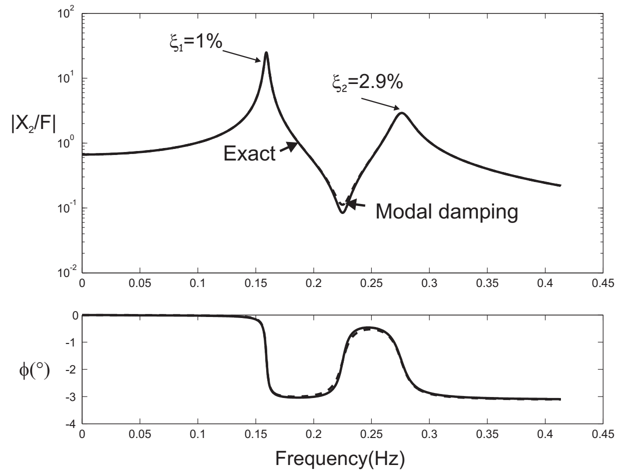

Figure 84: Bode diagram for mass 2 of the two dofs system with a non-proportionnal damping: comparison between the exact solution and the approximation using the modal damping model for a low value of damping

Let us now assume that the damping coefficient is $b = 0.2Ns/m$. The modal damping coefficients are $\xi_1 = 5\%$ et $\xi_2 = 14.43\%$ which cannot be considered as small damping anymore. In this case, as shown in Figure 85, the modal damping model deviates from the exact solution.

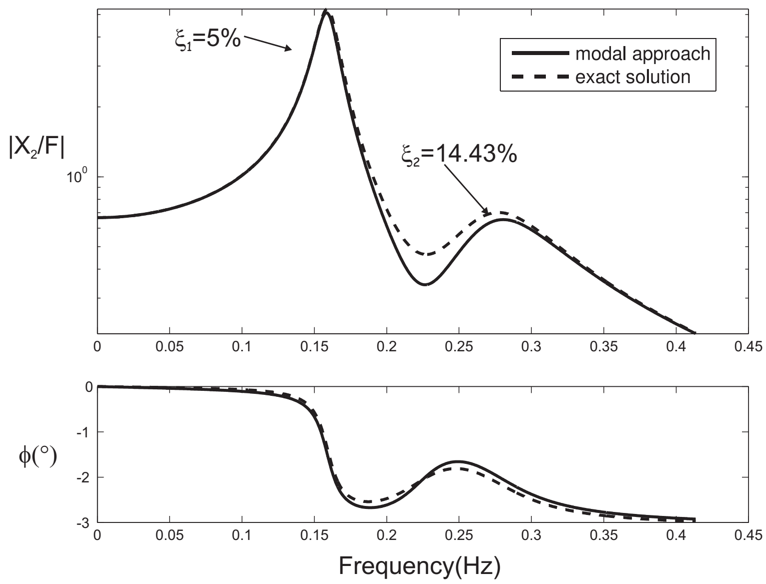

Figure 85: Bode diagram for mass 2 of the two dofs system with a non-proportionnal damping: comparison between the exact solution and the approximation using the modal damping model for a high value of damping

5.3 MDOF application: the tuned mass damper

A tuned mass damper (TMD) is a device that it attached to a primary structure in order to damp its vibrations. The first type of tuned mass damper we are going to study is a mass-spring system . In this study, we assume that the primary system is modeled by an equivalent 1 DOF system (Figure 86).

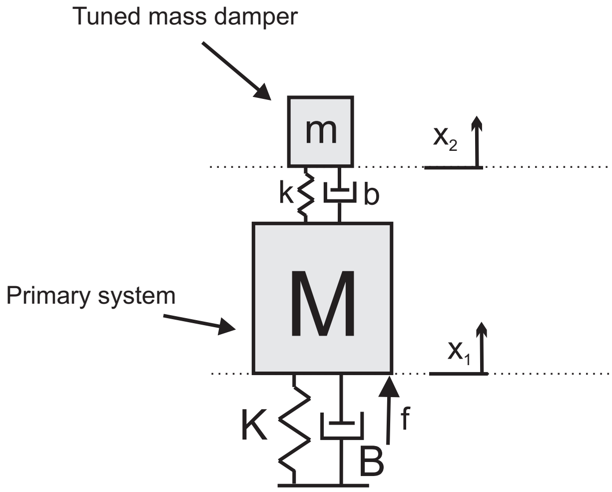

Figure 86: A mass-spring tuned mass damper (TMD) attached to a primary structure modeled as a 1 DOF system

The equations of motions of this 2 DOFs system are:

$$\begin{bmatrix} M & 0 \\ 0 & m \end{bmatrix} \begin{Bmatrix} \ddot{x_1} \\ \ddot{x_2} \end{Bmatrix} + \begin{bmatrix} B+b & -b \\ -b & b \end{bmatrix} \begin{Bmatrix} \dot{x_1} \\ \dot{x_2} \end{Bmatrix} \begin{bmatrix} K+k & -k \\ -k & k \end{bmatrix} \begin{Bmatrix} x_1 \\ x_2 \end{Bmatrix} = \begin{Bmatrix} f \\ 0 \end{Bmatrix}$$

In the frequency domain, we have $x_1(t) = X_1 e^{i\omega t}$, $x_2(t) = X_2 e^{i\omega t}$, and $f(t) = F e^{i\omega t}$ which leads to:

$$\begin{bmatrix} K+k+i\omega(B+b)-\omega^2 M & -(k+i\omega b) \\ -(k+i\omega b) & k-\omega^2 m + i\omega b \end{bmatrix} \begin{Bmatrix} X_1 \\ X_2 \end{Bmatrix} = \begin{Bmatrix} F \\ 0 \end{Bmatrix}$$

we solve for the displacement of the primary system X_1:

$$X_1/F = \frac{k-\omega^2 m + i\omega b}{(K+k+i\omega(B+b)-\omega^2 M)(k-\omega^2 m+i\omega b)-(k+i\omega b)^2}$$

Let us first consider the case where there is no damping in the TMD ($b = 0$). In this case, we have:

$$X_1/F = \frac{k-\omega^2 m}{(K+k+i\omega B-\omega^2 M)(k-\omega^2 m)-k^2}$$

We see that the displacement of the primary structure X_1 will be zero at a frequency given by

$$\omega = \sqrt{\frac{k}{m}}$$

which is the natural frequency ω_n of the TMD. If one wishes to cancel the vibration at the resonant frequency of the primary structure $\Omega = \sqrt{K/M}$, we need to have

$$\omega_n = \Omega$$

We define the frequency ratio $\nu = \omega_n/\Omega$. In order to cancel the vibration at the resonant frequency of the primary structure, we need to have $\nu = 1$: the TMD is ”tuned” to the eigenfrequency of the primary structure. Figure 87 shows the Bode diagram of X_1 for the primary structure with and without the TMD. The addition of the TMD results in an anti-resonance at the natural frequency of the primary structure Ω. The amplitude of the vibration is also reduced in a narrow frequency band around Ω. Outside this frequency band, the amplitude of vibration is increased, and there are now two resonant peaks leading to a very large amplification around the two eigenfrequencies of the system. The use of such a device is interesting only if the excitation source is in a narrow band around the natural frequency. Otherwise, although the amplitude around the resonance is decreased, it is increased at other frequencies, so the problem is only shifted in frequency.

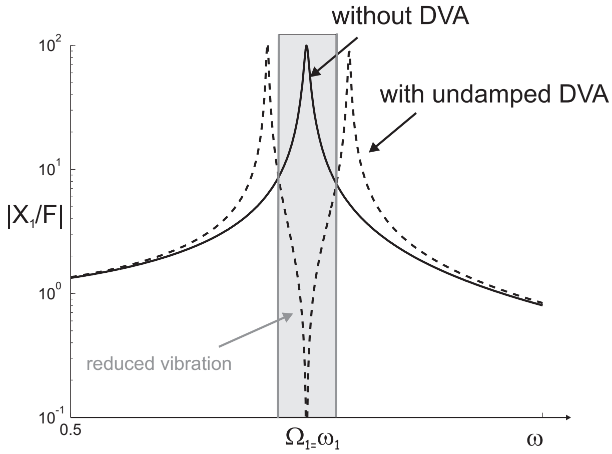

Figure 87: Effect of an undamped TMD on the primary structure's response X_1

If one wishes to lower the vibration of the primary structure X_1 in a wide frequency band around its natural frequency Ω, it is necessary to introduce damping in the TMD ($b \neq 0$). Figure 88 shows the response of the system for different values of b and for a tuning parameter $\nu = 1$. The mass ratio defined as $\mu = m/M$ is equal to 3%.

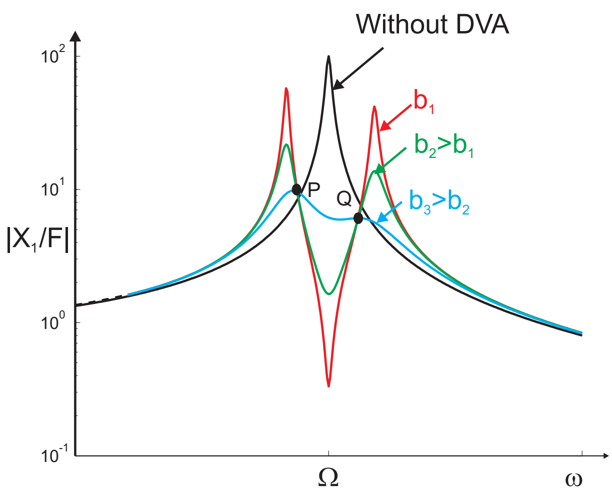

Figure 88: Effect of a damped TMD on the primary structure's response X_1

Note the existence of two points P and Q where all the curves for the different values of b cross. The optimal tuning of a TMD consists in finding the parameters m, k and b such that the two points

P and Q are at the same height, and such that the response X_1 is maximum at these two points. Den Hartog derived simple equations which lead to an approximation of this optimal TMD. The equation leading to the same height for P and Q is given by

$$\nu = \frac{1}{1+\mu} \tag{34}$$

In general, the value of the mass m is chosen a priori. For practical reasons, it is chosen such that μ does not exceed a few percents of the mass of the primary system. Equation (34) is then used to determine the value of k. The optimal damping is then found with

$$\xi = \sqrt{\frac{3\mu}{8(1+\mu)}} = \frac{b}{2\sqrt{km}} \tag{35}$$

which gives the optimal value for b. The response of the primary structure with an optimal TMD is shown in Figure 89.

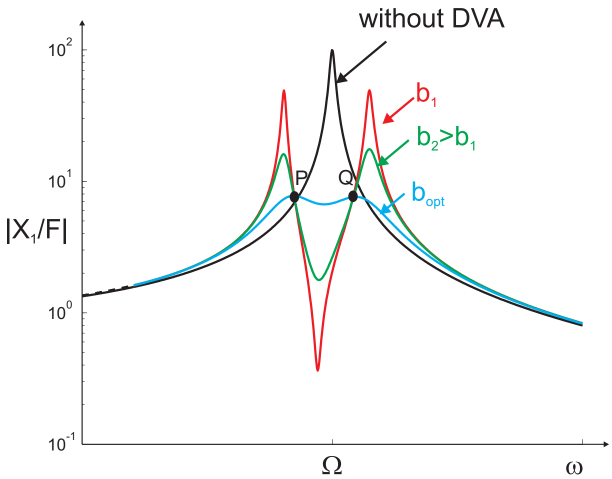

Figure 89: Effect of the optimal TMD on the primary structure's response X_1

There are many examples of installation of TMDs on civil engineering structures, such as:

- The Millenium Bridge, for which this solution was adopted due to the large vibrations induced by pedestrians walking on the bridge which led to the closure of the bridge directly after its opening.

http://www.gerb.com

- The John Hancock Tower in Boston (1976), where two TMDs consisting of large steel blocks of approx 5.2x5.2x1m (weighting 270 Tons) were installed at the top of the tower (tuned to 0.14 Hz).

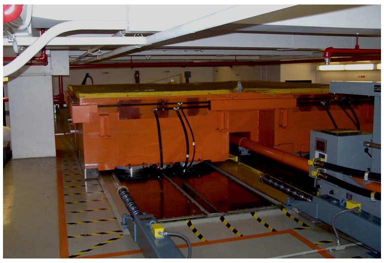

http://www.lemessurier.com

- The city corp Center in New York (1977), where 1 TMD of 400 Tons acting in two directions has been installed (tuned to 0.16 Hz).

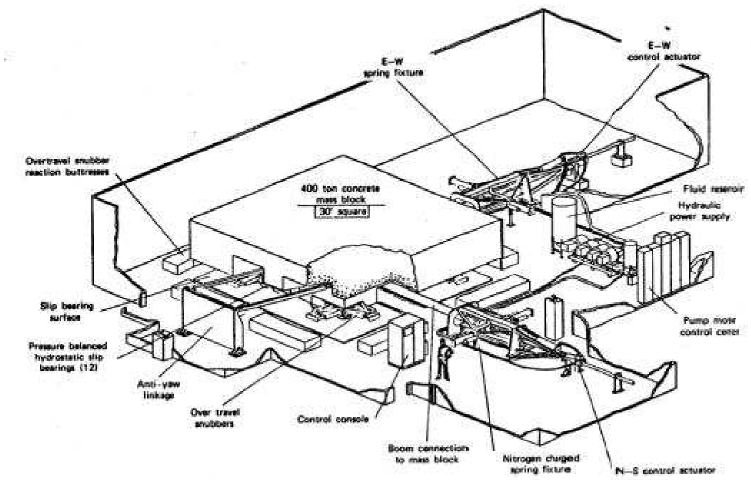

http://www.estructura.it

- The Chiba Port Tower (Japan - 1986), where 1 TMD of 15 Tons acting in two directions has been installed (0.44 Hz).

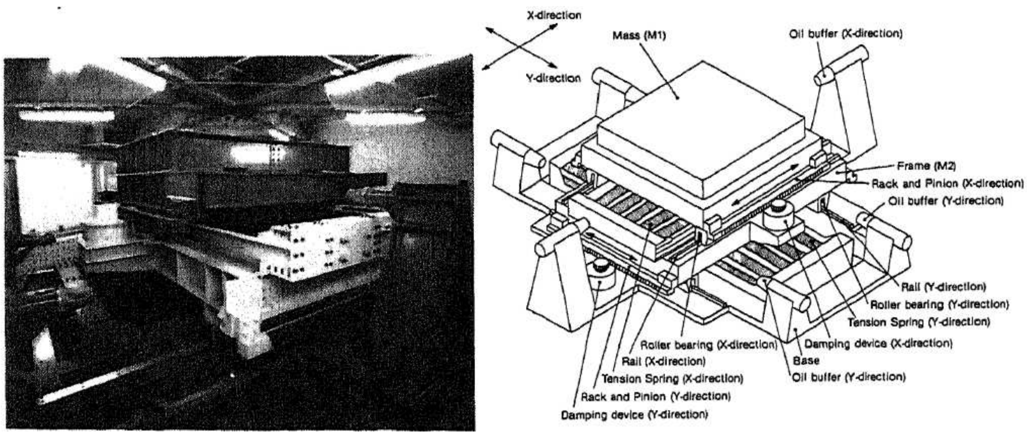

http://www.iitk.ac.in

The two following movies demonstrate the efficiency of a TMD applied to a host structure:

```
Undamped pendulum tuned mass damper:
             http://www.youtube.com/watch?v=bqJadkufes4
Tuned mass damper on a bridge:
             http://www.youtube.com/watch?v=e01_3mUGeyw
```

The second type of TMD we are going to study is the pendulum TMD. Instead of a mass-spring system, a pendulum is attached to the primary structure (Figure 91). Here again, the primary structure is modeled as a one DOF system. Note that the direction of motion is always horizontal for this type of TMD. A mass-spring TMD can be implemented to damp the motion either in the horizontal, or the vertical direction.

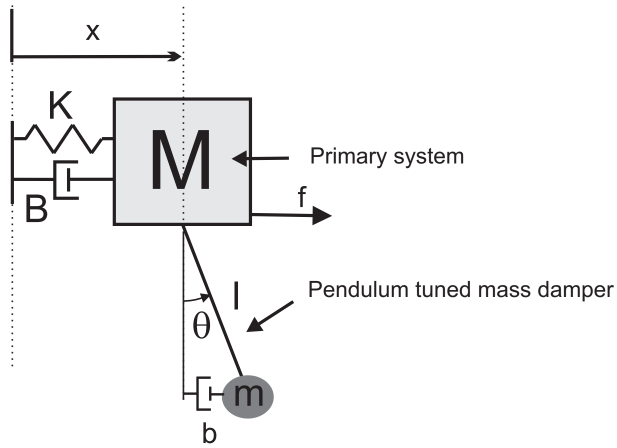

Figure 90: A pendulum TMD attached to a primary structure modeled as a 1 DOF system

The equations of the PTMD attached to the primary structure are non-linear. After linearization (θ small $\Rightarrow \cos\theta \simeq 1$, $\sin\theta \simeq \theta$ and $\dot{\theta}^2$ neglected), they are given by:

$$\begin{aligned} (M+m)\ddot{x} + ml\ddot{\theta} + Kx + B\dot{x} &= f \\ m(\ddot{x} + l\ddot{\theta}) + mg\theta + &= 0 \end{aligned}$$

In the frequency domain, we have $x(t) = Xe^{i\omega t}$, $\theta(t) = \Theta e^{i\omega t}$ and $f(t) = Fe^{i\omega t}$ which leads to:

$$\begin{bmatrix} K + i\omega B - \omega^2(M+m) & -ml\omega^2 - i\omega bl \\ -\omega^2 m & mg + i\omega bl - \omega^2 ml \end{bmatrix} \begin{Bmatrix} X \\ \Theta \end{Bmatrix} = \begin{Bmatrix} F \\ 0 \end{Bmatrix}$$

We solve the equation for the displacement of the primary structure X

$$\frac{X}{F} = \frac{\frac{mg}{l} + i\omega b - \omega^2 m}{(K + i\omega B - \omega^2(M+m))(\frac{mg}{l} + i\omega b - \omega^2 m) - \omega^2 m(i\omega b + \omega^2 m)}$$

Let us first consider the case where there is no damping in the PTMD, we have:

$$\frac{X}{F} = \frac{\frac{mg}{l} - \omega^2 m}{(K + i\omega B - \omega^2(M+m))(\frac{mg}{l} - \omega^2 m) - (\omega^2 m)^2}$$

Let us define

$$\omega_n = \sqrt{\frac{g}{l}}$$

which is the eigenfrequency of the undamped TMD and

$$\Omega = \sqrt{\frac{K}{M}}$$

which is the eigenfrequency of the primary structure without the TMD. In order to cancel the vibration at the eigenfrequency of the primary structure, we need to have $\nu = 1$ where

$$\nu = \frac{\omega_n}{\Omega}$$

Figure 91 shows the response of the primary structure X with and without PTMD ($\nu = 1$) and for several values of the mass of the pendulum. Note that the eigenfrequency of a pendulum only depends on its length, and not on its mass, so the tuning is not altered when the mass is increased. We see that the two peaks are further apart as the mass increases. As in the case of the mass-spring TMD, when there is no damping, the vibration can be canceled at the resonant frequency of the primary structure, but we note the appearance of two peaks away from that resonant frequency. The device is therefore only suited when one wants to decrease the vibration in a narrow frequency band around the resonance (the frequency band can be made larger if one increases the mass of the PTMD).

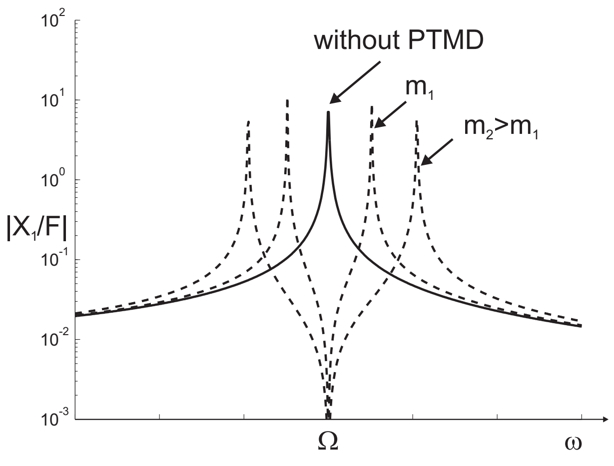

Figure 91: Response of the primary structure to which and undamped PTMD is attached

Let us now consider the case of the damped PTMD. As the equations are different from the mass-spring TMD, we cannot apply equations (34) and (35). The first tuning rule is given by:

$$\nu = \sqrt{\frac{2}{(2+3\mu)(1+2\mu)}}$$

The second rule is much more complex and given by:

$$r = \frac{\sqrt{2}\sqrt{\mu}\sqrt{3\sqrt{\mu}\sqrt{3\,\mu^2+4\,\mu+1}\sqrt{3\,\mu+2}-9\,\mu^2-11\,\mu-3}}{\sqrt{-3\,\mu^2-5\,\mu+\sqrt{\mu}\sqrt{3\,\mu^2+4\,\mu+1}\sqrt{3\,\mu+2}-2\sqrt{3\,\mu+2}\,(4\,\mu+2)}}$$

with

$$r = \frac{b}{2m\Omega}$$

This expression can be fairly well approximated by a fifth order polynomial:

$$r = -4351\mu^4 + 1074\mu^3 - 99.1\mu^2 + 4713\mu + 0.0167$$

for values of $\mu < 0.1$.
The response of the primary system with an optimal PTMD is represented on Figure 92.

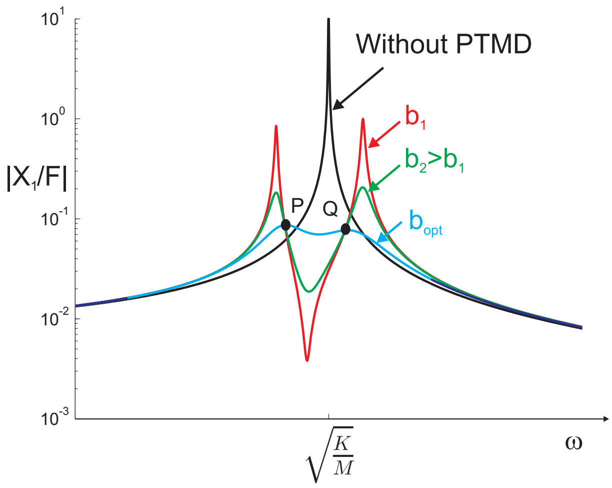

Figure 92: Response of the primary structure to which an optimal damped PTMD is attached

The most famous PTMD is the one in the Taipei 101 building (Figure 93), in Taiwan. The damper consist of a steel sphere 6 meters across and weighting 728 tons, suspended from the 92nd to the 87th floor.

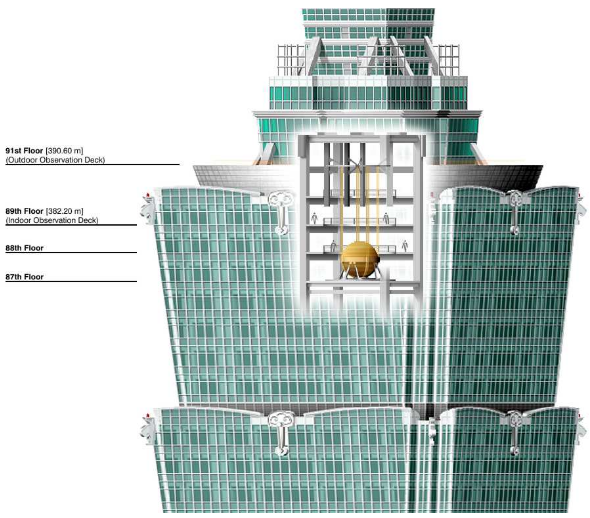

Figure 93: The Taipei 101 building with a PTMD (http://en.wikipedia.org/wiki/Tuned_mass_damper)

For more details on the building and the attached PTMD, see:

Taipei Discovery Channel: http://www.youtube.com/watch?v=xF7foZ-oiSo
Taipei 101 sketch of pendulum: http://www.youtube.com/watch?v=uybEXOkkrsw
Taipei TMD Motion on May 12, 2008 : http://www.youtube.com/watch?v=NYSgd1XSZXc

Additional movies (not played in class)

Citicorp Center
http://www.youtube.com/watch?v=TZhgTewKhTQ
http://www.youtube.com/watch?v=4fUwgH0gOWo
http://www.youtube.com/watch?v=IBjyB8EY2m4#t=2

6 Continuous systems

In the previous chapters, we have studied systems which can be simplified and modeled as masses connected with springs and dampers. In the real world, structures are always continuous. Some continuous structures can be simplified and be modeled as beams or bars, while others cannot. In the first part of this section, we will discuss the computation of the dynamic response of bars and beams. The second part will be devoted to the computation of the dynamic response of more general continuous structures. A continuous system can be seen as the limit when n tends to infinity of a n dofs system. A continuous system therefore has an infinite number of eigenfrequencies and mode shapes.

6.1 Beams and bars

6.1.1 Boundary conditions for beams and bars

If we consider a bar in traction, the displacement is in the x direction (Figure 94). At $x = 0$ and $x = L$, the bar can either be free or fixed. A fixed condition corresponds to $x = 0$, while a free condition corresponds to the absence of an applied normal force $N = E\varepsilon = E\frac{du}{dx}$, which we usually simplify to $u' = \frac{du}{dx}$=0 (Figure 95).

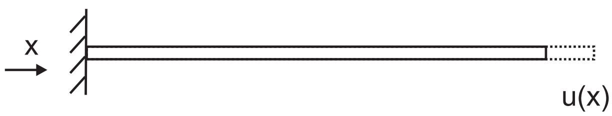

Figure 94: Bar in traction: the displacement is in the x direction

Figure 95: Boundary conditions for bars in traction

If we consider a beam in bending, the displacement is in the y direction (Figure 96). At $x = 0$ and $x = L$, there are four possible boundary conditions. The first two boundary conditions are linked to the vertical displacement which is either fixed ($y = 0$) or free (the shear force $T = -EIy^{III} = 0$, which can be simplified to $y^{III} = 0$), while the second set of boundary conditions is linked to the rotation which is either fixed ($y' = 0$) or free (the bending moment $M = -EIy'' = 0$, which can be simplified to $y'' = 0$) (Figure 97).

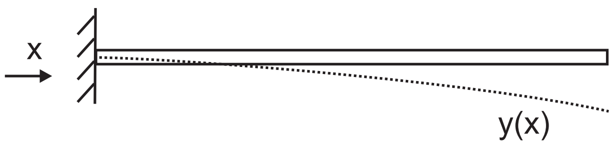

Figure 96: Bar in bending: the displacement is in the y direction

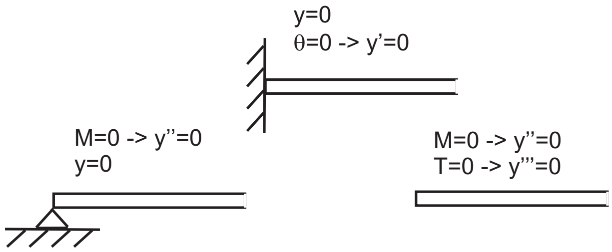

Figure 97: Boundary conditions for beams in bending

6.1.2 Bar in traction: equation of motion

The equation of motion for a bar in traction can be found by isolating a small part of the bar of length dx as shown in Figure 98:

$$-N + p(x,t)\,dx + N + dN = (\rho A \ddot{u}(x,t))\,dx$$

where $p(x,t)$ is the load per unit of length in direction x, ρ is the density of the material (kg/m^3) and A is the area of the section of the bar. This expression leads to

$$\frac{dN}{dx} = \frac{\partial}{\partial x}\left(EA\frac{\partial u}{\partial x}\right) = EA\frac{\partial^2 u(x,t)}{\partial x^2} = \rho A \ddot{u}(x,t) - p(x,t)$$

assuming EA is constant. We therefore have

$$EA\frac{\partial^2 u(x,t)}{\partial x^2} - \rho A \ddot{u}(x,t) = -p(x,t) \tag{36}$$

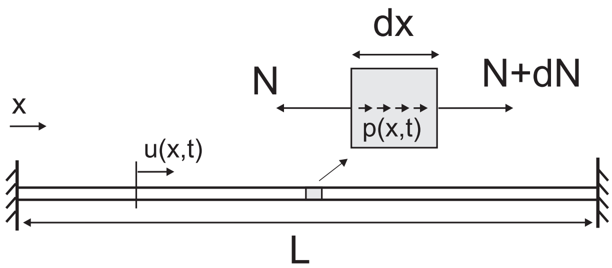

Figure 98: Equilibrium of a small part of a bar of length dx

6.1.3 Bar in traction: mode shapes and eigenfrequencies

Assuming $u(x,t) = U(x)e^{i\omega t}$, the mode shapes and eigenfrequencies are the solution of the equation of motion with the right-hand side equal to 0:

$$EA\frac{d^2U}{dx^2} + \rho A \omega^2 U = 0$$

which can be rewritten

$$\frac{d^2U}{dx^2} + \frac{\rho}{E}\omega^2 U = 0$$

This equation is of the second order for the variable x, the general solution can therefore be written $U(x) = Ae^{rx}$ and the characteristic equation is given by:

$$r^2 + \frac{\rho}{E}\omega^2 = 0$$

The two roots are

$$r_{1,2} = \pm i\omega\sqrt{\frac{\rho}{E}}$$

and the general solution is:

$$U(x) = Acos(\omega\sqrt{\frac{\rho}{E}}x) + Bsin(\omega\sqrt{\frac{\rho}{E}}x)$$

The constants A and B are a function of the boundary conditions. For a fixed-fixed bar, we have:

$$\begin{aligned} U(0) &= 0 \Rightarrow A = 0 \\ U(L) &= Bsin(\omega\sqrt{\frac{\rho}{E}}L) = 0 \end{aligned}$$

There exists a non-trivial solution if we have

$$\omega\sqrt{\frac{\rho}{E}}L = n\pi \qquad n = 1, ..., \infty$$

The eigenfrequencies are therefore given by

$$\omega_n = n\frac{\pi}{L}\sqrt{\frac{E}{\rho}} \qquad n = 1, ..., \infty$$

and the associated mode shapes

$$U(x)_n = sin(\frac{n\pi x}{L}) \qquad n = 1, ..., \infty$$

The three first traction mode shapes of a concrete cylinder are represented in Figure 99. The color code corresponds to the amplitude of displacement in the axial direction. One can see clearly the presence of nodes of vibration (zero displacement) in modes 2 and 3 (in addition to the faces of the cylinder which are also fixed).

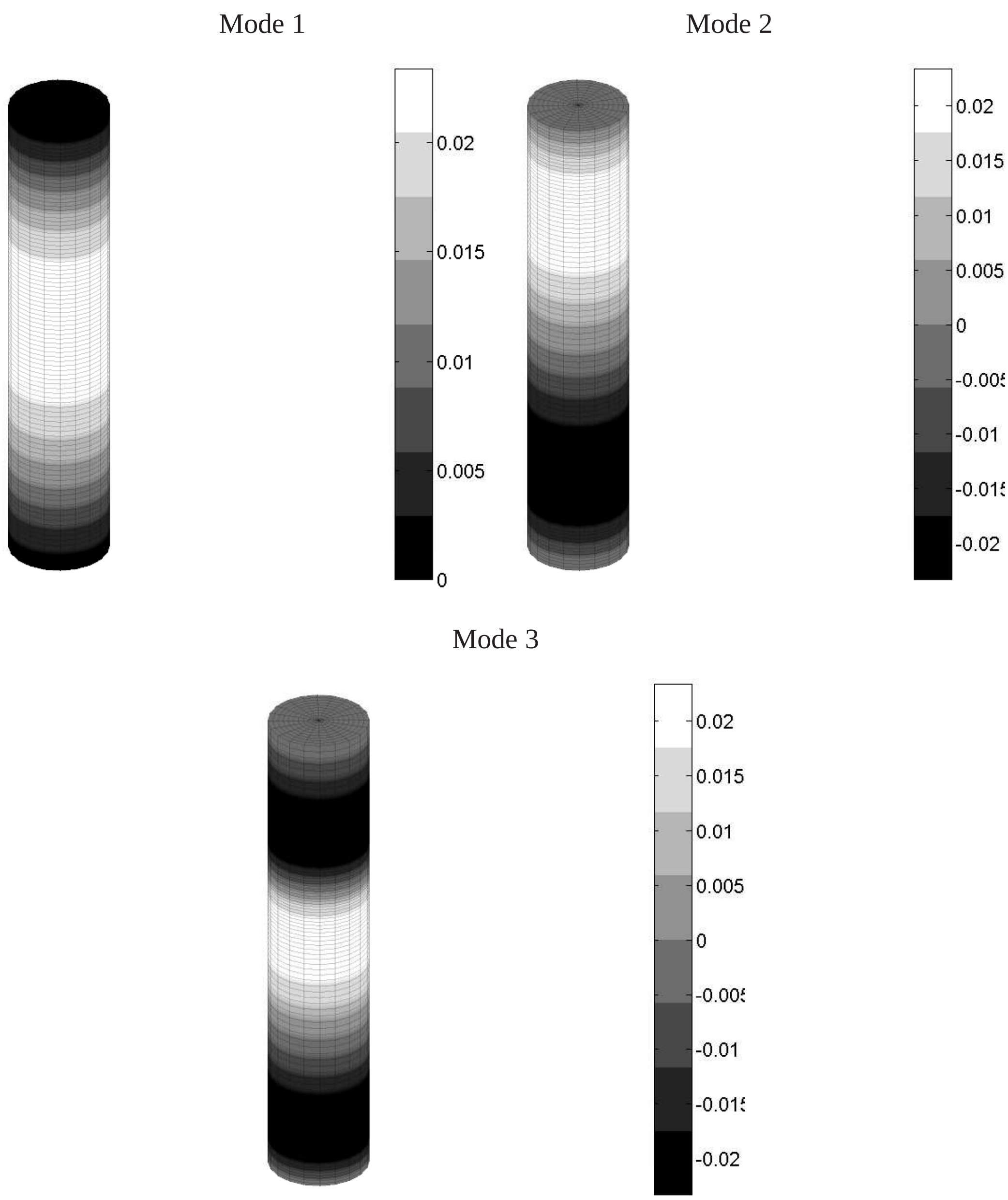

Figure 99: First three modes of a bar in traction

6.1.4 Bar in traction: orthogonality conditions

For bars in traction, the orthogonality conditions are given by:

$$\int_0^L \rho A U_i \, U_j \, dx = \delta_{ij} \mu_i$$

$$\int_0^L EA U_i' \, U_j' \, dx = \delta_{ij} \mu_i \omega_i^2$$

Proof: Let us consider two different mode shapes U_i and U_j where $\omega_i \neq \omega_j$:

$$\begin{aligned} EAU_i'' + \rho A \omega_i^2 U_i &= 0 \quad (37) \\ EAU_j'' + \rho A \omega_j^2 U_j &= 0 \quad (38) \end{aligned}$$

we multiply (37) by U_j and integrate from 0 to L, and multiply (38) by U_i and integrate from 0 to L.

$$\int_0^L \left(EAU_i'' + \rho A \omega_i^2 U_i \right) U_j \, dx = 0 \quad (39)$$

$$\int_0^L \left(EAU_j'' + \rho A \omega_j^2 U_j \right) U_i \, dx = 0 \quad (40)$$

Integrating by parts, we have

$$\int_0^L EAU_i'' U_j \, dx = \left[EAU_i' U_j \right]_0^L - \int_0^L EAU_i' U_j' \, dx$$

$$\int_0^L EAU_j'' U_i \, dx = \left[EAU_j' U_i \right]_0^L - \int_0^L EAU_j' U_i' \, dx$$

The terms

$$\left[EAU_i' U_j \right]_0^L$$

and

$$\left[EAU_j' U_i \right]_0^L$$

are always equal to zero because at $x = L$ and $x = 0$ we either have $U = 0$ or $U' = 0$. We thus have

$$\int_0^L EAU_i'' U_j \, dx = -\int_0^L EAU_i' U_j' \, dx$$

$$\int_0^L EAU_j'' U_i \, dx = -\int_0^L EAU_j' U_i' \, dx$$

replacing in (39) and (40) we have:

$$\int_0^L \left(-EAU_i' U_j' + \rho A \omega_i^2 U_i U_j \right) \, dx = 0 \quad (41)$$

$$\int_0^L \left(-EAU_j' U_i' + \rho A \omega_j^2 U_j U_i \right) \, dx = 0 \quad (42)$$

Substracting (42) from (41), we have:

$$\int_0^L \rho A (\omega_i^2 - \omega_j^2) U_i U_j \, dx = 0 \quad i \neq j$$

which leads to

$$\int_0^L \rho A U_i U_j \, dx = 0 \quad i \neq j \quad (43)$$

and defining

$$\mu_i = \int_0^L \rho A U_i^2 \, dx \quad (44)$$

(43) and (44) give the second orthogonality condition. We can rewrite (41):

$$\int_0^L EA\,U_i' U_j'\,dx = \int_0^L \rho A \omega_i^2 U_i U_j dx$$

and taking into account (43) and (44), we have:

$$\int_0^L EA\,U_i' U_j'\,dx = 0 \quad i \neq j$$

$$\int_0^L EA\,U_i'^2\,dx = \omega_i^2 \mu_i$$

which is the first orthogonality condition.

6.1.5 Bar in traction: projection in the modal basis

Starting from the equation of motion

$$EA\frac{\partial^2 u(x,t)}{\partial x^2} - \rho A \frac{\partial^2 u(x,t)}{\partial t^2} = -p(x,t)$$

we assume that the solution can be written as a function of the mode shapes:

$$u(x,t) = \sum_{i=1}^{\infty} U_i(x) z_i(t)$$

Plugging in the equation of motion, we get:

$$EA\sum_{i=1}^{\infty} U_i'' z_i - \rho A \sum_{i=1}^{\infty} U_i \ddot{z}_i = -p(x,t)$$

We multiply by U_j and integrate from 0 to L:

$$\int_0^L \left(EA \sum_{i=1}^{\infty} U_i'' z_i \right) U_j\,dx - \int_0^L \left(\rho A \sum_{i=1}^{\infty} U_i \ddot{z}_i \right) U_j\,dx = \int_0^L -p(x,t) U_j\,dx$$

and rearranging:

$$\int_0^L \left(EA \sum_{i=1}^{\infty} U_i'' U_j \right) z_i\,dx - \int_0^L \left(\rho A \sum_{i=1}^{\infty} U_i U_j \right) \ddot{z}_i\,dx = \int_0^L -p(x,t) U_j\,dx$$

We can then use the orthogonality conditions to have

$$\mu_i \ddot{z}_i + \mu_i \omega_i^2 z_i = F_i \tag{45}$$

with

$$F_i = \int_0^L p(x,t) U_i\,dx$$

Equation (45) is the equation of motion of a one dof system where

- μ_i is the modal mass
- ω_i is the angular eigenfrequency
- $\mu_i \omega_i^2$ is the stiffness
- F_i is the modal force

The solution of the equation of motion is therefore an infinite sum of the response of independent one dof systems.

6.1.6 Bar in traction: particular solution

Following the same approach as for the mdof systems studied in the previous chapter, we assume

$$u(x,t) = U(x)e^{i\omega t}$$
$$p(x,t) = P(x)e^{i\omega t}$$

and replace in (36) to get

$$EA\frac{d^2U(x)}{dx^2} + \rho A\omega^2 U(x) = -P(x)$$

We perform a projection in the modal basis:

$$U(x) = \sum_{i=1}^{\infty} U_i(x) Z_i$$

which leads to

$$\mu_i(\omega_i^2 - \omega^2)Z_i = \int_0^L P(x)U_i(x)$$

and

$$Z_i = \frac{\int_0^L P(x)U_i(x)}{\mu_i(\omega_i^2 - \omega^2)}$$

The harmonic solution is therefore:

$$U(x) = \sum_{i=1}^{\infty} \frac{\int_0^L P(x)U_i(x)}{\mu_i(\omega_i^2 - \omega^2)} U_i(x)$$

The solution is an infinite sum of sdof oscillator solutions, as shown in Figure 100.

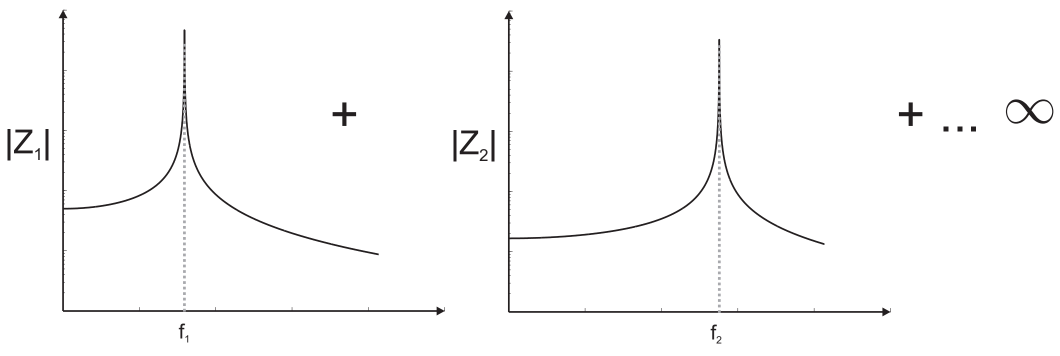

Figure 100: The response $X(\omega)$ is an infinite sum of the response of single dof systems with amplitude Z_i, i=1...n

At this point, it is interesting to note that although we have managed to transform the equation of motion into a set of independent equations, the number of equations is infinite, which poses a problem. The solution widely used is to truncate the sum in order to include only the n first mode shapes. The choice of n is dependent on the frequency range of interest for the computation. This is because a single mode has a significant influence on the response only at frequencies close to the associated eigenfrequency where the magnitude of the response is very high. A good rule of practice is to choose n such that

$$\omega < \frac{\omega_n}{1.5}$$

where ω is the maximum frequency in the frequency range of interest. This rule is purely empirical and is intended to make sure that all the modes with an eigenfrequency contained in the frequency band of interest are taken into account, with a safety margin. Figure 102 shows the example of a fixed-fixed bar of length L excited at a point located at a distance of $L/5$ and for which the displacement in the horizontal direction is computed at the same point where the excitation is applied (Figure 101). The exact solution is compared to a truncated solution where $n = 3$. The agreement is very good in the frequency band from 0 to 700 Hz. Note however that there are some discrepancies close to the anti-resonances. This is due to the contribution of the modes at higher frequencies which are not taken into account, and can be easily corrected with a so-called static correction. This is however out of the scope of this course.

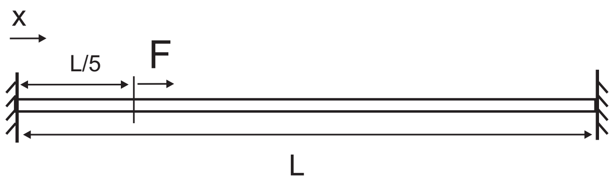

Figure 101: Fixed-fixed bar excited at L/5 in the horizontal direction

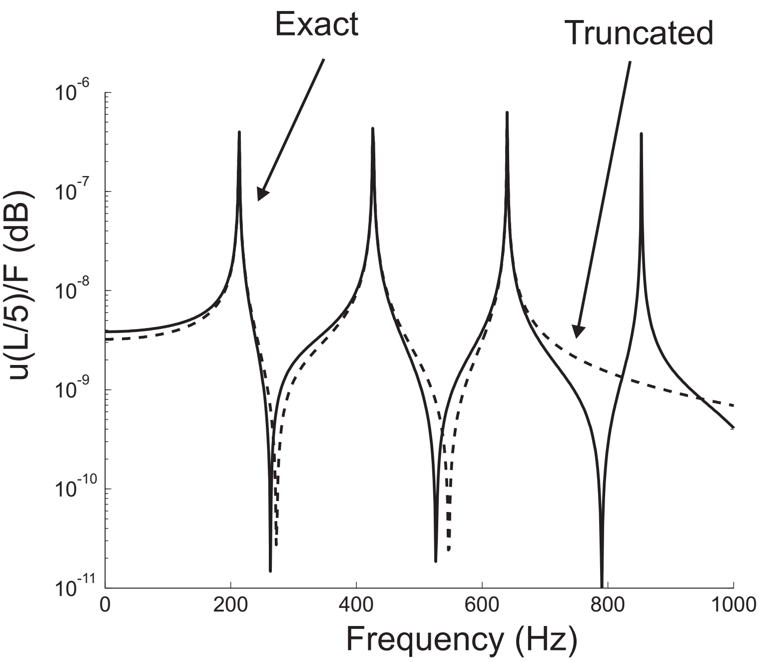

Figure 102: Comparison between the exact solution and a solution obtained by truncating the expansion in the modal basis to the third mode

6.1.7 Bar in traction: comparison with mdof systems

MDOF systems	Bar in traction

Orthogonality conditions

$\psi_i^T M \psi_j = \delta_{ij}\mu_i$	$\int_0^L \rho A U_i\, U_j\, dx = \delta_{ij}\mu_i$
$\psi_i^T K \psi_j = \delta_{ij}\mu_i\omega_i^2$	$\int_0^L EA U_i'\, U_j'\, dx = \delta_{ij}\mu_i\omega_i^2$

Projection in the modal basis

$$\boxed{\mu_i \ddot{z}_i + \mu_i \omega_i^2 z_i = F_i}$$

$F_i = \Psi^T F$	$F_i = \int_0^L p(x,t) U_i\, dx$

Response to harmonic excitation

$X(\omega) = \sum_{i=1}^{n} \frac{\psi_i^T F}{\mu_i(\omega_i^2 - \omega^2)} \psi_i$	$U(x) = \sum_{i=1}^{\infty} \frac{\int_0^L P(x) U_i(x)}{\mu_i(\omega_i^2 - \omega^2)} U_i(x)$

6.1.8 Beam in bending: equation of motion

The equation of motion for a beam in bending can be found by isolating a small part of the bar of length dx as shown in Figure 103:

$$-T + p(x,t)\,dx + T + dT = (\rho A\ddot{y})\,dx$$

where $p(x)$ is the vertical charge per unit of length. We know that $T = -EIy^{III}$ so that the equation of motion can be rewritten:

$$\frac{dT}{dx} = -EI\frac{d^4y}{dx^4} = \rho A\ddot{y} - p(x,t)$$

or

$$EI\frac{d^4y}{dx^4} + \rho A\ddot{y} = p(x,t)$$

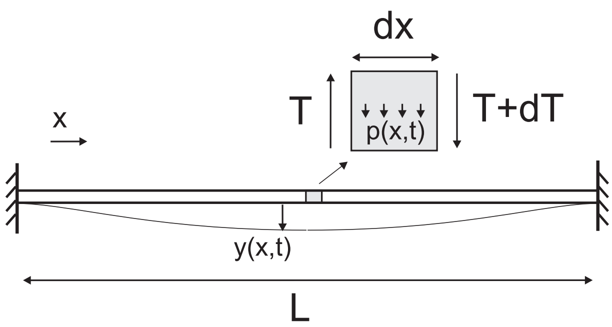

Figure 103: Equilibrium of a small part of a beam of length dx

6.1.9 Beam in bending: mode shapes and eigenfrequencies

Assuming $y(x,t) = Y(x)e^{i\omega t}$, the mode shapes and eigenfrequencies are the solution of the equation of motion with the right-hand side equal to 0:

$$EI\frac{d^4Y}{dx^4} - \rho A\omega^2 Y = 0$$

which can be rewritten:

$$\frac{d^4Y}{dx^4} - \frac{\rho A}{EI}\omega^2 Y = 0$$

Let us define

$$\xi^4 = \frac{\rho A}{EI}\omega^2$$

we have

$$\frac{d^4Y}{dx^4} - \xi^4 Y = 0$$

The characteristic equation is given by:

$$r^4 + \xi^4 = 0$$

It admits four roots

$$r_{1,2} = \pm i\xi$$
$$r_{3,4} = \pm\xi$$

and the general solution is written in the form

$$Y(x) = Acos(\xi x) + Bsin(\xi x) + Ccosh(\xi x) + Dsinh(\xi x)$$

The constants A, B, C and D depend on the boundary conditions

For a simply supported beam we have:

$$\begin{aligned} Y(0) &= A + C = 0 & \Rightarrow C = -A \\ Y''(0) &= \xi^2(-A + C) = 0 & \Rightarrow A = 0, C = 0 \end{aligned}$$

The solution therefore reduces to

$$Y(x) = Bsin\xi x + Dsinh\xi x$$

and taking into account the boundary conditions at $x = L$ we have:

$$Y(L) = B\sin\xi L + Dsinh\xi L = 0 \qquad (46)$$

$$Y''(L) = \xi^2(-B\sin\xi L + Dsinh\xi L) = 0 \qquad (47)$$

The system of equations admits a non trivial solution if the determinant is zero:

$$det\begin{pmatrix} \sin\xi L & sinh\xi L \\ -\sin\xi L & sinh\xi L \end{pmatrix} = 0$$

which leads to

$$\sin(\xi L)sinh(\xi L) = 0$$

Apart from the trivial solution $\xi = 0$, we have an infinite number of solutions corresponding to $\sin\xi L = 0$ which is true for

$$\xi L = n\pi \quad n = 1...\infty$$

We have

$$\xi^2 L^2 = \omega\sqrt{\frac{\rho A}{EI}}L^2$$

with $\xi L = n\pi$ which gives for the eigenfrequencies

$$\omega_n = \frac{n^2\pi^2}{L^2}\sqrt{\frac{EI}{\rho A}}$$

The mode shapes are obtained b replacing ξL by $n\pi$ in (46) , which leads to $D = 0$, and therefore

$$Y(x) = sin\frac{n\pi x}{L}$$

Mode shapes 1,5 and 10 are represented on Figure 104. This expression is identical to the mode-shapes of a bar in traction, but the motion here is in the vertical direction. The eigenfrequencies are proportional to the square root of the ratio of the bending rigidity EI and the mass per unit of length ρA. The difference with the bar in traction is the fact that the eigenfrequency is proportional to n for a bar in traction and to n^2 for a beam in bending. The eigenfrequencies are therefore equally spaced in frequency for a bar in traction but not for a beam in bending.

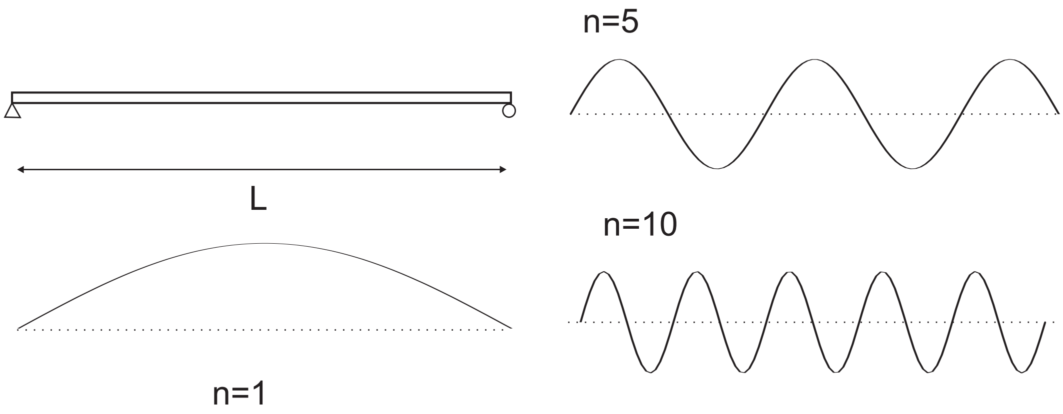

Figure 104: Bending modes 1,5 and 10 for a simply supported beam

For a double cantilever beam we have:

$$\begin{aligned} Y(0) &= A + C = 0 & \Rightarrow C = -A \\ Y'(0) &= \xi\,(B + D) = 0 & \Rightarrow D = -B \end{aligned}$$

So that the solution can be written

$$Y(x) = A(cos(\xi x) - cosh(\xi x)) + B(sin(\xi x) - sinh(\xi x))$$

Taking into account the boundary conditions at $x = L$ we have:

$$Y(L) = (cos\xi L - cosh\xi L)A + (sin\xi L - sinh\xi L)B = 0 \tag{48}$$

$$Y'(L) = (-sin\xi L - sinh\xi L)A + (cos\xi L - cosh\xi L)B = 0 \tag{49}$$

The system of equations admits a non trivial solution of

$$det \begin{pmatrix} cos\xi L - cosh\xi L & sin\xi L - sinh\xi L \\ -sin\xi L - sinh\xi L & cos\xi L - cosh\xi L \end{pmatrix} = 0$$

which leads to

$$cos\xi L = \frac{1}{cosh\xi L}$$

This equations does not admit an explicit solution. One way to solve it is to do it graphically. The first roots are represented on Figure 105.

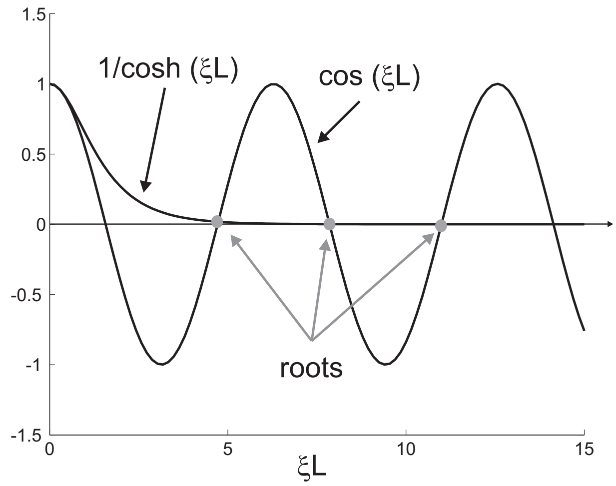

Figure 105: Roots of the equation allowing to compute the eigenfrequencies for a double cantilever beam

Let us note $\rho_n, n = 1, ...\infty$ with $\rho = \xi L$, we have:

$$\rho^2 = \xi^2 L^2 = \omega \sqrt{\frac{\rho A}{EI}} L^2$$

and the eigenfrequencies are:

$$\omega_n = \frac{\rho_n^2}{L^2} \sqrt{\frac{EI}{\rho A}} \qquad n = 1, ..., \infty$$

Note that a good approximation of the values of ρ_n is given by

$$\cos \rho = 0 \Rightarrow \rho_n = \frac{\pi}{2} + (n-1)\pi$$

and the mode shapes are obtained by replacing ξL with ρ_n in (48) which gives:

$$B = \frac{-\left(cos\rho_n - cosh\rho_n\right)}{sin\rho_n - sinh\rho_n} A =$$

and the mode shapes are given by (up to a constant)

$$Y_n(x) = (cos(\rho_n \frac{x}{L}) - cosh(\rho_n \frac{x}{L}) + \frac{-\left(cos\rho_n - cosh\rho_n\right)}{sin\rho_n - sinh\rho_n} (sin(\rho_n \frac{x}{L}) - sinh(\rho_n \frac{x}{L}))$$

There exists an infinity of eigenfrequencies and mode shapes, as for all continuous systems. The mode shapes of order $n = 1, 5, 10$ are represented in Figure 106.

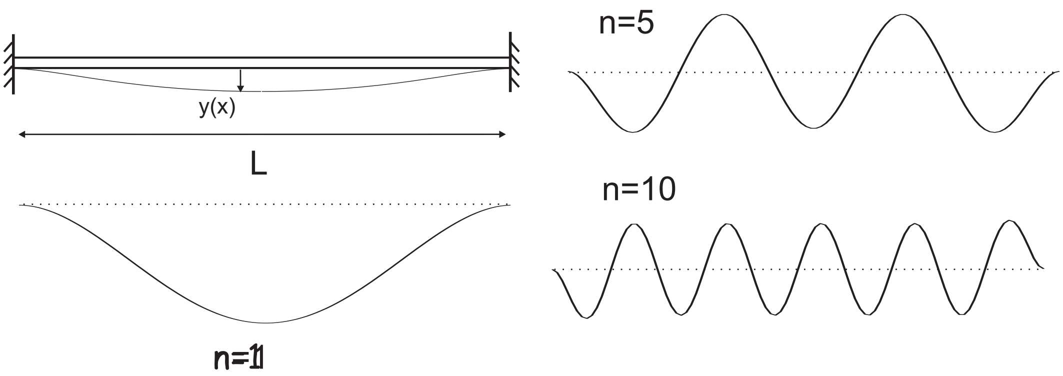

Figure 106: Mode shapes of a double cantilever beam ($n = 1, 5, 10$)

For a cantilever beam we have:

$$\begin{aligned} Y(0) &= A + C = 0 && \Rightarrow C = -A \\ Y'(0) &= \xi\,(B + D) = 0 && \Rightarrow D = -B \end{aligned}$$

So that the solution can be written

$$Y(x) = A(\cos(\xi x) - cosh(\xi x)) + B(\sin(\xi x) - sinh(\xi x))$$

Taking into account the boundary conditions at $x = L$ we have:

$$Y''(L) = (\cos\xi L + cosh\xi L)A + (\sin\xi L + sinh\xi L)B = 0 \tag{50}$$
$$Y'''(L) = (\sin\xi L - sinh\xi L)A - (\cos\xi L + cosh\xi L)B = 0 \tag{51}$$

The system of equations admits a non trivial solution of

$$det \begin{pmatrix} cos\xi L + cosh\xi L & sin\xi L + sinh\xi L \\ sin\xi L - sinh\xi L & -(cos\xi L + cosh\xi L) \end{pmatrix} = 0$$

which leads to

$$2\,(1 + cos\xi L cosh\xi L) = 0$$

$$cos\xi L = \frac{-1}{\cosh\xi L}$$

Again the solution cannot be solved analytically. Figure 107 represents the first roots of the equation. Let us note $\rho_n, n = 1, ...\infty$ with $\rho = \xi L$, we have:

$$\rho^2 = \xi^2 L^2 = \omega\sqrt{\frac{\rho A}{EI}}L^2$$

And the eigenfrequencies are:

$$\omega_n = \frac{\rho_n^2}{L^2}\sqrt{\frac{EI}{\rho A}} \qquad n = 1, ..., \infty$$

The first two roots are $\rho_1 = 1.876$ and ρ_2=4.693. The next roots are approximated by

$$\cos \xi L = 0 \Rightarrow \xi L = \pi/2 + (n-1)\pi$$

The mode shapes are obtained by replacing ξL with ρ_n in (50) which gives:

$$B = \frac{-(cos\rho_n + cosh\rho_n)}{sin\rho_n + sinh\rho_n} A =$$

and the mode shapes are given by (up to a constant)

$$Y_n(x) = (cos(\rho_n \frac{x}{L}) - cosh(\rho_n \frac{x}{L}) + \frac{-(cos\rho_n + cosh\rho_n)}{sin\rho_n + sinh\rho_n}(sin(\rho_n \frac{x}{L}) - sinh(\rho_n \frac{x}{L}))$$

There exists an infinity of eigenfrequencies and mode shapes, as for all continuous systems. The mode shapes of order $n = 1, 2, 5$ are represented in Figure 108.

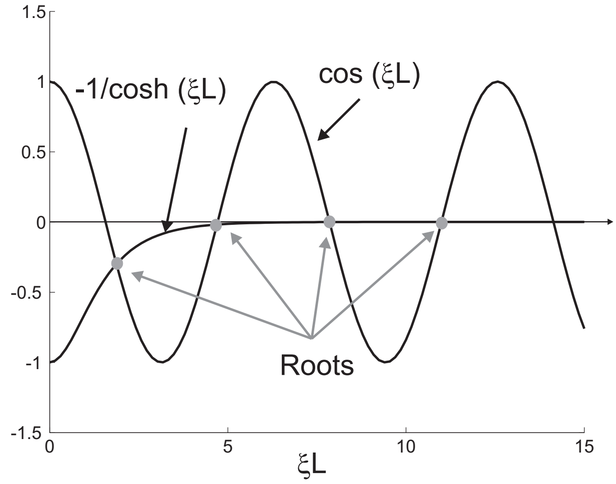

Figure 107: Roots of the equation allowing to compute the eigenfrequencies for a cantilever beam

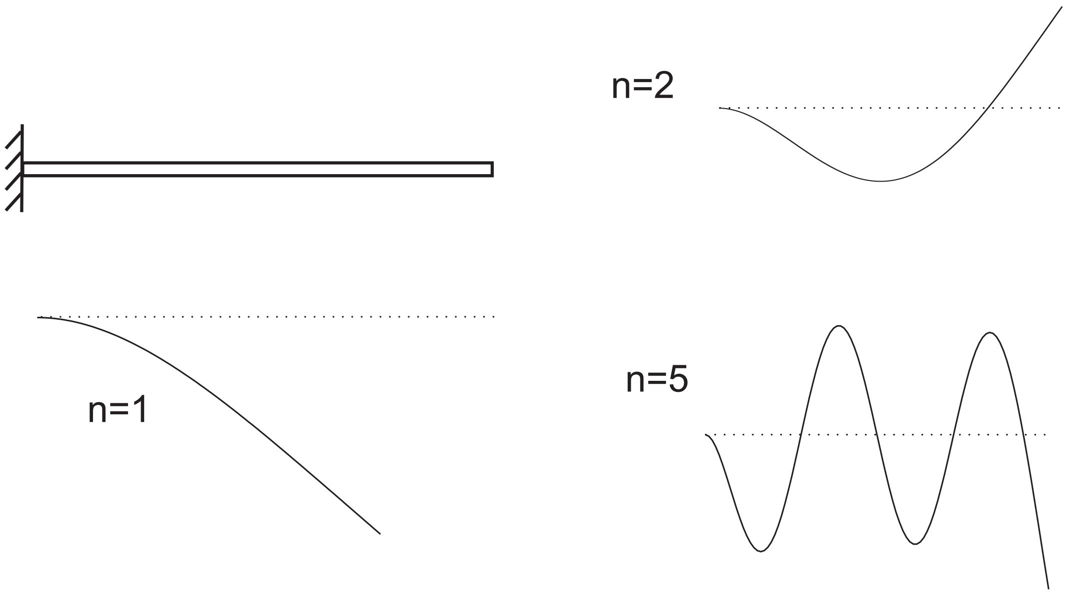

Figure 108: Mode shapes of a cantilever beam ($n = 1, 2, 5$)

6.1.10 Beam in bending: orthogonality conditions

For beams in bending, the orthogonality conditions are given by:

$$\int_0^L \rho A Y_i Y_j \, dx = \delta_{ij} \mu_i$$

$$\int_0^L EI Y_i'' Y_j'' \, dx = \delta_{ij} \mu_i \omega_i^2$$

Proof: Let us consider two different mode shapes Y_i and Y_j where $\omega_i \neq \omega_j$:

$$EIY_i^{IV} + \rho A \omega_i^2 Y_i = 0 \tag{52}$$

$$EIY_j^{IV} + \rho A \omega_j^2 Y_j = 0 \tag{53}$$

we multiply (52) by Y_j and integrate from 0 to L, and multiply (53) by Y_i and integrate from 0 to L.

$$\int_0^L \left(EIY_i^{IV} + \rho A \omega_i^2 Y_i \right) Y_j \, dx = 0 \tag{54}$$

$$\int_0^L \left(EIY_j^{IV} + \rho A \omega_j^2 Y_j \right) Y_i \, dx = 0 \tag{55}$$

Integrating twice by parts, we have

$$\begin{aligned} \int_0^L EI\, Y_i^{IV} Y_j \, dx &= \left[EI\, Y_i^{III} Y_j \right]_0^L - \int_0^L EI\, Y_i^{III} Y_j' \, dx + \\ &= \left[EI\, Y_i^{III} Y_j \right]_0^L - \left[EI\, Y_i'' Y_j' \right]_0^L + \int_0^L EI\, Y_i'' Y_j'' \, dx \end{aligned}$$

The term

$$\left[EI\, Y_i^{III} Y_j \right]_0^L$$

is always equal to zero because we either have $Y = 0$ or $T = 0$ (which leads to $T = -EIY^{III} = 0$) at the boundaries of the beam, and the term

$$\left[EI\,Y_i''Y_j'\right]_0^L$$

is also always equal to zero because we either have $Y' = 0$ or $M = 0$ at the boundaries of the beam (which leads to $-EIY'' = 0$). Finally, we obtain:

$$\int_0^L EI\,Y_i^{IV}Y_j\,dx = \int_0^L EI\,Y_j''Y_i''\,dx$$

and in the same way

$$\int_0^L EI\,Y_j^{IV}Y_i\,dx = \int_0^L EI\,Y_i''Y_j''\,dx$$

Therefore we have:

$$\int_0^L EI\,Y_j''Y_i'' \; + \rho A\omega_i^2 Y_j Y_i dx = 0 \tag{56}$$

$$\int_0^L EI\,Y_i''Y_j'' \; + \rho A\omega_j^2 Y_i Y_j dx = 0 \tag{57}$$

Substracting (57) from (56), we have:

$$\int_0^L \rho A(\omega_i^2 - \omega_j^2)Y_i\,Y_j\,dx = 0 \quad i \neq j \tag{58}$$

so that

$$\int_0^L \rho AY_i\,Y_j\,dx = 0 \quad i \neq j \tag{59}$$

and defining

$$\mu_i = \int_0^L \rho AY_i^2\,dx \tag{60}$$

(59) and (60) give the second orthogonality condition.
We can rewrite (56):

$$\int_0^L EI\,Y_j''Y_i'' \; = -\rho A\omega_i^2 Y_j Y_i dx$$

and taking into account (59) and (60), we have:

$$\int_0^L \; EI\,Y_i''Y_j''\,dx = 0 \quad i \neq j$$

$$\int_0^L \; EI\,(Y_i'')^2\,dx = \omega_i^2\mu_i$$

which is the first orthogonality condition.

6.1.11 Beam in bending: projection in the modal basis

Starting from the equation of motion

$$EI\frac{\partial^4 y(x,t)}{\partial x^4} + \rho A\frac{\partial^2 y(x,t)}{\partial t^2} = p(x,t)$$

we assume that the solution can be written as a function of the mode shapes

$$y(x,t) = \sum_{i=1}^{\infty} Y_i(x) z_i(t)$$

Plugging into the equation of motion, we have

$$EI\sum_{i=1}^{\infty} Y_i^{IV} z_i + \rho A\sum_{i=1}^{\infty} Y_i \ddot{z}_i = p(x,t)$$

We multiply by Y_j and integrate from 0 to L:

$$\int_0^L \left(EI\sum_{i=1}^{\infty} Y_i^{IV} z_i \right) Y_j\, dx + \int_0^L \left(\rho A\sum_{i=1}^{\infty} Y_i \ddot{z}_i \right) Y_j\, dx = \int_0^L p(x,t) Y_j\, dx$$

and rearranging

$$\int_0^L \left(EI\sum_{i=1}^{\infty} Y_i^{IV} Y_j \right) z_i\, dx + \int_0^L \left(\rho A\sum_{i=1}^{\infty} Y_i Y_j \right) \ddot{z}_i\, dx = \int_0^L p(x,t) Y_j\, dx$$

the orthogonality conditions are then used to obtain

$$\mu_i \ddot{z}_i + \mu_i \omega_i^2 z_i = F_i$$

$$F_i = \int_0^L p(x,t) Y_i\, dx$$

As in the case of the bar in traction, the equation of motion is transformed into an infinite number of equations of motions of a single dof. As discussed earlier, a truncation can be performed based on the frequency band of interest for the computation. Below is a link to a video showing the first modes of a cantilever beam.

`Cantilever beam modes : http://www.youtube.com/watch?v=uBZqa851uvw`

6.2 Complex structures

In many cases, the complexity of a structure does not allow one to use a beam or bar model in order to get an accurate model. There exist also solution for rectangular plates, but this will not be treated in this course. For more general cases, it is necessary to build an approximation by using numerical models, the most widely used being the finite element method. In the finite element method, the structure is divided in elements and contains nodes. For a general 3D model, there are three unknowns for each node: the displacement in the 3 directions. The displacement field is therefore given by:

$$
\left\{ \begin{array}{c} u(x,y,z) \\ v(x,y,z) \\ w(x,y,z) \end{array} \right\} = \left\{ \begin{array}{c} \sum_{i=1}^{n} u_i \phi_i(x,y,z) \\ \sum_{i=1}^{n} v_i \phi_i(x,y,z) \\ \sum_{i=1}^{n} w_i \phi_i(x,y,z) \end{array} \right\}
$$

where u, v, w are the displacement in the x, y and z direction, n is the number of nodes in the model, $\phi_i(x,y,z)$ are the shape functions and u_i, v_i, w_i are the nodal displacements of node i. An example of a finite element model of a bridge is presented in Figure 109.

Figure 109: Finite element model of the Pine Creek bridge lenticular truss bridge (http://fynitesolutions.com)

Another example is given in Figure 110. The study concerns the interaction of vehicles with the bridge. Once the finite element has been built, it is possible to obtain the stiffness and the mass matrices. The size of these matrices depends on the number of dofs of the structure modeled. For a structure modeled with 3D elements, the number of unknowns is $3n$ where n is the number of nodes. The matrices K and M are therefore $3n$ x $3n$ matrices. The undamped equations of motion are written in a matrix form:

$$
M\ddot{q} + Kq = F
$$

where

$$
q = \left\{ \begin{array}{c} u_1 \\ v_1 \\ w_1 \\ u_2 \\ \dots \\ w_n \end{array} \right\}
$$

is the vector of nodal unknowns. As this expression is identical to (27), the tools described in section 5.1 can be used to solve the system of equations. Based on the K and M matrices, the mode shapes and eigenfrequencies can be computed numerically. A few mode shapes of the bridge are represented on Figure 111. From that point, the same strategy as described for mdof systems can be followed to reduce the system of equations by projecting it in the modal basis. In general, the number of dofs in the model is not linked to the necessary accuracy, but rather to the necessity to comply with the complex geometry. For a bridge excited by wind and traffic, generally, only a few modes (up to

20 modes) are of interest. The truncation is therefore very efficient as it allows to go from several thousands of dofs to only 10-20 dofs.

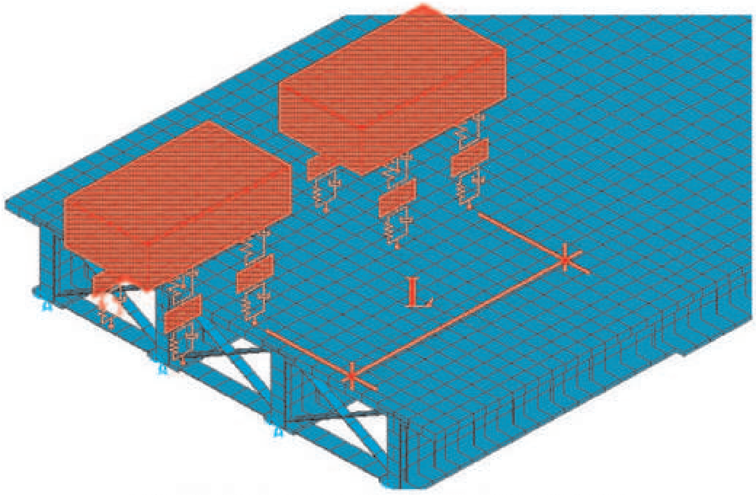

Figure 110: Finite element model of a bridge and vehicles crossing the bridge [http://www.scielo.br]

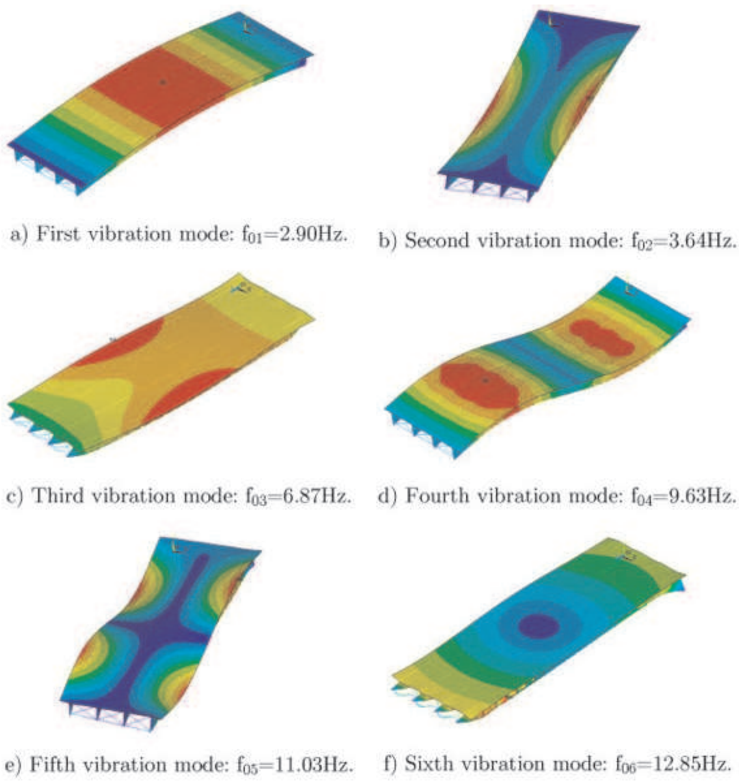

Figure 111: A few modes of the bridge presented in Figure 110 [http://www.scielo.br]

6.2.1 Modeling of damping

The equations of motion including the damping are written:

$$M\ddot{q} + C\dot{q} + Kq = F$$

The matrix C is difficult to obtain. This is because, as we have seen in Section 3.4.3, there are various sources of damping which are not easily quantified. Rayleigh damping is often used to build the damping matrix, but is gives a very poor fit to experimental data (only two parameters, no physical meaning). The damping matrix can be constructed using physical constitutive laws for the materials including dissipative effects (viscoelasticity, friction ...). This is rarely done because in practice, a lot of the damping comes from the joints which are usually represented by a simplified model for which the damping is unknown. The most common approach is to project the equations of motion in the modal domain and use the modal damping approach. The modal damping coefficients can either be measured on the real structure if it is available, or given by a flat value, usually equal to $\xi = 0.01$ for lightly damped structures.

6.2.2 Tuned mass damper attached to continuous structures

Let us take the example of a simply supported beam to which a TMD is attached at a distance d from the left-hand side (Figure 112). The TMD is replaced by a force f_d and the displacement at this point is noted y_d.

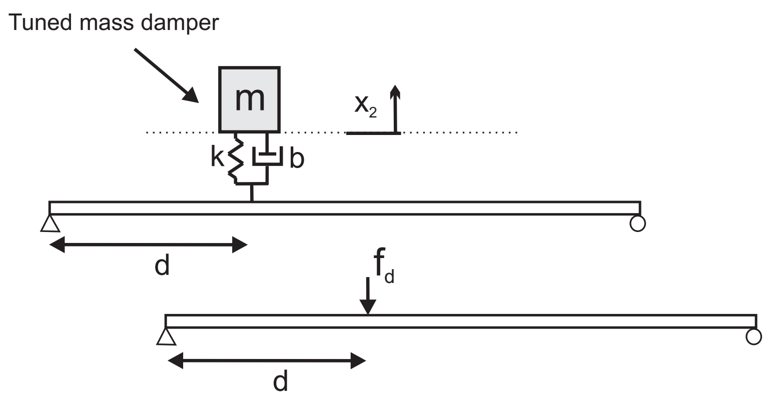

Figure 112: Simply supported beam equipped with a TMD

The projection on the modal basis leads to an infinite number of equations of the type:

$$\mu_i \ddot{z}_i + \mu_i \omega_i^2 z_i = \psi_i^T F \quad (61)$$

We make the assumption that around the eigenfrequency ω_i, the displacement can be approximated with a single mode:

$$x = \sum_{j=1}^{\infty} \psi_j z_j \simeq \psi_i z_i$$

The displacement at the position of the TMD is therefore

$$y(d) = \psi_i(d) z_i$$

and we can write

$$z_i = \frac{y(d)}{\psi_i(d)}$$

Replacing in (61) and noting that $\psi_i^T F = \psi_i(d) f_d$, we obtain:

$$\frac{\mu_i}{\psi_i^2(d)}\ddot{y}(d) + \frac{\mu_i \omega_i^2}{\psi_i^2(d)} y(d) = f_d$$

which can be written

$$M\ddot{y}(d) + Ky(d) = f_d$$

if we define

$$M = \frac{\mu_i}{\psi_i^2(d)}$$
$$K = \frac{\mu_i \omega_i^2}{\psi_i^2(d)}$$

The equation of motion has been reduced to a single dof (assuming that the displacement can be approximated by a single mode), and the formulae developed in Section 5.3 can be used. Figure 113 shows the example of the displacement in the middle of the beam excited by a force at the same location, with and without the TMD. The TMD is efficient to damp the first mode. Note that it is effective only in a narrow frequency band around the frequency to which it has been tuned.

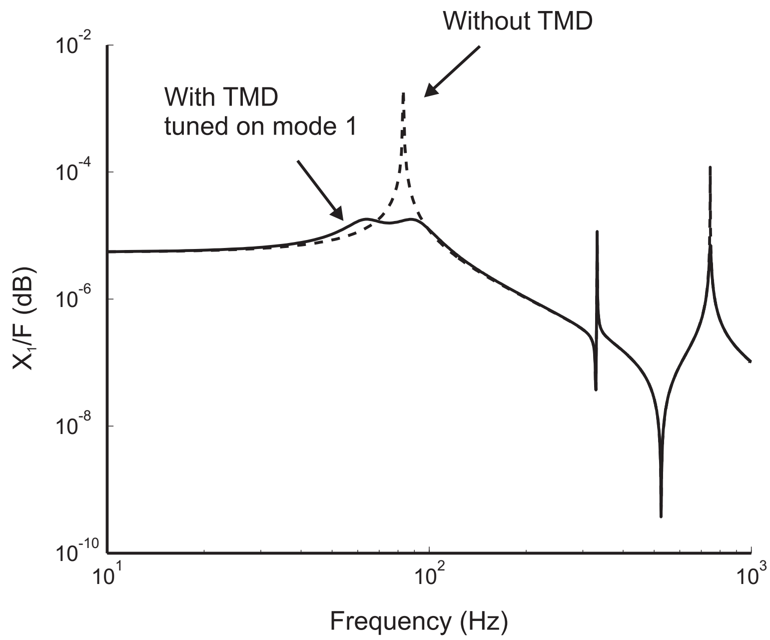

Figure 113: Displacement in the middle of the beam due to a force at the same location. Effect of the TMD

The following movie illustrates the efficiency of a TMD to damp the first mode shape of a cantilever beam.

`Beam with tuned mass damper: http://www.youtube.com/watch?v=fuCdZLQOrAw`